UNIVERSITÀ DI TORINO

Dipartimento di Biotecnologie Molecolari e Scienze per la Salute

Dottorato di Ricerca in
Scienze Biomediche ed Oncologia

Indirizzo: Immuno-diagnostica avanzata

XXXV Ciclo

TITOLO DELLA TESI

Analisi molecolare di forme aggressive di neoplasia endocrina per la identificazione di meccanismi di progressione e di potenziali nuovi bersagli terapeutici

Candidata: Vanessa Zambelli
Tutor: Prof. Marco Volante

Direttore della Scuola: Prof. Emilio Hirsch
Coordinatore di indirizzo: Prof.ssa Silvia Deaglio

Anni accademici: 2019/2020-2022/2023

Settore scientifico-disciplinare di afferenza: MED/08

“You are braver than you believe,
stronger than you seem
and smarter than you think"
– The Adventures of Winnie The Pooh-

A tutta la mia famiglia.

INDEX

1.0 OVERALL RESEARCH ACTIVITY

This present work summarizes the candidate's main research activities performed during the 4-year PhD program at the Doctoral School in Biomedical Sciences and Oncology of the University of Turin (Subject: "Advanced Immunodiagnostics"), under the supervision of Prof. Marco Volante.

The research interest has been mainly focused on the study of rare forms of aggressive endocrine and neuroendocrine tumors, in particular focusing on specific aspects in the molecular pathogenesis and in the identification of novel potential therapeutic targets.

What illustrated in the present work is related to studies still unpublished but completed, that are already submitted or in draft for publication. Additional studies that the Candidate performed during the PhD program, that are already published, are briefly mentioned in the Summary Table here below but are not described in detail in the present Thesis.

Study 1 and 2 are dedicated to the investigation of molecular mechanisms of tumor progression and on the identification of potentially druggable alterations in adrenocortical carcinoma.

In study 1, we focused our work on the analysis of mechanisms of progression of adrenal cortical carcinoma cases associated with a benign component. In most cases we found a common genotype in the two components that was enriched for additional molecular events in the malignant component that suggested to be main drivers of tumor progression. However, a subset of cases, even in the presence of a closely intermingled combination of the tumor components, showed a markedly different genotype, thus suggesting that in a subset of these cases clonal evolution was independent.

In study 2, we wanted to analyze clinical, pathological, and molecular characteristics of adrenocortical carcinomas with a defective mismatch repair (MMR) system, to establish their prevalence in a large cohort and their specific characteristics. MMR-deficient cases showed the presence in general of characteristics of more aggressive diseases and a genotype highly enriched for the presence of *TP53* mutations.

Study 3 and 4 are focused on the investigation of the molecular characteristics of poorly differentiated thyroid carcinomas. The two studies here present have a similar conceptualization as the two ones in adrenocortical carcinoma.

In study 3, our aims were to verify if, from a molecular point of view, poorly differentiated thyroid carcinomas derive from direct progression from well differentiated thyroid carcinomas or develop as new clonal events. We selected and analyzed separately tumor

components from cases having well-differentiated and poorly differentiated carcinoma areas and found that most of the cases were molecularly correlated. However, similarly to what we found in Study 1, a few cases were molecularly unrelated.
In study 4, we aimed to characterize a series of poorly differentiated thyroid carcinomas with multimodal molecular approach to identify potential targetable genes. Our results showed that cases could be segregated in molecularly different subgroups, and that, overall, a significant proportion of cases harbor molecular alterations of potential therapeutic interest.

Finally**, Study 5**, is investigating the molecular background of lung carcinoids with high proliferation index, with the aim of investigating their relationship with other forms of lung neuroendocrine neoplasms and specifically to determine the prevalence of genomic alterations of potential therapeutic relevance. As a result, we found that these tumors share molecular characteristics of both carcinoids and high-grade neuroendocrine carcinomas, with special reference to large cell neuroendocrine carcinoma, but overall have a distinct genotype. Moreover, as for what found in study 4 in the model of poorly differentiated carcinomas, lung carcinoids with high proliferation index have a high number of molecular alterations in genes that are potential therapeutic targets.

Overall research activity of the Candidate

Study Number	Authors	Title	Aim	Main results
Study 1	**Vanessa Zambelli**, Giulia Orlando, Giulia Vocino Trucco, Eleonora Duregon, Giulia Capella, Mauro Papotti, Marco Volante	Deep molecular analysis of matched samples of adrenocortical neoplasms with coexisting benign and malignant tumor components	To unveil mechanisms of progression from adrenal cortical adenoma to adrenal cortical carcinoma through deep molecular characterization of cases associated with both a benign and a malignant component within the same lesion.	In most of the samples, copy number variations, chromosomal arms loss/gain together with mutations in *TP53* and *TERT promoter* genes were the possible leading mechanisms of malignant transformation. However, some cases showed a polyclonal genotype thus suggesting an unrelated clonal development.
Study 2	**Vanessa Zambelli**, Giulia Vocino Trucco, Ida Rapa, Lorenzo Daniele, Mauro Papotti, Alfredo Berruti, Massimo Terzolo, Marco Volante	Pathological and molecular characteristics of adrenocortical carcinomas with mismatch repair deficiency	To analyze clinical, pathological and molecular characteristics of adrenocortical carcinomas with defective mismatch repair (MMR) system.	The prevalence of cases with altered expression of MMR proteins was about 9%. MSH6 loss was the most frequent and possibly related to non-genomic mechanisms of alteration. MMR deficient cases were particularly enriched in co-mutations in *TP53* gene.
Study 3	**Vanessa Zambelli**, Matthias Dettmer, Lorenzo Daniele, Jasna Metovic, Renaud Maire, Stefano Carollo, Jessica Giorcelli, Simona Vatrano, Susanna Cappia, Giovanni De Rosa, Aurel Perren, Mauro Papotti, Marco Volante	Molecular heterogeneity of poorly differentiated thyroid carcinomas associated with a well differentiated carcinoma component.	To characterize the molecular landmark of poorly differentiated carcinomas (PDTC) associated with a well-differentiated component (WDTC), to underpin possible molecular pathways of tumor progression and to verify a possible clonal origin for these tumors.	Most of the cases support the concept that PDTC may progress from WDTC through the acquisition of additional alterations mainly involving genes coding for tyrosine kinases and/or involved in the PI3K/AKT pathway. However, a minority of cases showed a polyclonal genotype.
Study 4	**Vanessa Zambelli**, Marta Fornaro, Giulia Orlando, Giulia Vocino Trucco, Ida Rapa, Francesca Napoli, Susanna Cappia, Lorenzo Daniele, Simonetta Piana, Mauro Papotti, Marco Volante	High prevalence of potential molecular therapeutic targets in poorly differentiated thyroid carcinoma	To characterize a series of PDTC, homogeneously coded according to the most recent WHO classification of thyroid tumors, by means of a multimodal molecular approach with the objective of identifying the prevalence and potential clinical usefulness of molecular targets for therapy	The main molecular subgroups were identified, *NRAS*-enriched, *TP53* enriched (mutually exclusive each other) and a *TERT promoter*-enriched. MMR altered cases were 11.9% and associated with *TP53* mutations. Four cases harbored gene fusions, including two cases harboring the *TBL1XR1-PIK3CA* fusion that has never been reported in thyroid cancer, so far.
Study 5	**Vanessa Zambelli**, Francesca Napoli, Susanna Cappia, Angela Listì, Ida Rapa, Luisella Righi, Fabrizio Tabbò, Jasna Metovic, Mauro Papotti, Giorgio Scagliotti, Silvia Novello, Marco Volante	High prevalence of potentially druggable molecular alterations in lung carcinoids with high proliferation index.	To investigate the genomic background of lung carcinoid with high proliferation index, with special reference to alterations in genes of potential therapeutic relevance.	Gene expression data and microRNA profiling posed these tumors in between carcinoids and LCNEC. Overall, 40% of cases harbored mutations (single or co-occurrent) in genes that are potential therapeutic targets, including those

				in DNA repair genes (31%), MMR (19%) and ERBB2 (15%).
/	Francesca Napoli, Ida Rapa, Umberto Mortara, Federica Massa, Stefania Izzo, Angelica Rigutto, **Vanessa Zambelli**, Claudio Bellevicine, Giancarlo Troncone, Mauro Papotti, Marco Volante	MicroRNA profiling predicts positive nodal status in papillary thyroid carcinoma in the preoperative setting	To assess the preoperative role of microRNAs (miRNAs) in predicting the nodal status of patients with papillary thyroid cancer.	In thyroid cytological samples, 4 miRNAs (miR-154-3p, miR-299-5p, miR-376a-3p, and miR-302E) were demonstrated to predict significantly pN-positive versus pN-negative status at surgery.
/	Francesca Bersani, Francesca Picca, Morena Deborah, Luisella Righi, Francesca Napoli, Mariangela Russo, Daniele Oddo, Giuseppe Rospo, Carola Negrino, Barbara Castella, Marco Volante, Angela Listì, **Vanessa Zambelli**, Federica Benso, Fabrizio Tabbò, Paolo Bironzo, Emanuele Monteleone, Valeria Poli, Filippo Pietrantonio, Federica Di Nicolantonio, Alberto Bardelli, Carola Ponzetto, Silvia Novello, Giorgio Scagliotti, Riccardo Taulli	Exploring circular MET RNA as a potential biomarker in tumors exhibiting high MET activity	To provide a comprehensive molecular characterization of circular MET RNA (circMET), an abundant and stable circRNA molecule encoded by *MET* exon 2.	Using publicly available bioinformatic tools, we discovered that the *MET* locus transcribes several circRNA molecules, but only one candidate, circMET, was particularly abundant. Deeper molecular analysis revealed that circMET levels positively correlated with MET expression and activity, especially in *MET*-amplified cells. We developed a circMET-detection strategy and, in parallel, we performed standard FISH and IHC analyses in the same specimens to assess whether circMET quantification could identify patients displaying high MET activity. Longitudinal monitoring of circMET levels in the plasma of selected patients revealed the early emergence of *MET* amplification as a mechanism of acquired resistance to molecular therapies.
/	Francesca Napoli, Angela Listì, **Vanessa Zambelli**, Gianluca Witel, Paolo Bironzo, Mauro Papotti, Marco Volante, Giorgio Scagliotti, Luisella Righi	Pathological Characterization of Tumor Immune Microenvironment (TIME) in Malignant Pleural Mesothelioma	To collect literature data on the role of the Tumor Immune Microenvironment in pleural mesothelioma to critically evaluate possible implications for clinical practice (Review)	The chronic inflammatory response to asbestos fibers leads to a unique tumor immune microenvironment (TIME), constituted by immunosuppressive cells, such as type 2 tumor-associated macrophages and T regulatory lymphocytes, plus the expression of several immunosuppressive factors, such as tumor-associated PD-L1. These data opens the way to the identification of novel potential tissue biomarkers.

2.0 AIMS

The general aim of this Thesis is to characterize rare aggressive endocrine cancers, in order to better understand their molecular background and to unravel novel potential therapeutic targets.

All models investigated in the present Thesis are aggressive forms of cancer that are characterized by an uncertain histogenesis, by an aggressive clinical course with poor response to standard therapeutic protocols, and by the lack of an individualized clinical and therapeutic approach.

In the different tumor models, we design 5 main studies with the specific sub aims:

a) to identify molecular pathways of tumor progression

b) to better characterize specific tumor subgroups

c) to define the prevalence and potential clinical impact of druggable alteration.

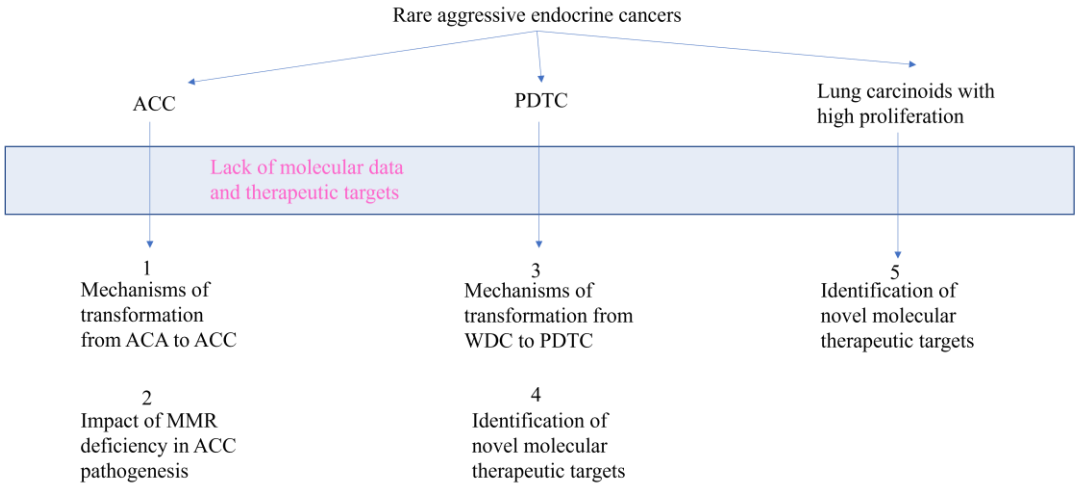

3.0 GENERAL METHODS

Tumor tissue samples analyzed in the present Thesis are detailed in the specific chapters. All material corresponds to series of formalin-fixed and paraffin embedded (FFPE) human tumor tissues.

Here below are listed all the products, the general procedures and technical protocols used in this 4-year PhD program, with a specific reference for each methos to the study where it has been employed.

3.1 Immunohistochemistry (Study 2, 4 and 5)

3.1.1 Mismatch repair status (Study 2 and 4)

The expression of mismatch repair (MMR) proteins was tested using immunohistochemistry (IHC) in an automated system (DakoCytomation Omnis, Dako) using the following antibodies (all from DakoCytomation): MLH1 (clone ES05), MSH2 (clone FE11), MSH6 (clone EP49) and PMS2 (clone EP51). Loss of nuclear expression for paired proteins (MLH1 and/or PMS2 or MSH2 and/or MSH6) or for MSH6 and PMS2 alone was considered as altered expression pattern. Non tumoral cells (peritumoral adrenal cortical or thyroid cells, inflammatory cells and/or endothelial cells) were used as positive internal control cells. Cases with an altered pattern were also tested for the presence of microsatellite instability (MSI) using genomic DNA extracted as described below.

Since thyroid and adrenocortical cancer-specific panels are not commercially available, all cases were analyzed using a kit clinically approved for colon and endometrial cancer (EasyPGX ready MSI KIT CE IVD, Diatech Pharmacogenetics) that includes the following markers: BAT25, BAT26, NR21, NR22, NR24, NR27, CAT25 and MONO27. Results are expressed as microsatellite stable (MSS), low microsatellite instability (MSI-low) and high microsatellite instability (MSI-high).

3.1.2 ALK (Study 5)

In all samples of lung neuroendocrine neoplasms that resulted positive for ALK fusion on RNA NGS testing, one five-micron thick section was cut, deparaffinized and tested for expression of ALK protein by using immunohistochemistry (IHC) (clone 5A4, Novocastra™, Leica) following manufacturer instructions, with an automated Dako Omnis System (Agilent Technologies, Santa Clara, CA, USA).

3.2 Fluorescence In Situ Hybridization (FISH) (Study 4 and 5)

To validate the *TBL1XRA-PIK3CA* fusion in poorly differentiated thyroid cancer, a FISH approach was applied on four-micron thick formalin-fixed paraffin-embedded section using a *TBL1XR1/PIK3CA* probe set (Empire Genomics, New York, US) following manufacturer instructions. The *TBL1XR1/PIK3CA* probe set consisted of DNA labeled in Spectrum Green and Spectrum Orange. The DNA probe set hybridizes to chromosome 3q26.32 (Green) and 3q26.32-q26.33 (Orange) in interphase nuclei (**Figure 1**).

RET and *NTRK2* FISH assays were performed on four-micron thick formalin-fixed paraffin-embedded (FFPE) section with ZytoLight™ SPEC *RET* and *NTRK2* Dual Color Break-Apart Probes (Zyto Vision, Bremerhaven, Germany) following manufacturer instructions.

The SPEC *RET* Dual Color Break-Apart Probe is a mixture of two direct labeled probes hybridizing to the 10q11.21 band. The orange fluorochrome direct labeled probe hybridizes proximal to the *RET* gene, the green fluorochrome direct labeled probe hybridizes distal to the gene (**Figure 2**).

The SPEC *NTRK2* Dual Color Break-Apart Probe is a mixture of two direct labeled probes hybridizing to the 9q21.32-q21.33 band. The green fluorochrome direct labeled probe hybridizes proximal to the *NTRK2* breakpoint region at 9q21.32-q21.33, the orange fluorochrome direct labeled probe hybridizes distal to the *NTRK2* breakpoint region at 9q21.33 (**Figure 3**).

For *PIK3CA* probe the presence of two green and red separated signals were considered as normal pattern, while altered partner was characterized by fused signals (yellow) and/or with multiple red and green signals without fusion signal.

For *RET* break-apart probe signal pattern consisting of two orange/green fusion signals were considered negative; one orange/green fusion signal, one orange signal, and a separate green signal were considered positive. Isolated green signals are the result of deletions proximal to the *RET* breakpoint region.

For *NTRK2* break-apart probe signal pattern consisting of two orange/green fusion signals were considered negative; one orange/green fusion signal, one orange signal, and a separate green signal were considered positive.

For each case, 100 non overlapping tumor cell nuclei were examined for the presence of yellow or green and orange, fluorescent signals. Cutoff values for all probes were set at >15% of nuclei with altered signals.

The sections were examined with an Olympus BX61 fluorescence microscope (Olympus Corporation, Tokyo, Japan) equipped with a triple-pass filter (DAPI/Green/Orange; Vysis, Downers Grove, IL, USA) with CytoVision® software version 7.6 (Leica Biosystems, Buffalo Grove, IL, USA).

3.3 Nucleic acid extraction (All studies)

Genomic DNA and RNA were extracted from the formalin-fixed paraffin-embedded tumor material. Enrichment of tumor cells was obtained by manual micro dissection under light microscopy from one to ten sections for each case. For NGS analysis, the selected material was extracted using Maxwell® RSC DNA FFPE kit (Promega Corporation, Madison, WI, USA) and Maxwell® RSC RNA FFPE kit (Promega Corporation, Madison, WI, USA) according to the manufacturer's instructions. Nucleic acids were quantified on QuantusTM fluorometer (Promega Corporation, Madison, WI, USA) using Quantifluor® DNA System (Promega Corporation, Madison, WI, USA) and Quantifluor® RNA System (Promega Corporation, Madison, WI, USA) following manufacturer's instructions. DNA quality was evaluated with Real Time PCR of *EGFR* Exon2 amplification through Rotor-Gene Q (Qiagen, Hilden, Germany) Real Time PCR instrument, the following primers were used for *EGFR*: EGFRex2b Fw (5'-GAAGATCATTTTCTCAGCCTCCA-3') and EGFRex2b Rw (5'-AGGAAAATCAAAGTCACCAACCT-3') (Diatech Pharmacogenetics, Jesi, AN, Italy). RNA quality was evaluated with Real Time PCR with beta-actin amplification through Rotor-Gene Q (Qiagen, Hilden, Germany) Real Time PCR instrument, the following primers were used for B-ACT: BACT Fw (5'-CCTTCCTGGGCATGGAGTCTTG-3') and BACT Rw (5'-GGAGCAATGATCTTGATCTTC-3').

For gene and microRNA expression analysis, total RNA (including miRNAs) was isolated using a different commercially available RNA extraction kit (miRNeasy FFPE kit, Qiagen, Hilden, Germany), according to the manufacturer's instructions. The concentration and the purity of RNA samples were determined by measuring the optical density (OD) 260/OD280.

3.4 Wide targeted next generation sequencing (All studies)

3.4.1 Focus Assay (Study 3)

Complementary DNA (cDNA) synthesis prior to library preparation for RNA panel was carried out using SuperScript™ VILO™ cDNA Synthesis Kit (11754050, Thermo Fisher Scientific, Waltham, MA, USA). Library preparation was carried out using the DNA Oncomine™ Focus Assay (Thermo Fisher Scientific, Waltham, MA, USA) and RNA Oncomine™ Focus Assay (Thermo Fisher Scientific, Waltham, MA, USA) following manufacturer's instructions using a total of 10 ng input DNA and or 15 ng input RNA. The Oncomine™ Focus DNA and RNA assay (Thermo Fisher Scientific, Waltham, MA, USA) comprises two separate panels (DNA and RNA) interrogating hotspot mutations in 35 genes, copy number variations in 19 genes and fusions in 23 genes (**Table 1**). DNA and RNA assay specificity and sensitivity were assessed using clinical samples with known molecular alterations, the Quantitative Multiplex Reference Standard cfDNA mild (Horizon Discovery, Waterbeach, UK,catalog) and the *ALK-RET-ROS1* Fusion FFPE RNA Reference standard (Horizon Discovery, Waterbeach, UK, RNA REF 1–4). Libraries were clonally amplified onto Ion Sphere Particles (ISP) using emulsion PCR in an Ion Chef System (Thermo Fisher Scientific, Waltham, MA, USA) according to the manufacturer's instructions. Enriched ISPs were loaded onto 530 chips accommodating eight DNA end eight RNA sample on a single chip and sequencing on the S5 sequencer (Thermo Fisher Scientific, Waltham, MA, USA), according to manufacturer's instructions.

3.4.2 Oncomine Comprehensive Assay V3 (Study 2, 4, 5)

Library preparation was carried out automatically using the DNA and RNA Oncomine™ Comprehensive Assay v3 (Thermo Fisher Scientific, Waltham, MA, USA) using a total from 10 to 40 ng input DNA and RNA in an Ion Chef System (Thermo Fisher Scientific, Waltham, MA, USA) following manufacturer's instructions. The Oncomine™ Comprehensive Assay v3 (Thermo Fisher Scientific, Waltham, MA, USA) comprises DNA panel which was designed to interrogate hotspot mutations (87), full exon coverage (48) and copy number variations (43) and RNA panel which was designed to interrogate fusion drivers (51) (**Table 2**). The prepared libraries were clonally amplified onto Ion Sphere Particles (ISP) using emulsion PCR in an Ion Chef System (Thermo Fisher Scientific, Waltham, MA, USA) according to the manufacturer's instructions. Enriched ISPs were loaded onto 540 chips accommodating eight DNA samples and eight RNA

samples on a single chip and sequencing on the Ion Torrent S5 Prime Studio™ (Thermo Fisher Scientific, Waltham, MA, USA), according to the manufacturer's instructions.

3.4.3 Oncomine Comprehensive Assay PLUS (Study 1)

Library preparation was carried out automatically using the DNA Oncomine™ Comprehensive Assay PLUS (Thermo Fisher Scientific, Waltham, MA, USA) using a total from 20 to 30 ng input DNA and in an Ion Chef System (Thermo Fisher Scientific, Waltham, MA, USA) following manufacturer's instructions. The Oncomine™ Comprehensive Assay PLUS (Thermo Fisher Scientific, Waltham, MA, USA) comprises DNA panel which was designed to interrogate hotspot mutations and CNV gain (185), full exon coverage (227) and TMB only genes (89) (**Table 3**).

The prepared libraries were clonally amplified onto Ion Sphere Particles (ISP) using emulsion PCR in an Ion Chef System (Thermo Fisher Scientific, Waltham, MA, USA) according to the manufacturer's instructions. Enriched ISPs were loaded onto 550 chips accommodating four DNA samples on a single chip and sequencing on the Ion Torrent S5 Prime Studio™ (Thermo Fisher Scientific, Waltham, MA, USA), according to the manufacturer's instructions.

3.5 Sanger sequencing for TERTp mutation analysis (Study 3 and 4)

To validate *TERT* promoter *(TERTp)* mutations that are difficult to detect in NGS analysis, as they are intronic, we performed Sanger sequencing analysis on all cases tested for DNA genomic alterations in NGS. *TERTp* region was sequenced for the detection of the two mutations C228T and C250T. Target region was amplified by conventional PCR with the following primes: *TERT* Fw (5'AGTGGATTCGCGGGCACAGA-3') and *TERT* Rw (5'-CAGCGCTGCCTGAAACTC-3'). A first step with Uracil-DNA Glycosylase (Thermo Fisher Scientific, Waltham, MA, USA) was performed on all samples, following manufacturer's instructions. Then, the PCR run in 50 μL reactions with 25μL of 2X Platinum™ Superfi™ II PCR Master Mix (Thermo Fisher Scientific, Waltham, MA, USA), 5μM of each primer and 10μL of gDNA. The amount of gDNA for each PCR varies from 5 to 100 ng, depending on sample's quality. PCR conditions consist of one cycle of 98°C for 1 min, 3 cycles of (98°C for 30s, 62°C for 30s, 72°C for 45s), followed by 35 cycles of (98°C for 30s, 60°C for 30s, 72°C for 45s), and final extension at 72°C for 5 min.

Resulting amplicons were visualized in 2% agarose gels and verified to have the expected size of 193 bp. *TERTp* sequences were generated by Sanger sequencing and sequencing was performed at Eurofins Genomics (Ebersberg, Germany). All samples were sequenced in both directions.

3.6 Bioinformatics and statistical analysis (All studies)

Pathological features, immunohistochemical and molecular results were correlated to clinical variables, using appropriate statistical tests (chi-square and t Student's test for qualitative and quantitative parameters correlation, and univariate analyses of both disease-free interval (from the date of diagnosis to first metastasis/recurrence) and disease-specific survival (from the date of diagnosis to death if related to the disease). All statistical analyses were performed using Graph Pad Prism 9.4.1 software.

3.6.1 Oncomine Focus assay data analysis (Study 3)

Analysis was carried out using Ion Torrent Suite™ Browser version 5.12 (Thermo Fisher Scientific, Waltham, MA, USA) and Ion Reporter™ version 5.10 (Thermo Fisher Scientific, Waltham, MA, USA). The Torrent Suite™ Browser was used to perform initial quality control check including chip loading density, median read length and number of mapped reads. The Coverage Analysis plugin was applied to all data and used to assess amplicon coverage for regions of interest. The Ion Reporter suite (Thermo Fisher Scientific, Waltham, MA, USA) was used to filter out known polymorphic variants. The variants were annotated by three genetic databases: the Single Nucleotide Polymorphism Database (dbSNP) (http://www.ncbi.nlm.nih.gov/ projects/ SNP/), the Catalogue of Somatic Mutations in Cancer (COSMIC) (http://cancer.sanger.ac.uk/cancergenome/projects/cosmic/) and the ClinVar database (http://www.ncbi.nlm.nih.gov/clinvar/). The prediction of the functional pathogenic effects of the missense variants to the protein structure and function were predicted in silico by PolyPhen-2 (https://ionreporter.thermofisher.com) and SIFT (https://ionreporter.thermofisher.com).

Missense variants predicted to be benign or tolerated in PolyPhen-2 and SIFT software were excluded, as well as variants having a frequency higher than 1% in all populations from the 1000 Genomes data.

Moreover, variants with altered allele depth ≤1000 base coverage and/or an allelic frequency ≤5% were also eliminated from the analysis. Significance of identified variants was checked using Alamut Visual v.2.15 (Interactive Biosoftware, Sophia Genetics, Boston, MA, USA). Any discrepancy in variant identification between Ion Reporter and Alamut was validated manually using the Integrative Genomics Viewer (Thorvaldsdóttir et al, 2013) All variants were re-evaluated according to the search engineVarSome.com (Kopanos et al, 2019).

Synonymous, benign and VUS mutations were excluded from analysis.

3.6.2 Oncomine Comprehensive assay V3 data analysis (Study 2, 4 and 5)

Analysis was carried out using Ion Torrent Suite™ Browser version 5.16 (Thermo Fisher Scientific, Waltham, MA, USA) and Ion Reporter™ version 5.16 (Thermo Fisher Scientific, Waltham, MA, USA). The Torrent Suite™ Browser was used to perform initial quality control including chip loading density, median read length and number of mapped reads. The Coverage Analysis plugin was applied to all data and used to assess amplicon coverage for regions of interest. For DNA analysis, the Ion Reporter suite (Thermo Fisher Scientific, Waltham, MA, USA) was used to filter out known polymorphic variants. The variants were annotated by genetic databases: The Single Nucleotide Polymorphism Database (dbSNP) (http://www.ncbi.nlm.nih.gov/ projects/ SNP/), Catalogue of Somatic Mutations in Cancer (COSMIC) (http://cancer.sanger.ac.uk/cancergenome/projects/cosmic/) and ClinVar database (http://www.ncbi.nlm.nih.gov/clinvar/).Variants with altered allele depth ≤100 base coverage and a variant allelic frequency ≤5% were eliminated from the analysis. Identified variants were checked for correct nomenclature using Alamut Visual Plus (Interactive Biosoftware, Sophia Genetics). Any discrepancies in variant identification, between Ion Reporter and Alamut, were validated manually using the Integrative Genomics Viewer (http://dx.doi.org/10.1093/bib/bbs017). Variants were annotated following ACGM guidelines (Richards et al,2015) and the search engine VarSomePremium.com (Kopanos et al, 2019).The prediction of functional effects of the variants that were find as Variants of Uncertain Significance (VUS) was assessed with 13 in silico tools (**Table 4**) (Tavtigian et al, 2006; Quang et al, 2015; Grantham, 2014; Felsenstein, 1981; Li et al, 2022; Schwarz et al, 2010; Pejaver et al, 2020; Choi et al, 2015; Ioannidis et al, 2016; Kumar et al, 2009) . VUS was qualified as Damaging when defined as such by at least 7 tools (Ticha et al, 2019). Synonymous mutations, missense variants called benign or tolerated and variants

showing a frequency higher than 1% in all populations from the 1000 Genomes data were excluded from the analysis.

3.6.3 Oncomine Comprehensive assay PLUS data analysis (Study 1)

Analysis was carried out using Ion Torrent Suite™ Browser version 5.18 (Thermo Fisher Scientific, Waltham, MA, USA) and Ion Reporter™ version 5.20 (Thermo Fisher Scientific, Waltham, MA, USA). The Torrent Suite™ Browser was used to perform initial quality control including chip loading density, median read length and number of mapped reads. The Coverage Analysis plugin was applied to all data and used to assess amplicon coverage for regions of interest.

The Ion Reporter suite (Thermo Fisher Scientific, Waltham, MA, USA) was used to filter out known polymorphic variants. The variants were annotated by genetic databases: The Single Nucleotide Polymorphism Database (dbSNP) (http://www.ncbi.nlm.nih.gov/ projects/ SNP/), Catalogue of Somatic Mutations in Cancer (COSMIC) (http://cancer.sanger.ac.uk/cancergenome/projects/cosmic/) and ClinVar database (http://www.ncbi.nlm.nih.gov/clinvar/).Variants with altered allele depth ≤100 base coverage and a variant allelic frequency ≤5% were eliminated from the analysis. Identified variants were checked for correct nomenclature using Alamut Visual Plus (Interactive Biosoftware, Sophia Genetics). Any discrepancies in variant identification, between Ion Reporter and Alamut, were validated manually using the Integrative Genomics Viewer (Thorvaldsdóttir et al, 2013). Variants were annotated following ACGM guidelines (Richards et al, 2015) and the search engine VarSome.com (Kopanos et al, 2019).

3.7 Quantitative PCR gene expression analysis (Study 5)

Complementary DNA was transcribed from 10 ng of RNA using M-MLV Reverse Transcriptase (Invitrogen, Carlsbad, California), according to standard protocols, in a final volume of 20 µl with the following conditions: 25° C for 10 min, 50° C for 37 min, and 70° C for 15 min. Reaction without RNA was added as a negative control for excluding any likely contamination of the mix.

TaqMan gene expression assays (Applied Biosystems) were used according to the manufacturer's instructions for ACTB (Hs01060665_g1), ASCL1 (HS00269932_m1), CHGA (Hs00154441_m1), DLL3 (Hs01085096_m1), INSM1 (Hs00357871_s1),

NEUROD1 (Hs01922995_s1), NOTCH1 (Hs01062014_m1), MYCL1 (Hs00420495_m1), POU2F3 (Hs00205009_m1) and YAP1 (Hs00902712_g1).Expression levels for all genes studied and the internal reference gene (β-actin) were examined using a fluorescence based real-time detection method (ABI PRISM 7900 Sequence Detection System—TaqMan; Applied Biosystems, Foster City, CA). Each measurement was performed in duplicate.

3.8 miRNA PCR Array (Study 5)

For global miRNA profiling in study 5, six cases, each, of lung neuroendocrine tumors/carcinoids with elevated proliferative index, typical carcinoids and LCNEC were analyzed. 500 ng of total RNA were retro-transcribed from the 18 chosen samples using MiScript II RT Kit (Qiagen, MD, USA) in a final volume of 20 μL. In the reaction mix were present 4 μL of miScript HI spec 5X buffer, 2 μL of 10X miScript nucleics mix and 2 μL of Reverse Transcriptase mix. Cycling condition were 37°C for 1 hour and 5 minutes at 95°C. At each 20 uL of cDNA obtained were added 310 μL of RNase-free water. This mix was then divided in three aliquots of 110 μL. Each aliquot was used for one 384 plate (3 in total) where different miRNA arrays were present. miScript® miRNA PCR Array System, Human genome V16.0 Complete (SABiosciences, Qiagen company, MD, USA) was used for the simultaneous detection of 1152 different miRNAs in the same sample. The mix for the reaction was prepared as follow: 2050 μl of QuantiTect SYBR green PCR master mix, 410 μL miScript universal primer, 1540 μL of RNase free water and 100 μL of diluted cDNA. 10 μL of this mix was dispensed in each 384 wells containing the miRNA array. The RT-PCR was performed using ABI 7900HT instrument (Applied Biosystems, Life technologies group). Cycling conditions were 95°C for 15 minutes followed by 40 cycles at 94°C for 30 seconds and 55°C.

3.9 Gene and miRNA data evaluation (Study 5)

The relative gene expression levels were expressed as ratios (differences between the Ct values) between 2 absolute measurements (genes of interest/internal reference gene). The ΔΔCt values were calculated subtracting ΔCt values of sample and ΔCt value of a pool of

RNA derived from normal different tissues (kidney, stomach, larynx, thyroid) and converted to ratio by the following formula: $2^{-\Delta\Delta Ct}$. PCR Array data analysis was performed using the http:/pcrdataanalysis.sabiosciences.com/miRNA tool.

For both gene and microRNA expression, rows and columns were clustered using the hierarchal clustering tool in Morpheus (https://software.broadinstitute.org/morpheus/documentation.htm) using the one minus Pearson correlation matrix and the average linkage method. The log2 fold change values were z-score adjusted before clustering.

The biological impact of microRNA deregulated among the different groups was evaluated identifying the pathways impaired by those genes targeted by at least 5 microRNAs using the STRING database (https://string-db.org/).

Figures and Tables

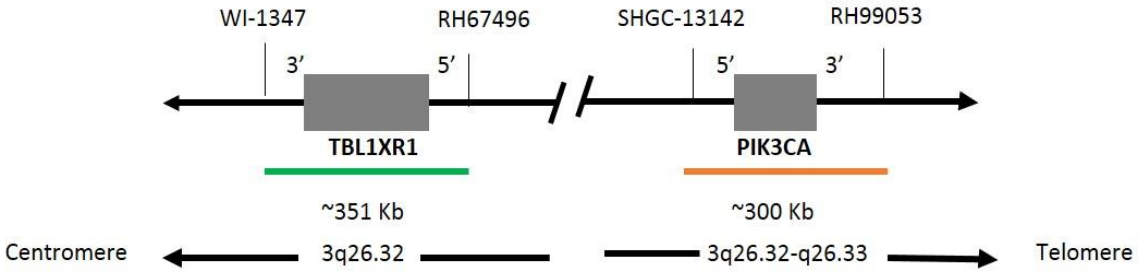

Figure 1: *TBL1XR1/PIK3CA* probe set, original.

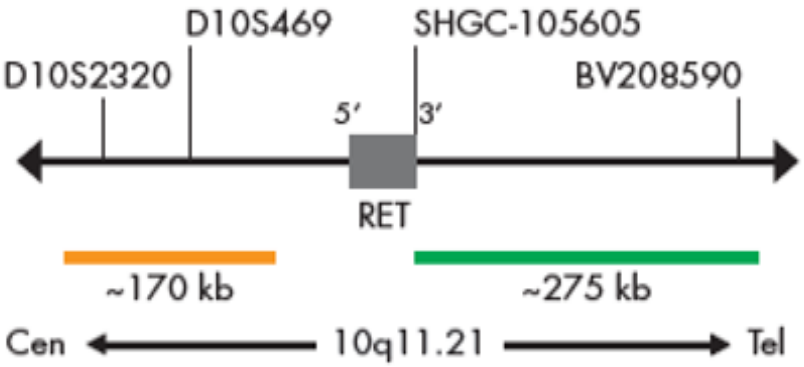

Figure 2: *RET* probe set, image from ZytoLight ® SPEC RET Dual Color Break Apart Probe.

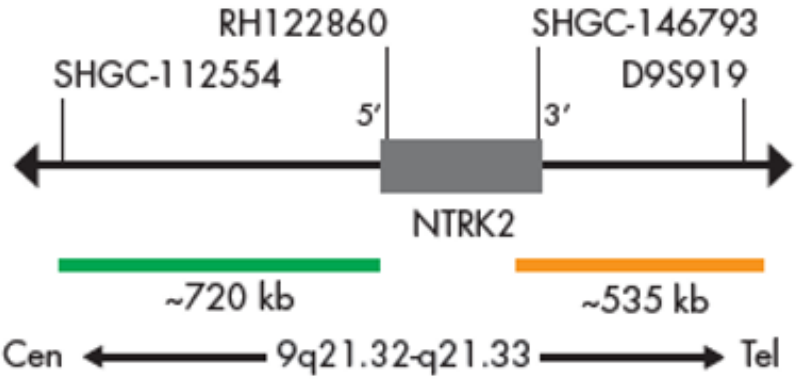

Figure 3: *NTRK2* probe set, image from ZytoLight ® SPEC NTRK2 Dual Color Break Apart Probe.

Oncomine Focus Assay	
Hotspot mutations	*AKT1, ALK, AR, BRAF, CDK4, CTNNB1, DDR2, EGFR, ERBB2, ERBB3, ERBB4, ESR1, FGFR2, FGFR3, GNA11, GNAQ, HRAS, IDH1, IDH2, JAK1, JAK2, JAK3, KIT, KRAS, MAP2K1, MAP2K2, MET, MTOR, NRAS, PDGFRA, PIK3CA, RAF1, RET, ROS1, SMO*
Copy number genes	*AKT1, ALK, AR, BRAF, CCND1, CDK4, CDK6, EGFR, ERBB2, FGFR1, FGFR2, FGFR3, FGFR4, KIT, KRAS, MET, MYC, MYCN, PDGFRA, PIK3CA*
Gene fusions	*ABL1, AKT3, ALK, AXL, BRAF, EGFR, ERBB2, ERG, ETV1, ETV4, ETV5, FGFR1, FGFR2, FGFR3, MET, NTRK1, NTRK2, NTRK3, PDGFRA, PPARG, RAF1, RET1, ROS1*

Table 1: List of all genes included in Oncomine Focus Panel

Oncomine Comprehensive Assay V3	
Hotspot mutations	*AKT1, AKT2, AKT3, ALK, AR, ARAF, AXL, BRAF, BTK, CBL, CCND1, CDK4, CDK6, CHEK2, CSF1R, CTNNB1, DDR2, EGFR, ERBB2, ERBB3, ERBB4, ERCC2, ESR1, EZH2, FGFR1, FGFR2, FGFR3, FGFR4, FLT3, FOXL2, GATA2, GNA11, GNAQ, GNAS, H3F3A, HIST1H3B, HNF1A, HRAS, IDH1, IDH2, JAK1, JAK2, JAK3, KDR, KIT, KNSTRN, KRAS, MAGOH, MAP2K1, MAP2K2, MAP2K4, MAPK1, MAX, MDM4, MED12, MET, MTOR, MYC, MYCN, MYD88, NFE2L2, NRAS, NTRK1, NTRK2, NTRK3, PDGFRA, PDGFRB, PIK3CB, PIK3CA,PPP2R1A, PTPN11, RAC1, RAF1, RET, RHEB, RHOA, ROS1, SF3B1, SMAD4, SMO, SPOP, SRC, STAT3, TERT, TOP1, U2AF1, XPO1.*
Full length genes	*ARID1A, ATM, ATR, ATRX, BAP1, BRCA1, BRCA2, CDK12, CDKN1B, CDKN2A, CDKN2B, CHEK1, CREBBP, FANCA, FANCD2, FANCI, FBXW7, MLH1, MRE11, MSH6, MSH2, NBN, NF1, NF2, NOTCH1, NOTCH2, NOTCH3, PALB2, PIK3R1, PMS2, POLE, PTCH1, PTEN, RAD50, RAD51, RAD51B, RAD51C, RAD51D, RNF43, RB1, SETD2, SLX4, SMARCA4, SMARCB1, STK11, TP53, TSC1, TSC2.*
Copy number genes	*AKT1, AKT2, AKT3, ALK, AXL, AR, BRAF, CCND1, CCND2, CCND3, CCNE1, CDK2, CDK4, CDK6, EGFR, ERBB2, ESR1, FGF19, FGF3, FGFR1, FGFR2, FGFR3, FGFR4, FLT3, IGF1R, KIT, KRAS, MDM2, MDM4, MET, MYC, MYCL, MYCN, NTRK1, NTRK2, NTRK3, PDGFRA, PDGFRB, PIK3CB, PIK3CA, PPARG, RICTOR, TERT.*
Gene fusions	*AKT2, ALK, AR, AXL, BRCA1, BRCA2, BRAF, CDKN2A, EGFR, ERBB2, ERBB4, ERG, ESR1, ETV1, ETV4, ETV5, FGFR1, FGFR2, FGFR3, FGR, FLT3, JAK2, KRAS, MDM4, MET, MYB, MYBL1, NF1, NOTCH1, NOTCH4, NRG1, NTRK1, NTRK2, NTRK3, NUTM1, PDGFRA, PDGFRB, PIK3CA, PRKACA, PRKACB, PTEN, PPARG, RAD51B, RAF1, RB1, RELA, RET, ROS1, RSPO2, RSPO3, TERT.*

Table 2: List of all genes included in Oncomine Comprehensive assay V3

Oncomine Comprehensive Assay PLUS	
CNV gains and Hotspot genes	*ABCB1, ABL2,ACVR1*,AKT1,AKT2,AKT3,ALK,AR,ARAF,ATP1A1*,AURKA, AURKC,AXL,BCL2,BCL2L12,BCL6,BCR*,BMP5*,BRAF,BTK*,CACNA1D*,CARD11,CBL,CCN D1,CCND2,CCND3,CCNE1,CD79B*,CDK4,CDK6,CHD4,CSF1R*,CTNNB1*, CTNND2,CUL1*,CYSLTR2*,DDR1,DDR2,DGCR8*,DROSHA*,E2F1*,EGFR,EIF1AX, EMSY,EPAS1*,ERBB2,ERBB3,ERBB4,ES1,EZH2,FAM135B,FGF19,FGF23,FGF3,FGF4, FGF7*,FGF9,FGFR1,FGFR2,FGFR3,FGFR4,FLT3,FLT4,FOXA1,FOXL2*,FOXO1*,FYN,GATA 2,GLI1*,GLI3,GNA11*,GNAQ*,GNAS,H1-4*,H2BC5*,H3-3A, H3-3B, H3C2* ,HIF1A* ,HRAS, IDH1*, IDH2,IGF1R, IKBKB, IL6ST*, IL7R, IRF4*, IRS4*, KDR, KIT, KLF4*, KLF5,KNSTRN*,KRAS,MAGOH, MAP2K1, MAP2K2*, MAPK1, MAX, MCL1, MDM2, MDM4,MECOM,MED12*,MEF2B, MET, MITF, MPL, MTOR, MYC, MYCL, MYCN,MYD88,MYOD1*,NFE2L2,NRAS,NSD2*,NT5C2*,NTRK1,NTRK2,NTRK3,NUP93*,PAX5 *,PCBP1,PDGFRA,PDGFRB,PIK3C2B,PIK3CA,PIK3CB,PIK3CD*,PIK3CG*,PIK3R2,PIM1,PL CG1,PPP2R1A,PPP6C, PRKACA, PTPN11, PTPRD*, PXDNL, RAC1, RAF1, RARA, RET,RGS7*,RHEB,RHOA*, RICTOR, RIT1, ROS1, RPL10*, RPS6KB1,RPTOR,SETBP1,SF3B1,SIX1*,SIX2*,SLCO1B3,SMC1A,SMO,SNCAIP*,SOS1*, SOX2*,SPOP,SRC,SRSF2*,STAT3,STAT5B,STAT6,TAF1,TERT,TGFBR1*,TOP1,TPMT, TRRAP*,TSHR*,U2AF1,USP8,WAS*,XPO1, YAP1,YES1,ZNF217,ZNF429.*
TMB only genes	*A1CF,ACSM2B,ADAM18,ANO4,ARMC4,AURKB,BRINP3,C6,C8A,C8B,CANX,CASR, CD163,CNTN6,CNTNAP4,CNTNAP5,COL11A1,DCAF4L2,DCDC1,GALNT17,GPR158, GRID2,HCN1,HLA-C,KCND2,KCNH7,KCNJ5,KEL,KIR3DL1,KRTAP21-1,KRTAP6-2, LRRC7,MARCO,NLRC5,NOL4,NRXN1,NYAP2,OR10G8,OR2G6,OR2L13,OR2L2,OR2L8, OR2M3,OR2T3,OR2T33,OR2T4,OR2W3,OR4A15,OR4C15,OR4C6,OR4M1,OR4M2, OR5D18,OR5F1,OR5L1,OR5L2,OR6F1,OR8H2,OR8I2,OR8U1,ORC4,PAK5,PCDH17, PDE1A, PDE1C,PLXDC2,POM121L12,PPFIA2,RBP3,REG1A,REG1B,REG3A,REG3G, RPTN, RUNDC3B,SH3RF2,SLC15A2,SLC8A1,SYT10,SYT16,TAPBP,TOP2A,TPTE, TRHDE, TRIM48,TRIM51,ZIM3,ZNF479,ZNF536.*
CDS genes	*ACVR1B,ACVR2A,ADAMTS12,ADAMTS2,AMER1,APC,ARHGAP35,ARID1A,ARID1B, ARID2,ARID5B,ASXL1,ASXL2,ATM♮,ATR,ATRX,AXIN1,AXIN2,B2M,BAP1,BARD1♮, BCOR,BLM,BMPR2,BRCA1♮,BRCA2♮,BRIP1♮,CALR*,CASP8,CBFB,CD274,CD276,CDC73,CDH 1,CDH10,CDK12♮,CDKN1A,CDKN1B,CDKN2A,CDKN2B,CDKN2C,CHEK1♮, CHEK2♮,CIC,CIITA*,CREBBP,CSMD3,CTCF,CTLA4,CUL3,CUL4A,CUL4B,CYLD, CYP2C9,CYP2D6*,DAXX,DICER1,DNMT3A,DOCK3,DPYD,DSC1,DSC3,ELF3,ENO1, EP300,EPCAM,EPHA2,ERAP1,ERAP2,ERCC2,ERCC4,ERCC5*,ERRFI1,ETV6,FANCA, FANCC,FANCD2,FANCE,FANCF,FANCG,FANCI,FANCL♮,FANCM,FAS*,FAT1,FBXW7, FUBP1,GATA3,GNA13,GPS2,HDAC2,HDAC9,HLA-A,HLA-B,HNF1A,ID3*,INPP4B, JAK1,JAK2,JAK3,KDM5C,KDM6A,KEAP1,KLHL13*,KMT2A,KMT2B,KMT2C, KMT2D,LARP4B,LATS1,LATS2,MAP2K4,MAP2K7,MAP3K1,MAP3K4,MAPK8,MEN1, MGA,MLH1,MLH3,MRE11,MSH2,MSH3,MSH6,MTAP,MTUS2*,MUTYH,NBN,NCOR1, NF1,NF2,NOTCH1,NOTCH2,NOTCH3,NOTCH4,PALB2♮,PARP1,PARP2,PARP3,PARP4, PBRM1,PDCD1,PDCD1LG2,PDIA3,PGD,PHF6,PIK3R1,PMS1,PMS2,POLD1,POLE, POT1,PPM1D,PPP2R2A,PRDM1,PRDM9,PRKAR1A,PSMB10*,PSMB8*,PSMB9*,PTCH1,PTEN ,PTPRT,RAD50,RAD51,RAD51B♮,RAD51C♮,RAD51D♮,RAD52,RAD54L♮,RASA1, RASA2,RB1,RBM10,RECQL4,RNASEH2A,RNASEH2B,RNASEH2C,RNF43,RPA1,RPL22*, RPL5*,RUNX1,RUNX1T1,SDHA,SDHB,SDHC,SDHD,SETD2,SLX4,SMAD2,SMAD4, SMARCA4,SMARCB1,SOCS1,SOX9,SPEN,STAG2,STAT1,STK11,SUFU,TAP1,TAP2, TBX3,TCF7L2,TET2,TGFBR2,TMEM132D*,TNFAIP3,TNFRSF14,TP53,TP63,TPP2,TSC1,TSC2, UGT1A1*,USP9X,VHL,WT1,XRCC2,XRCC3,ZBTB20*,ZFHX3,ZMYM3,ZRSR2.*

Table 3: List of all genes included in Oncomine Comprehensive assay PLUS (*CNV is not reported, ♮ Homologous recombination repair genes enabled for gene-level LOH).

Score name	Website	Basis	Score	Classification
Align GVGD	(http://agvgd.hci.utah.edu/agvgd_input.php)	Protein structure/function and evolutionary conservation	GVGD= Class C0, C15, C25, C35, C45, C55, or C65	C65: most likely C0: less likely.
DANN	(https://varsome.com)	Contrast annotations of fixed/nearly fixed derived alleles in humans with simulated variants	0.01 - 0.99	near 1 = "damaging"
FATHMM-MKL	(https://fathmm.biocompute.org.uk)	Evolutionary Conservation	p-values range: 0 - 1	< 0.5= "benign" > 0.5= "deleterious"
Grantham	(https://ionreporter.thermofisher.com)	Evolutionary Conservation	0 - 215	0-50= "conservative" 51-100= "moderately conservative" 101-150= "moderately radical" ≥151 "radical"
LRT	(https://sites.google.com/site/jpopgen/dbNSFP)	Evolutionary Conservation	0 - 1	Tolerated Unkown Damaging
Meta-RNN	(http://www.liulab.science/metarnn.html)	Integrate information from 28 high-level annotation scores (16 functional prediction scores including SIFT, Polyphen2_HDIV, Polyphen2_HVAR, MutationAssessor, PROVEAN, VEST4, M-CAP, REVEL, MutPred, MVP, PrimateAI, DEOGEN2, CADD, fathmm-XF, Eigen and GenoCanyon, 8 conservation scores including GERP, phyloP100way_vertebrate, phyloP30way_mammalian, phyloP17way_primate, phastCons100way_vertebrate, phastCons30way_mammalian, phastCons17way_primate and SiPhy, and 4 allele frequency information from the 1000 Genomes Project, ExAC, gnomAD exome, and gnomAD genome) and produce an ensemble prediction	0 - 1	< 0.5 = "Toerated" > 0.5 = "Damaging"

		model with a deep recurrent neural network (RNN).		
Mutation Assessor	(http://mutationassessor.org/r3)	Evolutionary Conservation	- 5.2 to 6.5	"Damaging" (Score - Min)/(Max-Min)= ≤ 0.65 "Tolerated" (Score - Min)/(Max-Min)= > 0.65
Mutation Taster	(https://www.mutationtaster.org)	Protein structure/function and evolutionary conservation	0.0-2.15 (does not affect forecast)	"disease causing" "disease causing automatic" "polymorphism" "polymorphism automatic"
MutPred	(http://mutpred.mutdb.org)	Evolutionary Conservation	0-1	≥ 0.5 "Damaging" < 0.5 "Benign"
Polyphen 2	(https://ionreporter.thermofisher.com)	Evolutionary Conservation/ protein structure/function	Two models: HumDiv: 0.00 - 1 HumVar: 0.00 - 1	0.0 - 0.15= "benign" 0.15 - 0.85= "possibily damaging" 0.85 - 1.0= "probably damaging"
Provean	(http://provean.jcvi.org)	Evolutionary conservation/Allignment and mesurement of similarity between variant sequence and protein sequence homolog	-40 -12.5 (threshold: -2.5)	≥ -2.5= "Deleterious" ≤ -2.5= "Neutral"
REVEL	(https://labworm.com/tool/revel)	Ensemble method for predicting the pathogenicity of missense variants based on a combination of scores from 13 individual tools: MutPred, FATHMM v2.3, VEST 3.0, PolyPhen-2, SIFT, PROVEAN, MutationAssessor, MutationTaster, LRT, GERP++, SiPhy, phyloP, and phastCons	From 0 to 1	≥ 0.5= "Deleterious" ≤ 0.5= "Neutral"
SIFT	(https://sift.bii.a-star.edu.sg)	Evolutionary Conservation	0.00 - 1	< 0.05= "Damaging" > 0.05= "Tolerated"

Table 4: List and characteristics of the different bioinformatic tools used for variant classification.

References

Choi Y, Chan AP. PROVEAN web server: a tool to predict the functional effect of amino acid substitutions and indels. Bioinformatics. 2015 Aug 15;31(16):2745-7.

Felsenstein J. Evolutionary trees from DNA sequences: a maximum likelihood approach. J Mol Evol. 1981;17(6):368-76.

Grantham R. Amino acid difference formula to help explain protein evolution. Science. 1974 Sep 6;185(4154):862.

Ioannidis NM, Rothstein JH, Pejaver V, Middha S, McDonnell SK, Baheti S, Musolf A, Li Q, Holzinger E, Karyadi D, Cannon-Albright LA, Teerlink CC, Stanford JL, Isaacs WB, Xu J, Cooney KA, Lange EM, Schleutker J, Carpten JD, Powell IJ, Cussenot O, Cancel-Tassin G, Giles GG, MacInnis RJ, Maier C, Hsieh CL, Wiklund F, Catalona WJ, Foulkes WD, Mandal D, Eeles RA, Kote-Jarai Z, Bustamante CD, Schaid DJ, Hastie T, Ostrander EA, Bailey-Wilson JE, Radivojac P, Thibodeau SN, Whittemore AS, Sieh W. REVEL: An Ensemble Method for Predicting the Pathogenicity of Rare Missense Variants. Am J Hum Genet. 2016 Oct 6;99(4):877-885.

Kopanos C, Tsiolkas V, Kouris A, Chapple CE, Albarca Aguilera M, Meyer R, Massouras A. VarSome: the human genomic variant search engine. Bioinformatics. 2019 Jun 1;35(11):1978-1980.

Kumar P, Henikoff S, Ng PC. Predicting the effects of coding non-synonymous variants on protein function using the SIFT algorithm. Nat Protoc. 2009;4(7):1073-81.

Li C, Zhi D, Wang K, Liu X. MetaRNN: differentiating rare pathogenic and rare benign missense SNVs and InDels using deep learning. Genome Med. 2022 Oct 8;14(1):115.

Pejaver V, Urresti J, Lugo-Martinez J, Pagel KA, Lin GN, Nam HJ, Mort M, Cooper DN, Sebat J, Iakoucheva LM, Mooney SD, Radivojac P. Inferring the molecular and phenotypic impact of amino acid variants with MutPred2. Nat Commun. 2020 Nov 20;11(1):5918.

Quang D, Chen Y, Xie X. DANN: a deep learning approach for annotating the pathogenicity of genetic variants. Bioinformatics. 2015 Mar 1;31(5):761-3.

Richards S, Aziz N, Bale S, Bick D, Das S, Gastier-Foster J, Grody WW, Hegde M, Lyon E, Spector E, Voelkerding K, Rehm HL; ACMG Laboratory Quality Assurance Committee. Standards and guidelines for the interpretation of sequence variants: a joint consensus recommendation of the American College of Medical Genetics and Genomics and the Association for Molecular Pathology. Genet Med. 2015 May;17(5):405-24.

Schwarz JM, Rödelsperger C, Schuelke M, Seelow D. MutationTaster evaluates disease-causing potential of sequence alterations. Nat Methods. 2010 Aug;7(8):575-6.

Tavtigian SV, Deffenbaugh AM, Yin L, Judkins T, Scholl T, Samollow PB, de Silva D, Zharkikh A, Thomas A. Comprehensive statistical study of 452 BRCA1 missense substitutions with classification of eight recurrent substitutions as neutral. J Med Genet. 2006 Apr;43(4):295-305.

Thorvaldsdóttir H, Robinson JT, Mesirov JP. Integrative Genomics Viewer (IGV): high-performance genomics data visualization and exploration. Brief Bioinform. 2013 Mar;14(2):178-92.

Ticha I, Hojny J, Michalkova R, Kodet O, Krkavcova E, Hajkova N, Nemejcova K, Bartu M, Jaksa R, Dura M, Kanwal M, Martinikova AS, Macurek L, Zemankova P, Kleibl Z, Dundr P. A comprehensive evaluation of pathogenic mutations in primary cutaneous melanomas, including the identification of novel loss-of-function variants. Sci Rep. 2019 Nov 19;9(1):17050.

4.0 ADRENOCORTICAL CARCINOMA

<u>Study 1:</u> Deep molecular analysis of matched samples of adrenocortical neoplasms with coexisting benign and malignant tumor components

Vanessa Zambelli[1], Giulia Orlando[2], Susanna Cappia[1], Giulia Vocino Trucco[3], Eleonora Duregon[2], Giulia Capella[2], Mauro Papotti[2], Marco Volante[1]

[1]Department of Oncology, University of Turin, San Luigi Hospital, Orbassano, Turin, Italy

[2]Department of Oncology, University of Turin, Città della Salute e della Scienza Hospital, Turin, Italy

[3]Department of Medical Sciences, University of Turin, Città della Salute e della Scienza Hospital, Turin, Italy

[4]Pathology Unit, San Luigi Hospital, Orbassano, Turin, Italy

[5]Pathology Unit, Mauriziano Hospital, Turin, Italy

[6]Pathology Unit, Reggio Emilia Hospital, Reggio Emilia, Italy

(paper status: manuscript in preparation)

<u>Study 2:</u> Pathological and molecular characteristics of adrenocortical carcinomas with mismatch repair deficiency

Vanessa Zambelli[1], Giulia Vocino Trucco[2], Ida Rapa[3], Lorenzo Daniele[4], Mauro Papotti[5], Alfredo Berruti[6], Massimo Terzolo[7], Marco Volante[1]

[1]Department of Oncology, University of Turin, San Luigi Hospital, Orbassano, Turin, Italy

[2]Department of Medical Sciences, University of Turin, Città della Salute e della Scienza Hospital, Turin, Italy

[3]Pathology Unit, San Luigi Hospital, Orbassano, Turin, Italy

[4]Pathology Unit, Mauriziano Hospital, Turin, Italy

[5]Department of Oncology, University of Turin, Città della Salute e della Scienza Hospital, Turin, Italy

[6]Medical Oncology Unit, Department of Medical and Surgical Specialties, Radiological Sciences and Public Health, University of Brescia, Brescia, Italy

[7]Department of Clinical and Biological Sciences, University of Turin, San Luigi Hospital, Orbassano, Turin, Italy

(paper status: submitted)

Adrenal tumors are very common, affecting 3% to 10% of human population, and the majority are small benign nonfunctional adrenocortical adenomas (ACA) (Mansmann et al, 2014). Adrenocortical Carcinoma (ACC), in contrast, is a very rare disease as defined by the National Institutes of Health Office of Rare Diseases Research, with a prevalence of fewer than 200000 patients in the United States (Viani et al, 2009). In adults the majority of ACC are found in the female gender (Luton et al, 1990), and the median age of diagnosis is in the fifth to the sixth decade, with the German ACC Registry recommending a median age of 46 years at diagnosis (Fassnacht et al, 2009).

ACCs have a varied presentation in adults: 40-60% of patients present with signs and symptoms of adrenal steroid hormone excess. Pediatric ACCs are generally rare and can be a part of familiar cancer syndromes (Kim et al, 2023). Hormone hypersecretion, apart from being responsible for heterogeneous clinical presentations, has been also associated with outcome, being cortisol secretion a predictor of poor prognosis (Ikeya et al, 2020). Patients that do not present hormonal excess have abdominal mass effect or are discovered incidentally through imaging for unrelated medical conditions (Fassnacht et al, 2009; Else et al, 2014). In children, 90% of cases arise from hormonal excess (Michalkiewicz et al, 2004).

Pathological diagnosis is based on the application of scoring systems and/or diagnostic algorithms. The Weiss score has widely been used since its introduction in 1984 to diagnose ACC (Weiss, 1984). It consists of nine histopathological parameters relating to tumor invasion, tumor cell properties, tumor structure and mitotic rate to predict the malignant potential of the tumor (Pittaway et al, 2019). Subsequently, it has been modified into the Weiss Revised Index, that consist of five parameters with a greater weight on mitotic rate and tumor cell type (Aubert et al.,2002). Since both are difficult to apply and are affected by low reproducibility, other scores/systems have been developed. Among them, the one gaining major interest is the Helsinki Score, that in addition to mitotic index and necrosis includes the use of Ki-67 proliferation index (Pennanen et al, 2015). Ki-67 index *per se* has been suggested to help to refine the diagnosis and prognosis of ACC (Ikeya et al, 2020). In fact, a Ki-67 index ≥5% has been proposed some years ago to differentiate ACC from ACA (Schmitt et al, 2006). Moreover, Ki-67 index is considered a prognostic marker, as it has been suggesting that patients with a Ki-67 index >10% have a high risk of recurrence (Fassnacht et al, 2018).

Most ACCs are sporadic, but up to 10% of cases can be associated with a hereditary cancer syndrome (HCS) (Hofstedter et al, 2023).

The most frequent are:

- Li Fraumeni syndrome (LFS), that develops childhood ACC, because of germline *TP53* gene mutations; in LFS approximately 3% to 10% of LFS-associated cancers are ACC, and 50% to 80% of ACC cases in children are in the context of LFS (Li et al,1988; Bouregard et al, 2008; Rodriguez-Galindo et al, 2005; Wagner et al, 1994; Valrey et al, 1999);
- Beckwith-Wiedemann syndrome (BWS) spectrum disorders, that can increase the risk of ACC (Else et al, 2014); this syndrome consists genetically of alteration of DNA methylation of the 11p15 locus where the coding region of *IGF2,* the cell cycle regulator *CDKN1C* and the non-translated RNA H19 are located (Weksberg et al, 2005);
- Multiple endocrine neoplasia type 1 (MEN1), that is caused by mutation in the *MEN1* gene on chromosome 11q13; its manifestations are hyperparathyroidism, foregut neuroendocrine tumors and pituitary adenomas. A fraction of MEN1 patients will develop adrenal lesions (20-50%), being 14% of these malignant (Skogseid et al, 2015; Waldmann et al, 2007; Gatta et al, 2012);
- Lynch syndrome (LS), caused by mutation of genes involved in DNA mismatch repair pathway, as *MSH2*, *MSH6*, *PMS2* and *MLH1*; patients with Lynch syndrome have an increased risk of developing cancer, in particular colorectal and endometrial cancer (Stoffel et al, 2019). The prevalence of Lynch syndrome in patients with ACC is around 3%, that is comparable to the prevalence in colon and endometrial cancer, which is estimated to be around 2 to 5 % (Raymond et al, 2013);

The number of therapeutic alternatives in ACC is very limited, and the only curative treatment is complete surgical rejection. More than 50% of patients, after 5 years, develop relapse of their disease (Glover et al, 2013), with a significant proportion of distant metastases (Bianchini et al, 2021).

The only drug that has been approved from the US Food and Drug Administration is mitotane, an inhibitor of steroidogenesis, both for treatment of cases at relapse after surgery and for palliation (Assié et al, 2007). However, given the rarity of ACC, randomized prospective trials evaluating adjuvant mitotane are nonexistent, and most retrospective studies are limited by small sample size and/or single-institution bias (Postlewait et al, 2016). Unfortunately, toxicities due to mitotane are common and

include lethargy, somnolence, vertigo, paresthesia, anorexia, nausea, vomiting, hormonal dysregulation, and skin changes (Williamson et al, 2000; Baudin et al, 2001).

In the presence of cases with an aggressive clinical course, the current standard practice recommendations support combination therapy regiments associating mitotane with chemotherapy agents such as etoposide, doxorubicin, and cisplatin (Bianchini et al, 2021; Postlewait et al, 2016). By contrast, target therapies in ACC are under clinical investigation but largely miss specific targets or biomarkers (Kenney et al, 2023).

Therefore, there has been an emerging interest on performing Next Generation Sequencing (NGS) on ACCs in order to detect genomic alteration that could be used to guide targeted therapies for the treatment of this rare disease (Ross et al,2014).

Main pathways involved in ACC cancerogenesis are the insulin growth factor 2 (IGF-2), the Wnt/ß-catenin and the p53/Rb pathways (Espiard et al, 2014).

TP53 gene mutations are associated with more aggressive tumors and with a poor outcome (Libè et al, 2007; Ragazzon et al, 2010; Hescot et al, 2022). In a recent study it has been shown that *TP53* is one of the most frequent genetic alterations in ACC, together with *BRD9*, *TERT*, *CTNNB1*, *CDK4*, *FLT4* and *MDM2* (Hescheler et al, 2022)

Wnt/ß-catenin pathway is relatively conservative in evolution, since it has important effects on ontogeny, cell differentiation, apoptosis, and necrosis (MacDonald et al, 2009). It is activated by ß-catenin that is coded by the *CTNNB1* gene. Mutations in *CTNNB1* gene can inactivate the Wnt/ß-catenin pathway, leading to a higher risk of developing adrenocortical tumors, both benign and malignant (Zhou et al, 2020).

The gene and protein overexpression of insulin-like growth factor (IGF) II is observed in the majority of ACC (Scicluna et al, 2022). The *IGF2* gene is located within 90 kb from the *H19* gene in chromosomal region 11p15.5 (Larsson et al, 2013). The *IGF2- H19* is subjected to parental imprinting, which is frequently lost in cancer by the loss of imprinting, leading to the overexpression of *IGF2/IGFII* (Ogawa et al, 1993; Weksberg et al, 1993).

Among other pathways involved in ACC pathogenesis, the Mismatch Repair (MMR) system attracted great attention in the last years due to possible clinical implications related to the possible use of immunotherapy. MMR is part of the DNA damage repair pathway, and germline mutations in MMR genes are responsible for cancer development (Lynch et al, 2009; Latham et al, 2019; Wang, 2016), causing hypermutability or

microsatellite instability (MSI). The presence of MSI using molecular tools and/or testing the expression of MMR proteins through immunohistochemistry (IHC) are generally used for Lynch syndrome screening in different cancer types (Carethers et al.,2015; Li et al.,2021; Olave et al.,2022). In ACC, MMR defects are poorly studies but recent data claim that a significant proportion of cases, up to about 14%, harbor mutations in MMR genes (Pozdeyev et al.,2021).

References

Assié G, Antoni G, Tissier F, Caillou B, Abiven G, Gicquel C, Leboulleux S, Travagli JP, Dromain C, Bertagna X, Bertherat J, Schlumberger M, Baudin E. Prognostic parameters of metastatic adrenocortical carcinoma. J Clin Endocrinol Metab. 2007 Jan;92(1):148-54.

Aubert S, Wacrenier A, Leroy X, Devos P, Carnaille B, Proye C, Wemeau JL, Lecomte-Houcke M, Leteurtre E. Weiss system revisited: a clinicopathologic and immunohistochemical study of 49 adrenocortical tumors. Am J Surg Pathol. 2002 Dec;26(12):1612-9.

Baudin E, Pellegriti G, Bonnay M, Penfornis A, Laplanche A, Vassal G, Schlumberger M. Impact of monitoring plasma 1,1-dichlorodiphenildichloroethane (o,p'DDD) levels on the treatment of patients with adrenocortical carcinoma. Cancer. 2001 Sep 15;92(6):1385-92.

Bianchini M, Puliani G, Chiefari A, Mormando M, Lauretta R, Appetecchia M. Metabolic and Endocrine Toxicities of Mitotane: A Systematic Review. Cancers (Basel). 2021 Oct 5;13(19):5001.

Bougeard G, Sesboüé R, Baert-Desurmont S, Vasseur S, Martin C, Tinat J, Brugières L, Chompret A, de Paillerets BB, Stoppa-Lyonnet D, Bonaïti-Pellié C, Frébourg T; French LFS working group. Molecular basis of the Li-Fraumeni syndrome: an update from the French LFS families. J Med Genet. 2008 Aug;45(8):535-8.

Carethers JM, Stoffel EM. Lynch syndrome and Lynch syndrome mimics: The growing complex landscape of hereditary colon cancer. World J Gastroenterol. 2015 Aug 21;21(31):9253-61.

Else T, Kim AC, Sabolch A, Raymond VM, Kandathil A, Caoili EM, Jolly S, Miller BS, Giordano TJ, Hammer GD. Adrenocortical carcinoma. Endocr Rev. 2014 Apr;35(2):282-326.

Espiard S, Bertherat J. The genetics of adrenocortical tumors. Endocrinol Metab Clin North Am. 2015 Jun;44(2):311-34.

Fassnacht M, Johanssen S, Quinkler M, Bucsky P, Willenberg HS, Beuschlein F, Terzolo M, Mueller HH, Hahner S, Allolio B; German Adrenocortical Carcinoma Registry Group; European Network for the Study of Adrenal Tumors. Limited prognostic value of the 2004 International Union Against Cancer staging classification for adrenocortical carcinoma: proposal for a Revised TNM Classification. Cancer. 2009 Jan 15;115(2):243-50.

Fassnacht M, Dekkers OM, Else T, Baudin E, Berruti A, de Krijger R, Haak HR, Mihai R, Assie G, Terzolo M. European Society of Endocrinology Clinical Practice Guidelines on the management of adrenocortical carcinoma in adults, in collaboration with the European Network for the Study of Adrenal Tumors. Eur J Endocrinol. 2018 Oct 1;179(4):G1-G46.

Fassnacht M, Allolio B. Clinical management of adrenocortical carcinoma. Best Pract Res Clin Endocrinol Metab. 2009 Apr;23(2):273-89.

Gatta-Cherifi B, Chabre O, Murat A, Niccoli P, Cardot-Bauters C, Rohmer V, Young J, Delemer B, Du Boullay H, Verger MF, Kuhn JM, Sadoul JL, Ruszniewski P, Beckers A, Monsaingeon M, Baudin E, Goudet P, Tabarin A. Adrenal involvement in MEN1. Analysis of 715 cases from the Groupe d'etude des Tumeurs Endocrines database. Eur J Endocrinol. 2012 Feb;166(2):269-79.

Glover AR, Ip JC, Zhao JT, Soon PS, Robinson BG, Sidhu SB. Current management options for recurrent adrenocortical carcinoma. Onco Targets Ther. 2013 Jun 6;6:635-43.

Hescheler DA, Hartmann MJM, Riemann B, Michel M, Bruns CJ, Alakus H, Chiapponi C. Targeted Therapy for Adrenocortical Carcinoma: A Genomic-Based Search for Available and Emerging Options. Cancers (Basel). 2022 May 31;14(11):2721.

Hescot S, Faron M, Kordahi M, Do Cao C, Naman A, Lamartina L, Hadoux J, Leboulleux S, Pattou F, Aubert S, Scoazec JY, Al Ghuzlan A, Baudin E. Screening for Prognostic Biomarkers in Metastatic Adrenocortical Carcinoma by Tissue Micro Arrays Analysis Identifies P53 as an Independent Prognostic Marker of Overall Survival. Cancers (Basel). 2022 Apr 29;14(9):2225.

Hofstedter R, Sanabria-Salas MC, Di Jiang M, Ezzat S, Mete O, Kim RH. FLCN-Driven Functional Adrenal Cortical Carcinoma with High Mitotic Tumor Grade: Extending the Endocrine Manifestations of Birt-Hogg-Dubé Syndrome. Endocr Pathol. 2023 Jun;34(2):257-264.

Ikeya A, Nakashima M, Yamashita M, Kakizawa K, Okawa Y, Saitsu H, Sasaki S, Sasano H, Suda T, Oki Y. CCNB2 and AURKA overexpression may cause atypical mitosis in Japanese cortisol-producing adrenocortical carcinoma with TP53 somatic variant. PLoS One. 2020 Apr 14;15(4):e0231665.

Kenney L, Hughes M. Adrenocortical Carcinoma: Role of Adjuvant and Neoadjuvant Therapy. Surg Oncol Clin N Am. 2023 Apr;32(2):279-287.

Kim JH, Choi Y, Hwang S, Yoon JH, Kim GH, Yoo HW, Choi JH. Clinical Characteristics and Long-Term Outcomes of Adrenal Tumors in Children and Adolescents. Exp Clin Endocrinol Diabetes. 2023 Oct;131(10):515-522.

Larsson C. Epigenetic aspects on therapy development for gastroenteropancreatic neuroendocrine tumors. Neuroendocrinology. 2013;97(1):19-25.

Latham A, Srinivasan P, Kemel Y, Shia J, Bandlamudi C, Mandelker D, Middha S, Hechtman J, Zehir A, Dubard-Gault M, Tran C, Stewart C, Sheehan M, Penson A, DeLair D, Yaeger R, Vijai J, Mukherjee S, Galle J, Dickson MA, Janjigian Y, O'Reilly EM, Segal

N, Saltz LB, Reidy-Lagunes D, Varghese AM, Bajorin D, Carlo MI, Cadoo K, Walsh MF, Weiser M, Aguilar JG, Klimstra DS, Diaz LA Jr, Baselga J, Zhang L, Ladanyi M, Hyman DM, Solit DB, Robson ME, Taylor BS, Offit K, Berger MF, Stadler ZK. Microsatellite Instability Is Associated With the Presence of Lynch Syndrome Pan-Cancer. J Clin Oncol. 2019 Feb 1;37(4):286-295.

Li FP, Fraumeni JF Jr, Mulvihill JJ, Blattner WA, Dreyfus MG, Tucker MA, Miller RW. A cancer family syndrome in twenty-four kindreds. Cancer Res. 1988 Sep 15;48(18):5358-62.

Li X, Liu G, Wu W. Recent advances in Lynch syndrome. Exp Hematol Oncol. 2021 Jun 12;10(1):37.

Libè R, Groussin L, Tissier F, Elie C, René-Corail F, Fratticci A, Jullian E, Beck-Peccoz P, Bertagna X, Gicquel C, Bertherat J. Somatic TP53 mutations are relatively rare among adrenocortical cancers with the frequent 17p13 loss of heterozygosity. Clin Cancer Res. 2007 Feb 1;13(3):844-50.

Luton JP, Cerdas S, Billaud L, Thomas G, Guilhaume B, Bertagna X, Laudat MH, Louvel A, Chapuis Y, Blondeau P, et al. Clinical features of adrenocortical carcinoma, prognostic factors, and the effect of mitotane therapy. N Engl J Med. 1990 Apr 26;322(17):1195-201.

Lynch HT, Lynch PM, Lanspa SJ, Snyder CL, Lynch JF, Boland CR. Review of the Lynch syndrome: history, molecular genetics, screening, differential diagnosis, and medicolegal ramifications. Clin Genet. 2009 Jul;76(1):1-18.

MacDonald BT, Tamai K, He X. Wnt/beta-catenin signaling: components, mechanisms, and diseases. Dev Cell. 2009 Jul;17(1):9-26.

Mansmann G, Lau J, Balk E, Rothberg M, Miyachi Y, Bornstein SR. The clinically inapparent adrenal mass: update in diagnosis and management. Endocr Rev. 2004 Apr;25(2):309-40.

Michalkiewicz E, Sandrini R, Figueiredo B, Miranda EC, Caran E, Oliveira-Filho AG, Marques R, Pianovski MA, Lacerda L, Cristofani LM, Jenkins J, Rodriguez-Galindo C,

Ribeiro RC. Clinical and outcome characteristics of children with adrenocortical tumors: a report from the International Pediatric Adrenocortical Tumor Registry. J Clin Oncol. 2004 Mar 1;22(5):838-45.

Ogawa O, Eccles MR, Szeto J, McNoe LA, Yun K, Maw MA, Smith PJ, Reeve AE. Relaxation of insulin-like growth factor II gene imprinting implicated in Wilms' tumour. Nature. 1993 Apr 22;362(6422):749-51.

Olave MC, Graham RP. Mismatch repair deficiency: The what, how and why it is important. Genes Chromosomes Cancer. 2022 Jun;61(6):314-321.

Pennanen M, Heiskanen I, Sane T, Remes S, Mustonen H, Haglund C, Arola J. Helsinki score-a novel model for prediction of metastases in adrenocortical carcinomas. Hum Pathol. 2015 Mar;46(3):404-10.

Pittaway JFH, Guasti L. Pathobiology and genetics of adrenocortical carcinoma. J Mol Endocrinol. 2019 Feb 1;62(2):R105-R119.

Postlewait LM, Ethun CG, Tran TB, Prescott JD, Pawlik TM, Wang TS, Glenn J, Hatzaras I, Shenoy R, Phay JE, Keplinger K, Fields RC, Jin LX, Weber SM, Salem A, Sicklick JK, Gad S, Yopp AC, Mansour JC, Duh QY, Seiser N, Solorzano CC, Kiernan CM, Votanopoulos KI, Levine EA, Staley CA, Poultsides GA, Maithel SK. Outcomes of Adjuvant Mitotane after Resection of Adrenocortical Carcinoma: A 13-Institution Study by the US Adrenocortical Carcinoma Group. J Am Coll Surg. 2016 Apr;222(4):480-90.

Pozdeyev N, Fishbein L, Gay LM, Sokol ES, Hartmaier R, Ross JS, Darabi S, Demeure MJ, Kar A, Foust LJ, Koc K, Bowles DW, Leong S, Wierman ME, Kiseljak-Vassiliades K. Targeted genomic analysis of 364 adrenocortical carcinomas. Endocr Relat Cancer. 2021 Aug 16;28(10):671-681.

Ragazzon B, Libé R, Gaujoux S, Assié G, Fratticci A, Launay P, Clauser E, Bertagna X, Tissier F, de Reyniès A, Bertherat J. Transcriptome analysis reveals that p53 and {beta}-catenin alterations occur in a group of aggressive adrenocortical cancers. Cancer Res. 2010 Nov 1;70(21):8276-81.

Raymond VM, Everett JN, Furtado LV, Gustafson SL, Jungbluth CR, Gruber SB, Hammer GD, Stoffel EM, Greenson JK, Giordano TJ, Else T. Adrenocortical carcinoma is a lynch syndrome-associated cancer. J Clin Oncol. 2013 Aug 20;31(24):3012-8.

Rodriguez-Galindo C, Figueiredo BC, Zambetti GP, Ribeiro RC. Biology, clinical characteristics, and management of adrenocortical tumors in children. Pediatr Blood Cancer. 2005 Sep;45(3):265-73.

Ross JS, Wang K, Rand JV, Gay L, Presta MJ, Sheehan CE, Ali SM, Elvin JA, Labrecque E, Hiemstra C, Buell J, Otto GA, Yelensky R, Lipson D, Morosini D, Chmielecki J, Miller VA, Stephens PJ. Next-generation sequencing of adrenocortical carcinoma reveals new routes to targeted therapies. J Clin Pathol. 2014 Nov;67(11):968-73.

Schmitt A, Saremaslani P, Schmid S, Rousson V, Montani M, Schmid DM, Heitz PU, Komminoth P, Perren A. IGFII and MIB1 immunohistochemistry is helpful for the differentiation of benign from malignant adrenocortical tumours. Histopathology. 2006 Sep;49(3):298-307.

Scicluna P, Caramuta S, Kjellin H, Xu C, Fröbom R, Akhtar M, Gao J, Shi H, Kjellman M, Almgren M, Höög A, Zedenius J, Ekström TJ, Bränström R, Lui WO, Larsson C. Altered expression of the *IGF2-H19* locus and mitochondrial respiratory complexes in adrenocortical carcinoma. Int J Oncol. 2022 Nov;61(5):140.

Skogseid B, Rastad J, Gobl A, Larsson C, Backlin K, Juhlin C, Akerström G, Oberg K. Adrenal lesion in multiple endocrine neoplasia type 1. Surgery. 1995 Dec;118(6):1077-82.

Stoffel E, Mukherjee B, Raymond VM, Tayob N, Kastrinos F, Sparr J, Wang F, Bandipalliam P, Syngal S, Gruber SB. Calculation of risk of colorectal and endometrial cancer among patients with Lynch syndrome. Gastroenterology. 2009 Nov;137(5):1621-7.

Varley JM, McGown G, Thorncroft M, James LA, Margison GP, Forster G, Evans DG, Harris M, Kelsey AM, Birch JM. Are there low-penetrance TP53 Alleles? evidence from childhood adrenocortical tumors. Am J Hum Genet. 1999 Oct;65(4):995-1006.

Viani GA, Stefano EJ, Afonso SL. Higher-than-conventional radiation doses in localized prostate cancer treatment: a meta-analysis of randomized, controlled trials. Int J Radiat Oncol Biol Phys. 2009 Aug 1;74(5):1405-18.

Wagner J, Portwine C, Rabin K, Leclerc JM, Narod SA, Malkin D. High frequency of germline p53 mutations in childhood adrenocortical cancer. J Natl Cancer Inst. 1994 Nov 16;86(22):1707-10.

Waldmann J, Bartsch DK, Kann PH, Fendrich V, Rothmund M, Langer P. Adrenal involvement in multiple endocrine neoplasia type 1: results of 7 years prospective screening. Langenbecks Arch Surg. 2007 Jul;392(4):437-43.

Wang Q. Cancer predisposition genes: molecular mechanisms and clinical impact on personalized cancer care: examples of Lynch and HBOC syndromes. Acta Pharmacol Sin. 2016 Feb;37(2):143-9.

Weiss LM. Comparative histologic study of 43 metastasizing and nonmetastasizing adrenocortical tumors. Am J Surg Pathol. 1984 Mar;8(3):163-9.

Weksberg R, Shen DR, Fei YL, Song QL, Squire J. Disruption of insulin-like growth factor 2 imprinting in Beckwith-Wiedemann syndrome. Nat Genet. 1993 Oct;5(2):143-50.

Weksberg R, Shuman C, Smith AC. Beckwith-Wiedemann syndrome. Am J Med Genet C Semin Med Genet. 2005 Aug 15;137C(1):12-23.

Williamson SK, Lew D, Miller GJ, Balcerzak SP, Baker LH, Crawford ED. Phase II evaluation of cisplatin and etoposide followed by mitotane at disease progression in patients with locally advanced or metastatic adrenocortical carcinoma: a Southwest Oncology Group Study. Cancer. 2000 Mar 1;88(5):1159-65.

Zhou T, Luo P, Wang L, Yang S, Qin S, Wei Z, Liu J. CTNNB1 Knockdown Inhibits Cell Proliferation and Aldosterone Secretion Through Inhibiting Wnt/β-Catenin Signaling in H295R Cells. Technol Cancer Res Treat. 2020 Jan-Dec;19:1533033820979685.

4.1 Study 1

Deep molecular analysis of matched samples of adrenocortical neoplasms with coexisting benign and malignant tumor components

Aim

To unveil mechanisms of progression from adrenal cortical adenoma to adrenal cortical carcinoma through deep molecular characterization of cases with coexistence of both a benign and a malignant component within the same lesion.

Methods

DNA extraction; Next Generation Sequencing, OCA Plus Assay.

Patients and tissue samples

From a large series of 418 samples of ACC collected at San Luigi Hospital, Orbassano, Turin, we selected 15 cases that were characterized by the coexistence of a morphologically recognizable benign/adenomatous component within the same lesion (4% of the series). All cases were re-assessed by a pathologist to confirm ACC diagnosis and evaluate adequacy of leftover FFPE material for molecular analyses. Seven cases met inclusion criteria for NGS testing. Match pairs of benign and malignant components were obtained by means of stereo-microscopically assisted manual microdissection (performed in all cases by the same pathologist) from serial sections.

Results

Pathological characteristics

The histological subtype of the 7 cases analyzed was conventional in four cases, oncocytic predominant in two and myxoid focal in one. Three cases were high and four were low grade according to the WHO 2022 classification. One representative case is illustrated in **Figure 1_1**.

Next generation sequencing analysis

The number of total gene mutations (including not only pathogenic mutation but also benign mutations and VUS mutations) that have been found is showed in **Figure 1_2** into Venn diagrams.

In most of the cases there is a slight increase in the number of mutations in the carcinoma component, although 1 case (S_1) displayed a higher number of mutations in the benign component.

Regarding pathogenic mutations, only, one sample was not informative due to the lack of pathogenetic alterations. The *TERT* promoter mutation c. -124 C>T occurred in two cases, both lacking pathogenetic variants in the benign component. Two other cases showed the presence of a single pathogenic mutation occurring in both the benign and the malignant component (*CTNNB1* and *FANCA*, respectively), with an additional co-mutation in *TP53* and *NF1*. Then, last two cases presented the same mutation profile adenoma and carcinoma components, one with *FANCD2* and *GNAS* co-mutations, and one with *NQO1* mutation.

Mismatch repair status was stable in all four cases that passed QC control in both tumor components (**Figure 1_3**).

Tumor mutational burden (TMB) was rather low, ranging from 0.95 to 6.65 in all samples. In most of the cases (71.4%), TMB was stable or increased in the carcinoma component, while in two cases TMB was higher in the adenoma component (**Figure 1_4**).

Loss of heterozygosity (LOH) analysis was assessable using the OCA Plus panel in 14 genes (the names of the genes are showed in **Figure 1_5**). Two out of 7 cases were not informative, not showing LOH in the adenoma or carcinoma component. Three cases showed either the presence of LOH exclusively in the malignant component or co-occurrence of LOH in both components with additional loci lost in the malignant sample. In the last two cases, the LOH profile was completely different between the two components: in case S_7, a higher number of LOH was observed in the adenoma component whereas in case S_1 both components were altered but none of the altered gene was in common between the two components (**Figure 1_5**).

Oncomine comprehensive assay PLUS detects copy number variations (CNV) and chromosomal arms alterations in terms of losses and gains. In the majority of cases (5/7 cases, 71.4%) there is an increasing number of CNV loss/gain and chromosomal arms loss/gain in the carcinoma component **(Figure 1_6)**. The other two cases had a completely discordant results, showing a high number of CNV and chromosomal arms loss/gain in both components.

Based on the overall agreement of molecular features in the tumor components, for each analysis (including pathogenic gene mutations, TMB, LOH and CNV/chromosomal arms) samples were coded as follows **(Figure 1_7)**:

a) monoclonal-homogeneous, when there was a predominant molecular overlapping between the two components;

b) monoclonal-heterogeneous, when a few molecular alterations were shared in the two components, but the malignant component was enriched for additional molecular alteration;

c) polyclonal, when molecular alterations were predominantly mutually exclusive between the two sample, thus molecularly unrelated.

As a summary of integrated molecular findings, most of the cases are in agreement with the hypothesis of a direct progression from adenoma to carcinoma, with 3 cases characterized by the acquisition of CNV alterations, one by *TERT promoter* mutation in association with CNVs, and one by *TP53* mutation and CNV. By contrast, two cases were more suggestive for a polyclonal origin due to a predominant heterogeneous, partly mutually exclusive, genotype.

Discussion

ACC with a benign associated component exist but have been very rarely described in the literature (Ranganathan et al, 2005). In a previous molecular study investigating both adrenocortical adenomas and carcinomas, it was shown that a high number of molecular alterations were present in benign and in malignant tumors, supporting a model of multi-step tumor progression (Ronchi et al, 2013). However, a molecular analysis of ACC cases with a coexistent benign component has not been conducted, so far.

Therefore, we retrieved from a very large collection of ACC samples a set of cases morphologically showing a combination of benign and malignant tumor components. The

fifteen cases recognized to have such features are indicative that this type of lesions is not extremely rare, but represents about 4% of ACC, at least in our series of cases.

The molecular analysis was limited to 7 cases due to the incomplete availability of leftover tumor tissue material and/or a suboptimal quality of the tissue that prevented an adequate quality of nucleic acids for the deep NGS testing planned in the study.

Genomic alterations were both exclusively identified in the ACC component or shared with the benign tumor tissue counterpart. Gene mutations exclusively detected in the ACC component were TERTp (2 cases), NF1 (one case) and TP53 (one case), thus showing that alterations in these genes are a hallmark of malignancy. Other mutations were all shared by both benign and malignant components and included mutations in genes involved in the b-catenin/Wnt pathway (CTNNB1, one case), the DNA repair mechanisms (FANCD2 and FANCA, one case, each), G-protein regulation (GNAS, one case) and cell cycle regulation (NQO1, one case). Most shared or malignant-specific mutations detected have been already described in ACC. TP53 mutations are among the most frequent in ACC (Assié et al, 2014; Hescheler et al, 2022). CTNNB1 and GNAS mutations are known to occur

in adrenocortical adenomas, also (Wu et al, 2022). Germline NF1 mutations are related to the onset of ACC in the context of neurofibromatosis type 1 syndrome (Minkiewicz et al, 2020), but in our case the NF1 mutation occurred in the ACC component only, thus demonstrating to occur as a somatic event. Interestingly, mutations in NQO1 gene have never been found in adrenocortical carcinoma, so far, but are described as pathogenetic event in other cancer types (Chao et al, 2006).

The analysis of microsatellite instability was not informative, both because of the high number of inadequate cases and the absence of cases showing an instable pattern.

TMB, as assessed by using the assay employed in this study, was also moderately informative due to a general low index, although the majority of cases showed a slight increase in the malignant as compared to the benign component. Although not directly comparable due to different methods of investigation, out data on low TMB are apparently different from recent data claiming a significant rate of cases with high TMB (Araujo-Castro et al, 2021), that was also correlated with worse clinical outcome (Luo et al, 2022). With all the limitations due to our small sample size and method of estimation, our data seem to suggest that ACC cases associated with a benign component harbor a low number of overall mutations as compared to “pure” ACC cases.

LOH analysis was limited in the NGS panel to a small number of genes, but was informative in 5 cases, with heterogeneous profiles. In three cases, some LOH were shared by the two components with additional LOH events in the malignant counterpart, whereas two other cases clearly showed mutually exclusive profiles. This overall picture was even more evident for CNV and chromosomal arms analysis. Also in this context, some cases showed almost mutually exclusive profiles in the two components. Therefore, at variance with genomic data related to mutational profiles that were supportive of a clonal multistep progression in all informative cases, LOH and CNV data were indicative, at least in some cases, of an unrelated clonal evolution even in cases where the two tumor components were closely intermingled.

In fact, an integrated overview of molecular data was supportive of the existence of cases following two different models of evolution:

a) 5 cases were consistent with a model of monoclonal evolution from the benign to the malignant component mediated by the acquisition of gene mutations (i.e. TERTp or TP53), or by the increased number of chromosomal alterations;

b) in 2 cases the benign and malignant components were molecularly unrelated, with special reference to CNV and LOH profiles, supporting a polyclonal evolution.

Figures

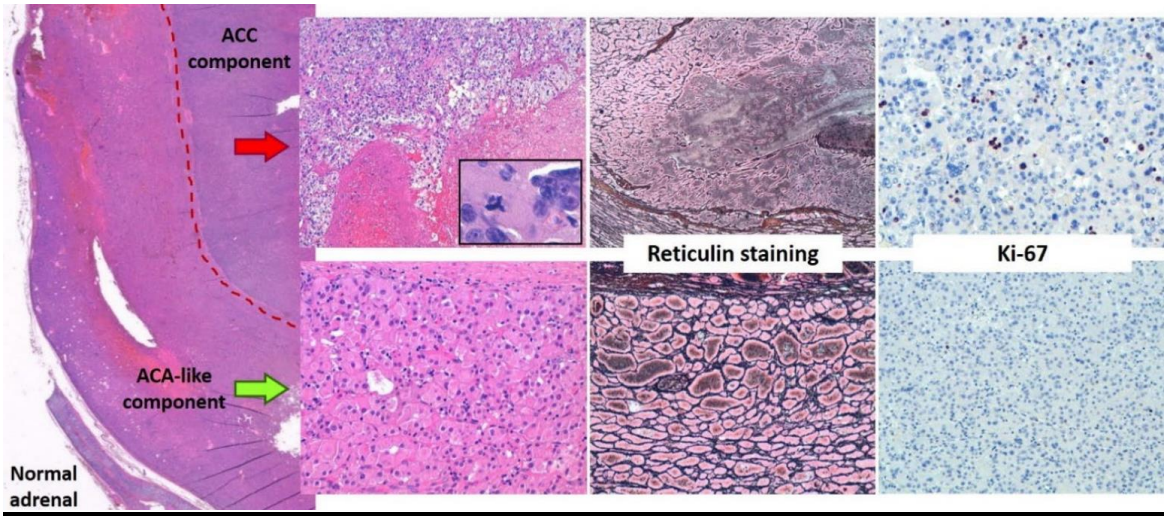

Figure 1_1: A case of ACC (upper panels, with atypia, necrosis, atypical mitotic figures, disrupted reticulin framework and moderate Ki-67 index) with abrupt transition from a predominant peripheral adenoma-like component (lower panels, with no or necrosis, low mitotic index with no atypical mitotic figures, intact reticulin framework and very low Ki-67 index). ACA: adrenocortical adenoma. ACC: adrenocortical carcinoma

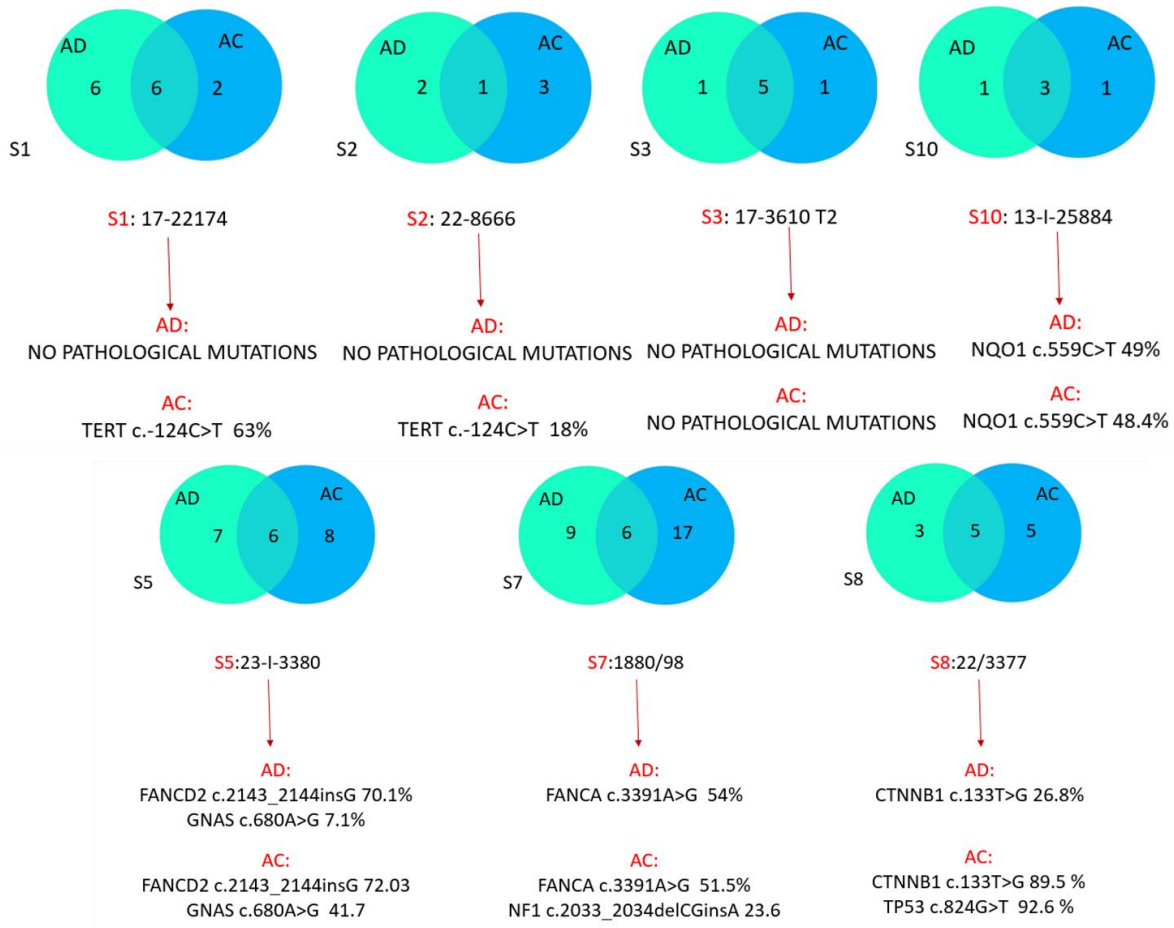

Figure 1_2: Venn diagrams showing number of gene mutations (including benign, VUS and pathogenic); list of pathogenic mutations related to each case.

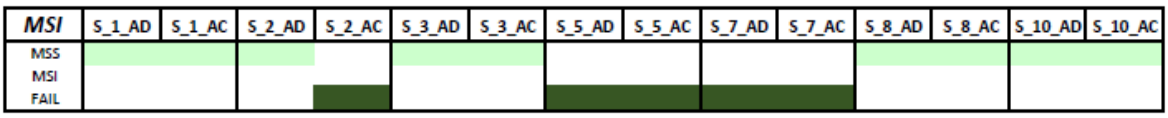

Figure 1_3: Microsatellite instability summary of cases. Fail is due to QC fail.

TMB	S_1_AD	S_1_AC	S_2_AD	S_2_AC	S_3_AD	S_3_AC	S_5_AD	S_5_AC	S_7_AD	S_7_AC	S_8_AD	S_8_AC	S_10_AD	S_10_AC
	2.84	1.89	0.95	0.95	2.84	3.79	2.85	2.85	6.65	3.81	2.85	4.75	0.95	0.95

Figure 1_4: Tumor mutational burden

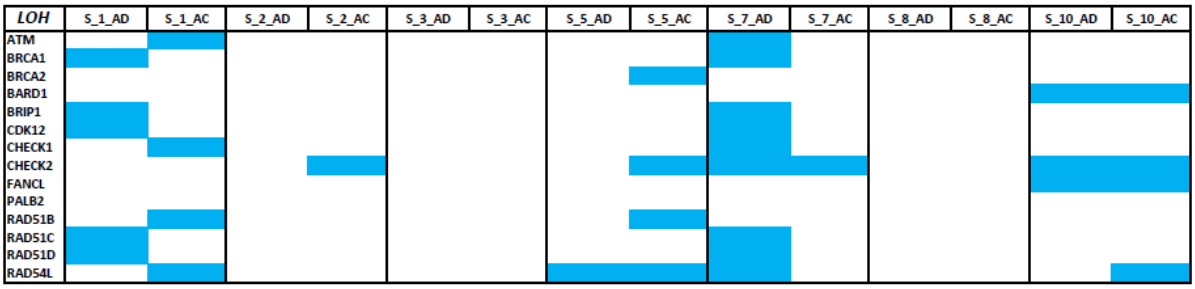

Figure 1_5: Loss of heterozygosity of the 14 genes analyzed by the assay.

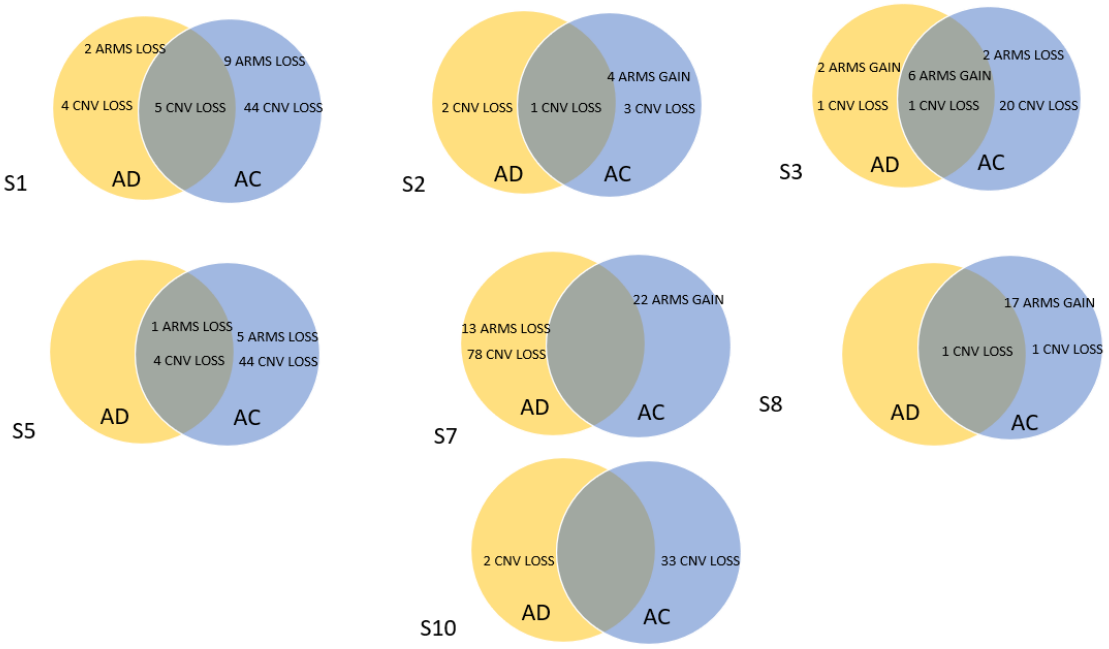

Figure 1_6: Number of copy number variation and arms loss/gain of all samples in both components.

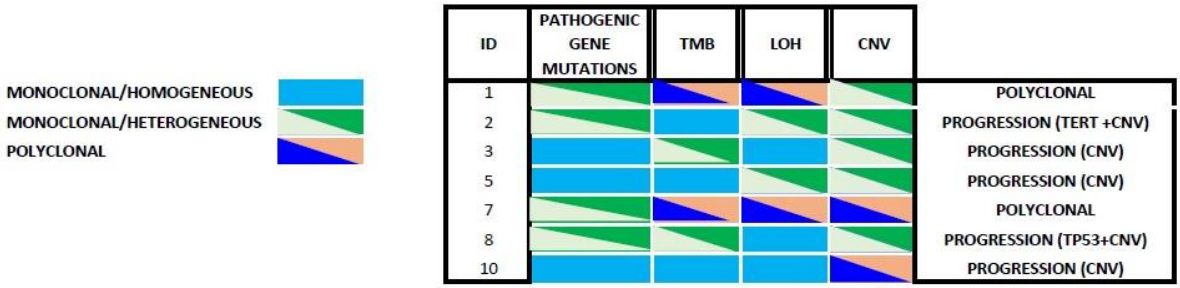

Figure 1_7: Summary of the results obtained from the different analyses.

References

Araujo-Castro M, Pascual-Corrales E, Molina-Cerrillo J, Alonso-Gordoa T. Immunotherapy in Adrenocortical Carcinoma: Predictors of Response, Efficacy, Safety, and Mechanisms of Resistance. Biomedicines. 2021 Mar 16;9(3):304.

Assié G, Letouzé E, Fassnacht M, Jouinot A, Luscap W, Barreau O, Omeiri H, Rodriguez S, Perlemoine K, René-Corail F, Elarouci N, Sbiera S, Kroiss M, Allolio B, Waldmann J, Quinkler M, Mannelli M, Mantero F, Papathomas T, De Krijger R, Tabarin A, Kerlan V, Baudin E, Tissier F, Dousset B, Groussin L, Amar L, Clauser E, Bertagna X, Ragazzon B, Beuschlein F, Libé R, de Reyniès A, Bertherat J. Integrated genomic characterization of adrenocortical carcinoma. Nat Genet. 2014 Jun;46(6):607-12.

Chao C, Zhang ZF, Berthiller J, Boffetta P, Hashibe M. NAD(P)H:quinone oxidoreductase 1 (NQO1) Pro187Ser polymorphism and the risk of lung, bladder, and colorectal cancers: a meta-analysis. Cancer Epidemiol Biomarkers Prev. 2006 May;15(5):979-87.

Hescheler DA, Hartmann MJM, Riemann B, Michel M, Bruns CJ, Alakus H, Chiapponi C. Targeted Therapy for Adrenocortical Carcinoma: A Genomic-Based Search for Available and
Emerging Options. Cancers (Basel). 2022 May 31;14(11):2721.

Kopanos C, Tsiolkas V, Kouris A, Chapple CE, Albarca Aguilera M, Meyer R, Massouras A. VarSome: the human genomic variant search engine. Bioinformatics. 2019 Jun 1;35(11):1978-1980.

Luo Y, Chen Q, Lin J. Identification and validation of a tumor mutation burden-related signature combined with immune microenvironment infiltration in adrenocortical carcinoma. Math Biosci Eng. 2022 May 12;19(7):7055-7075

Minkiewicz I, Wilbrandt-Szczepańska E, Jendrzejewski J, Sworczak K, Korwat A, Śledziński M. CO-OCCURRENCE OF ADRENOCORTICAL CARCINOMA AND GASTROINTESTINAL STROMAL TUMOR IN A PATIENT WITH NEUROFIBROMATOSIS TYPE 1 AND A HISTORY OF ENDOMETRIAL CANCER. Acta Endocrinol (Buchar). 2020 Jul-Sep;16(3):353-358.

Ranganathan S, Lynshue K, Hunt JL, Kane T, Jaffe R. Unusual adrenal cortical tumor of unknown biologic potential: a nodule in a nodule in a nodule. Pediatr Dev Pathol. 2005 Jul-Aug;8(4):483-8.

Ronchi CL, Sbiera S, Leich E, Henzel K, Rosenwald A, Allolio B, Fassnacht M. Single nucleotide polymorphism array profiling of adrenocortical tumors--evidence for an adenoma carcinoma sequence? PLoS One. 2013 Sep 16;8(9):e73959.

Wu WC, Peng KY, Lu JY, Chan CK, Wang CY, Tseng FY, Yang WS, Lin YH, Lin PC, Chen TC, Huang KH, Chueh JS, Wu VC. Cortisol-producing adenoma-related somatic mutations in unilateral primary aldosteronism with concurrent autonomous cortisol secretion: their prevalence and clinical characteristics. Eur J Endocrinol. 2022 Sep 14;187(4):519-530.

4.2 Study 2

Pathological and molecular characteristics of adrenocortical carcinomas with mismatch repair deficiency

Aim

The aim of this project was to investigate prevalence, clinical, pathological and molecular characteristics of MMR-deficient ACCs.

Methods

DNA extraction; immunohistochemistry (MMR proteins); microsatellite instability analysis; Next Generation Sequencing, OCA v3 assay.

Patients and tissue samples

From the same database used for study 1 including 418 samples of ACC collected at San Luigi Hospital, Orbassano, Turin, we randomly selected 120 cases based on availability of residual FFPE material adequate for all analyses planed in this study. All cases were re-assessed by a pathologist to confirm ACC diagnosis and to select the most representative tumor paraffin block. For molecular analyses, tumor cell enrichment was obtained by means of stereo-microscopically assisted manual microdissection (performed in all cases by the same pathologist) from serial sections.

Results

Prevalence of altered MMR protein expression

Out of the 120 ACCs tested, the majority (109/120, 91%) showed a preserved immunohistochemical expression of MMR proteins. By contrast, 11 out of 120 cases

(9.1%) showed an altered MMR protein expression profile. Among these cases, the most common alteration was the loss of MSH6, observed in 8 out of 11 cases (72%). This loss was either isolated (5 cases) or combined with the loss of MSH2 (3 cases). Conversely, the remaining cases showed an alteration in both MLH1 and PMS2 protein expression (3/11 cases, 27%) (**Figure 2_1**).

Association of MMR-deficient pattern with clinical and pathological characteristics

Main clinical and pathological characteristic of MMR-deficient cases were correlated with those lacking MMR alterations. Altered expression of MMR proteins was associated significantly with non-oncocytic histotype (p=0.03), and higher T stage (pT3-pT4 in 7/11, 64%; p=0.006). Moreover, MMR deficient cases were associated although with a borderline statistical significance with higher Weiss and Helsinki scores and Ki67 index. No associations were found with the other clinical and pathological factors (**Table 2_1**)

Concordance between loss of MMR protein expression and MSI status assessed by Real-time PCR and with DNA NGS analysis

ACC cases with altered MMR protein expression, were investigated at the molecular level to detect both the presence of microsatellite instability (MSI) and the occurrence of mutations in MMR genes.

For MSI analysis, we employed a Real-time PCR kit designed for MSI testing in colorectal and endometrial cancer. Interestingly, this analysis did not show a microsatellite unstable phenotype in any of the MMR-deficient case as assessed by immunohistochemistry (**Figure 2_2**).

Next-Generation sequencing (NGS) analysis detected overall 10 mutations in genes coding for MMR proteins. The genomic/phenotypic profile was concordant in 7/11 cases (64%) (**Figure 2_3**). In the discrepant cases, one case displayed MSH2 and MLH1 mutations with MSH6 protein loss, whereas in the remaining three cases (two with MSH2/MSH6 loss and one with MLH1/PMS2 loss), no mutations in mismatch repair gene were found.

Genomic characteristics of MMR deficient ACC

Subsequent molecular characterization of the MMR-deficient cases through DNA NGS analysis unveiled these cases to carry additional mutations (7 ± 4 mutations). Among these alterations, *TP53* mutations were the most common (82%), followed by mutations in genes related to chromatin remodeling, such as *ARID1A* (46%), *ATM* (36%), *SMARCA4* (36%),

and *ATRX* (27%). Importantly, every MMR-deficient case exhibited at least one mutation in the aforementioned chromatin remodeling genes. Additional frequent molecular alterations involved *NF1* (27%), *TSC2* (27%), *BAP1* (18%), *CTNNB1* (18%), *ERBB2* (18%), *MDM2* (18%), *NOTCH1* (18%), *PIK3R1* (18%), *RAD50* (18%), *RB1* (18%) (**Figure 2_4**).

Heterogeneity of MMR pattern and genotype in metachronous tumor samples of one case

Among the 11 MMR-deficient ACC cases, one case had altered protein pattern (MSH6 loss) in the sample corresponding to a local recurrence but not in the primary tumor sample. DNA NGS analysis showed that the primary lesion had a relatively limited number of mutations, primarily involving *TP53*, *CTNNB1* with a high allelic frequency. Moreover, a *NOTCH3* mutation was also detected but a very low frequency. Both *TP53* and *CTNNB1* mutations were retained in the recurrent MMR-deficient sample, that harbored a more complex genotype with several co-mutations with variable allelic frequencies (**Figure 2_5**).

Discussion

In the field of endocrine pathology, the relationship between the adreno-cortical carcinoma (ACC) and the MMR system has recently garnered increased attention. This heightened interest stems from several factors. Firstly, ACC has been reported to be potentially linked to the spectrum of MMR system-related disorders, but this aspect remains to be confirmed (Domènech et al, 2021; Mete et al, 2022). Secondly, there is a growing body of evidence suggesting that in certain endocrine malignancies the MMR status may serve as a significant prognostic indicator (Santos et al, 2018; Rocha et al, 2021; Wong et al, 2019; Teuber et al, 2021; Park et al, 2020). However, whether this could relate to ACC as well, including its potential utility in screening ACC patients for Lynch syndrome remains to be demonstrated (Domenech et al, 2021; Raymond et al, 2013). Lastly, the role of MMR status in determining the eligibility for immunotherapy in ACC remains to be validated, and this aspect is particularly relevant considering its potential clinical implications (Casey et al, 2018; Pozdeyev et al, 2021).

In this setting, this study makes a valuable contribution to better understanding ACC with MMR deficiency. In particular, it provides evidence of the association of MMR deficiency with unfavorable clinicopathological characteristics and highlights the presence of alternative pathways for MMR instability.

Adrenocortical carcinoma (ACC) is an exceptionally aggressive and rare malignancy, with an incidence of approximately 0.7-2 cases per million in the United States (Libè, 2019). Among these cases, the prevalence of MMR instability is reported to be low, varying from 3 to 13.7% (Else et al, 2014; Darabi et al, 2021; Pozdeyev et al, 2021), and with the most frequent alterations involving MSH2 (Domenech et al, 2021) or MLH1 (Brondani et al, 2020).

Similarly, in our series of surgically resected ACCs, only a minority (11 out of 120, or 9.1%) showed alterations in MMR protein expression, confirming both the presence as well as the rarity of this finding in ACC. Moreover, even though occasional alterations in MSH2 or MLH1 were reported, the loss of MSH6 was, by a significant margin, the most frequently observed alteration in our cohort, making this study the first to document such a finding.

Regarding clinical implications, our series clearly established a noteworthy connection between cases showing altered MMR protein expression and clinical characteristics that are typically associated with a more aggressive disease course. In particular, altered MMR protein expression was found to be significantly associated with a higher pathological T-stage (T3, T4). Additionally, while not quite reaching statistical significance, there was a trend indicating a positive association between MMR deficiency and elevated Weiss and Helsinki scores, as well as a high Ki-67 proliferation index. These findings gain particular significance when considered alongside recent evidence suggesting a link between MSH6 alterations in ACC and a worse prognosis (Chen et al, 2023).

The presence of MMR-deficient profile as assessed by immunohistochemistry was not associated with microsatellite instability using a commercial panel designed for colon and endometrial cancer. These results suggest that the profile of microsatellite instability is tumor and/or tissue specific and is influenced by the type of alteration affecting the MMR pathway. As an example, recently MSH6 loss has been associated even in endometrial cancer with a low sensitivity of PCR-based panels used to identify the presence of microsatellite instability (Adachi et al, 2023).

Genomic data in MMR-deficient cases were also contributing to the characterization of these cases. First, in 4 cases the immunohistochemical results were not correlated with the presence of mutations in MMR genes. This observation claimed that non genomic regulation but rather epigenetic mechanisms (such as methylation) might be responsible for a MMR-deficient phenotype, at least in a subset of cases. The single case in which we could compare primary tumor and tumor tissue sample related to a metachronous recurrence is strongly supportive of this scenario. In fact, whereas the primary tumor was MMR-proficient, the tumor at recurrence was MMR-deficient due to MSH6 protein loss. The IHC profile was non associated with significant mutations in MMR genes, if not for mutations in MSH2 and MLH1 with a very low allelic frequency, and probably arising as a consequence of defective DNA repair mechanisms. Moreover, MMR-deficient cases had peculiar co-occurring gene mutations that are different to what expected by overall data available in ACC. In particular, a very high frequency of TP53 mutations was observed (more than 80%) as compared to the 20% expected (Ragazzon et al, 2010). Finally, mutations in chromatin-remodeling gens were highly prevalent, with almost all cases of MMR-deficient ACC harboring at least one mutation in genes belonging to this pathway.

Figures and Tables

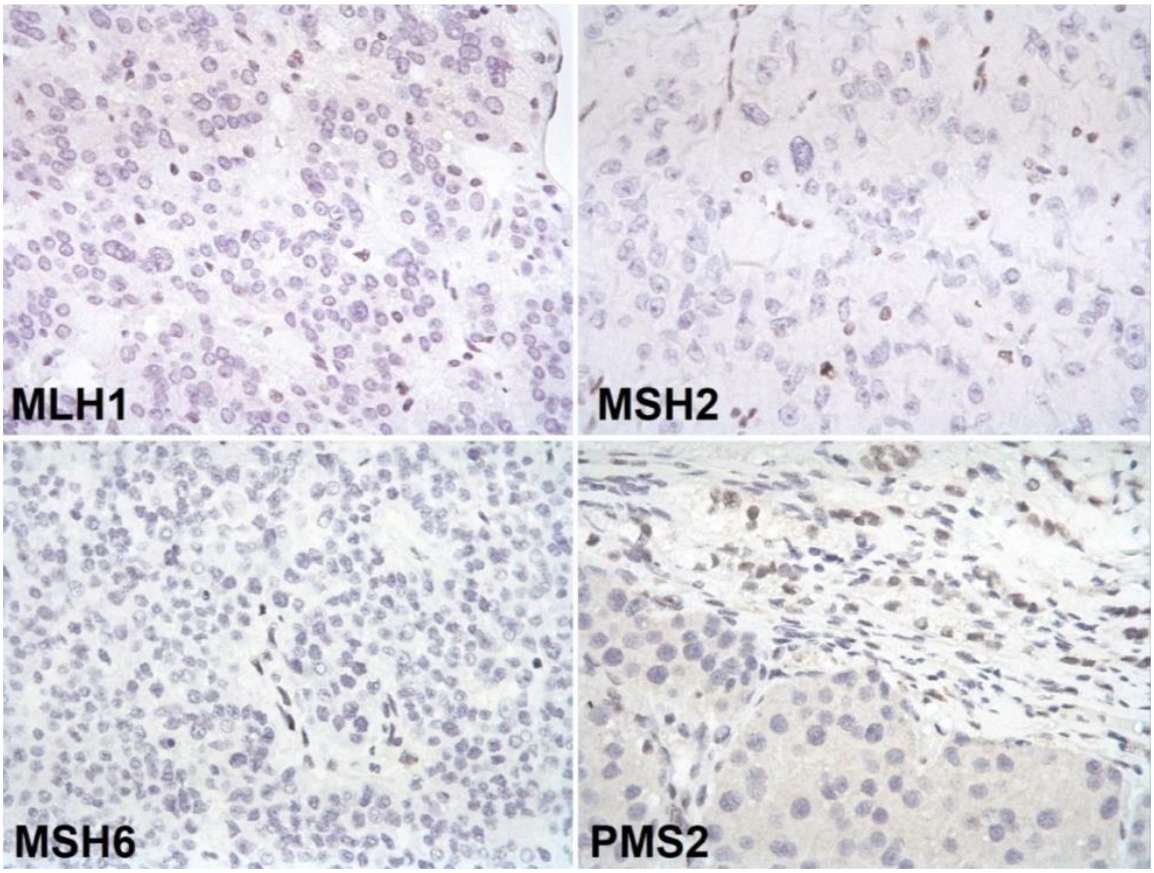

Figure 2_1: Patterns of loss of nuclear expression of MMR proteins in ACC. Endothelial or peritumoral cortical cells served as positive internal controls.

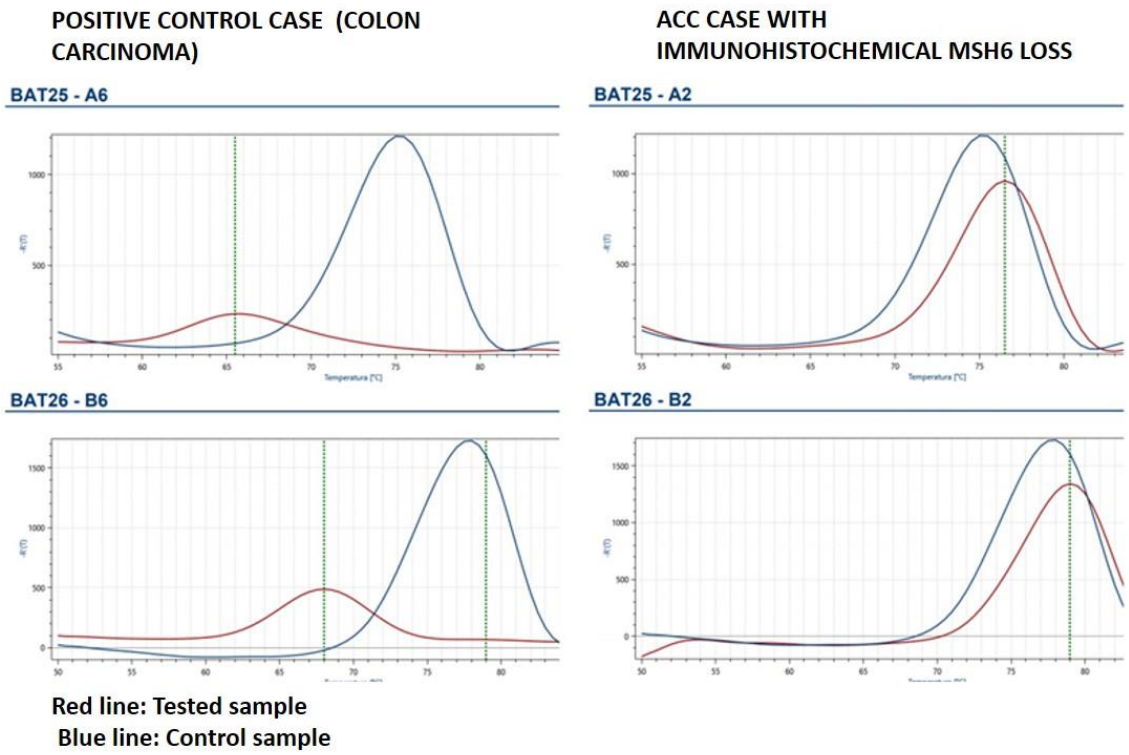

Figure 2_2: Examples of profiles of amplification of microsatellite regions tested in the assay applied in our study to detect the presence of microsatellite instability. The ACC sample with MSH6 protein loss showed a stable profile as compared to the colon cancer sample used as positive control.

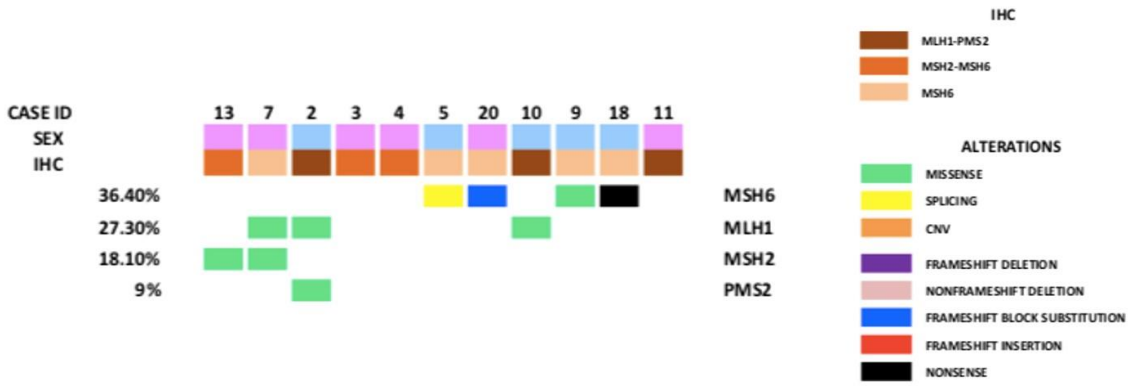

Figure 2_3: Correlation between IHC results and genomic alterations in MMR genes.

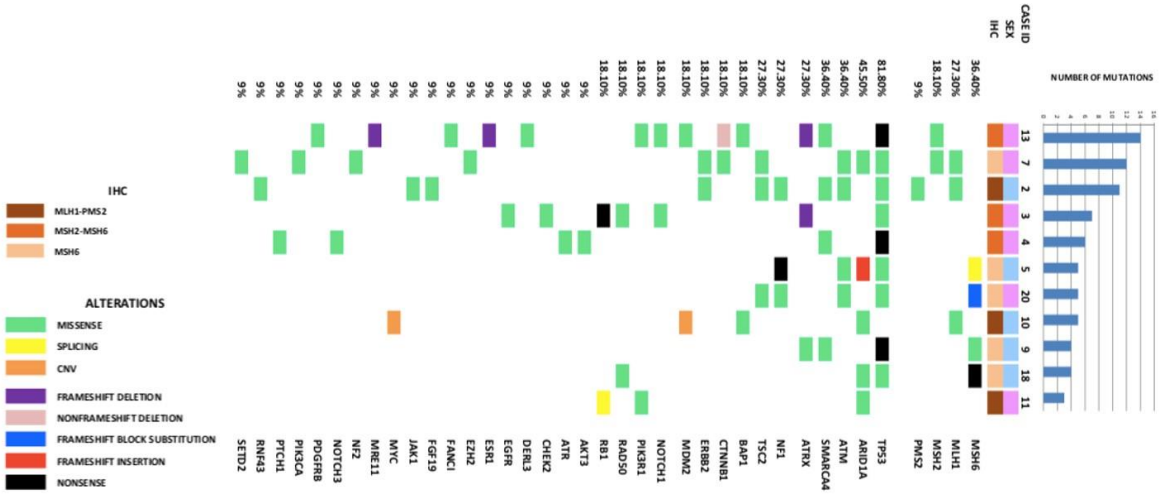

Figure 2_4: Main molecular alterations in ACC cases showing MMR deficiency.

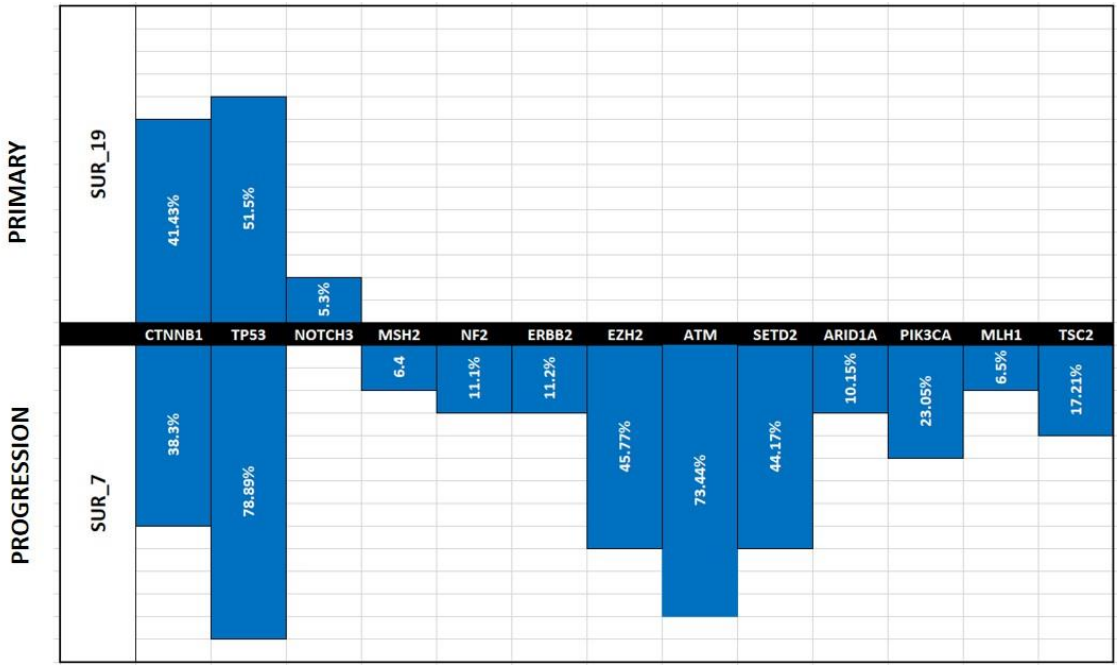

Figure 2_5: Comparative genomic analysis in one ACC case with MMR-proficient primary adrenal lesion and MMR-deficient recurrence. Percentages in the histograms represent allelic frequencies.

Parameter		**MMR-deficient (#11)**	**MMR-proficient (#109)**	**p-value**
Sex	M	5	46	0.99
	F	6	62	
Age	average, yrs [range]	56 [37-69]	49 [18-66]	0.13
Functionality	Not secreting	1	18	0.78
	Cortisol	2	15	
	Other	1 (androgens)	9 (5 cortisol+androgens; 3 androgens; 1 aldosterone+cortisol)	
	Not known	7	67	/
Diameter	average, cm [range]	12.7 [4.3-13.7]	11.5 [0.7-24.3]	0.44
Weight	average, g [range]	600.3 [321-810]	619.8 [64-2800]	0.94
Predominant subtype	Conventional	8	84	0.03
	Oncocytic	1	22	
	Mixoid	2	2	
	Sarcomatoid	0	1	
Weiss score	average [range]	8 [4-9]	6.9 [3-9]	0.06
Helisnki score	average [range]	39.9 [14-73]	30.5 [7-78]	0.13
Ki-67 index	average [range]	32.4 [11-65]	22.9 [1-70]	0.10
Stage pT	1-2	4	66	0.006
	3-4	7	18	
Stage pN	Nx	6	93	/
	N0	3	10	0.99
	N1	2	6	

Table 2_1: Clinical and pathological correlates.

References

Adachi S, Kimata JI, Hanami K, Adachi K, Igarashi T, Liang SG, Ishida Y, Fujino T, Yamazaki K. Applicability of the FDA-approved Immunohistochemical Panel for Identification of MMRd Phenotype in Uterine Endometrioid Carcinoma. Appl Immunohistochem Mol Morphol. 2023 Oct 20.

Brondani VB, Montenegro L, Lacombe AMF, Magalhães BM, Nishi MY, Funari MFA, Narcizo AM, Cardoso LC, Siqueira SAC, Zerbini MCN, Denes FT, Latronico AC, Mendonca BB, Almeida MQ, Lerario AM, Soares IC, Fragoso MCBV. High Prevalence of Alterations in DNA Mismatch Repair Genes of Lynch Syndrome in Pediatric Patients with Adrenocortical Tumors Carrying a Germline Mutation on *TP53*. Cancers (Basel). 2020 Mar 7;12(3):621.

Casey RT, Giger O, Seetho I, Marker A, Pitfield D, Boyle LH, Gurnell M, Shaw A, Tischkowitz M, Maher ER, Chatterjee VK, Janowitz T, Mells G, Corrie P, Challis BG. Rapid disease progression in a patient with mismatch repair-deficient and cortisol secreting adrenocortical carcinoma treated with pembrolizumab. Semin Oncol. 2018 Jun;45(3):151-155.

Chen G, Chen P, Zhou J, Luo G. Pan-Cancer Analysis of Histone Methyltransferase KMT2D with Potential Implications for Prognosis and Immunotherapy in Human Cancer. Comb Chem High Throughput Screen. 2023;26(1):83-92.

Darabi S, Braxton DR, Eisenberg BL, Demeure MJ. Molecular genomic profiling of adrenocortical cancers in clinical practice. Surgery. 2021 Jan;169(1):138-144.

Domènech M, Grau E, Solanes A, Izquierdo A, Del Valle J, Carrato C, Pineda M, Dueñas N, Pujol M, Lázaro C, Capellà G, Brunet J, Navarro M. Characteristics of Adrenocortical Carcinoma Associated With Lynch Syndrome. J Clin Endocrinol Metab. 2021 Jan 23;106(2):318-325.

Else T, Kim AC, Sabolch A, Raymond VM, Kandathil A, Caoili EM, Jolly S, Miller BS, Giordano TJ, Hammer GD. Adrenocortical carcinoma. Endocr Rev. 2014 Apr;35(2):282-326.

Libé R. Clinical and molecular prognostic factors in adrenocortical carcinoma. Minerva Endocrinol. 2019 Mar;44(1):58-69.

Mete O, Erickson LA, Juhlin CC, de Krijger RR, Sasano H, Volante M, Papotti MG. Overview of the 2022 WHO Classification of Adrenal Cortical Tumors. Endocr Pathol. 2022 Mar;33(1):155-196.

Park D, Airi R, Sherman M. Microsatellite instability driven metastatic parathyroid carcinoma managed with the anti-PD1 immunotherapy, pembrolizumab. BMJ Case Rep. 2020 Sep 23;13(9):e235293.

Pozdeyev N, Fishbein L, Gay LM, Sokol ES, Hartmaier R, Ross JS, Darabi S, Demeure MJ, Kar A, Foust LJ, Koc K, Bowles DW, Leong S, Wierman ME, Kiseljak-Vassiliades K. Targeted genomic analysis of 364 adrenocortical carcinomas. Endocr Relat Cancer. 2021 Aug 16;28(10):671-681.

Ragazzon B, Libé R, Gaujoux S, Assié G, Fratticci A, Launay P, Clauser E, Bertagna X, Tissier F, de Reyniès A, Bertherat J. Transcriptome analysis reveals that p53 and {beta}-catenin alterations occur in a group of aggressive adrenocortical cancers. Cancer Res. 2010 Nov 1;70(21):8276-81.

Raymond VM, Everett JN, Furtado LV, Gustafson SL, Jungbluth CR, Gruber SB, Hammer GD, Stoffel EM, Greenson JK, Giordano TJ, Else T. Adrenocortical carcinoma is a lynch syndrome-associated cancer. J Clin Oncol. 2013 Aug 20;31(24):3012-8.

Rocha ML, Schmid KW, Czapiewski P. The prevalence of DNA microsatellite instability in anaplastic thyroid carcinoma - systematic review and discussion of current therapeutic options. Contemp Oncol (Pozn). 2021;25(3):213-223.

Santos LS, Silva SN, Gil OM, Ferreira TC, Limbert E, Rueff J. Mismatch repair single nucleotide polymorphisms and thyroid cancer susceptibility. Oncol Lett. 2018 May;15(5):6715-6726.

Teuber J, Reinhardt A, Reuss D, Hähnel S, Unterberg A, Beynon C. Aggressive pituitary adenoma in the context of Lynch syndrome: a case report and literature review on this rare coincidence. Br J Neurosurg. 2021 Aug 25:1-6.

Wong KS, Lorch JH, Alexander EK, Nehs MA, Nowak JA, Hornick JL, Barletta JA. Clinicopathologic Features of Mismatch Repair-Deficient Anaplastic Thyroid Carcinomas. Thyroid. 2019 May;29(5):666-673.

5.0. POORLY DIFFERENTIATED THYROID CANCER

<u>Study 3</u>: Molecular heterogeneity of poorly differentiated thyroid carcinomas associated with a well differentiated carcinoma component.

Vanessa Zambelli[1], Matthias Dettmer[2], Lorenzo Daniele[3], Jasna Metovic[4], Renaud S. Maire[2], Stefano Carollo[1], Jessica Giorcelli[1], Simona Vatrano[1], Susanna Cappia[1], Giovanni De Rosa[3], Aurel Perren[2], Mauro G. Papotti[4*], Marco Volante[1*].

[1]Department of Oncology, University of Turin, San Luigi Hospital, Orbassano, Turin, Italy

[2]Institute of Pathology, University of Bern, Bern, Switzerland

[3]Pathology Unit, Mauriziano Hospital, Turin, Italy

[4]Department of Oncology, University of Turin, Città della Salute e della Scienza Hospital, Turin, Italy

(paper status: submitted)

<u>Study 4</u>: High prevalence of potential molecular therapeutic targets in poorly differentiated thyroid carcinoma.

Vanessa Zambelli[1], Marta Fornaro[1], Giulia Orlando[2], Giulia Vocino Trucco[3], Ida Rapa[4], Francesca Napoli[1], Susanna Cappia[1], Lorenzo Daniele[5], Simonetta Piana[6], Mauro Papotti[2]*, Marco Volante[1]*.

[1]Department of Oncology, University of Turin, San Luigi Hospital, Orbassano, Turin, Italy

[2]Department of Oncology, University of Turin, Città della Salute e della Scienza Hospital, Turin, Italy

[3]Department of Medical Sciences, University of Turin, Città della Salute e della Scienza Hospital, Turin, Italy

[4]Pathology Unit, San Luigi Hospital, Orbassano, Turin, Italy

[5]Pathology Unit, Mauriziano Hospital, Turin, Italy

[6]Pathology Unit, Reggio Emilia Hospital, Reggio Emilia, Italy

(paper status: submitted)

Thyroid cancer has a wide spectrum of morphologies and behaviors that include the most common and indolent tumors as well as the most aggressive and rapidly lethal malignancies (Asa et al, 2019).

Follicular cell-derived tumors constitute the majority of thyroid neoplasm, and the 2022 WHO classification of endocrine tumors has organized these neoplasms into three categories: benign neoplasms, low-risk neoplasms, and malignant neoplasms (Baloch et al, 2022).

Poorly differentiated thyroid carcinoma (PDTC), together with differentiated high-grade thyroid carcinoma (DHGTC), are rare thyroid malignancies that are both recognized by the new WHO classification as high-grade non-anaplastic follicular cell-derived carcinomas with an intermediate prognosis (Baloch et al, 2022).

The term "poorly differentiated (PD) thyroid carcinoma" has been proposed 20 years ago to define non-follicular, non-papillary thyroid carcinomas, which produced thyroglobulin and were unrelated to anaplastic carcinoma, showing an intermediate clinical behavior between follicular or papillary and anaplastic carcinomas (Volante et al, 2008).

PDTC and DHGTC are intermediate forms of thyroid cancer that are classified between differentiated thyroid carcinomas and anaplastic thyroid carcinomas (Cracolici, 2023). In particular, well differentiated thyroid carcinoma (WDTC) accounts for 90-95% of thyroid carcinoma and is further subtyped into papillary thyroid carcinoma (PTC) and follicular thyroid carcinoma (FTC) (Duan et al,2019). In contrast, PDTC represent less than 5% of all newly diagnosed thyroid malignancies, they generally affect patients in the fifth to sixth decade of life with a slight female predominance (Volante et al, 2007; Wong et al, 2019; Asioli et al, 2010) and have a mean survival, after diagnosis of only 3.2 years (Landa et al, 2016).

While there was a universal agreement on the recognition of PDTC, pathologist differed on histologic definition (Ibrahimpasic et al, 2019). Some of them lean on a solid/trabecular growth pattern alone (Volante et al, 2004), while head and neck pathologists at Memorial Sloane Kettering Cancer Center (MSKCC) used high mitotic rate and/or tumor necrosis to diagnose this tumor (Hiltzik et al, 2006). In 2006, in order to unify the concept of PDTC, a group of internationally recognized thyroid experts met in Turin and elaborated the "Turin consensus", an algorithm based on high-grade features and growth pattern (Volante et al, 2007; Dettmer et al, 2020; Volante et al, 2021).

Turin criteria include:

a) presence of a solid/trabecular/insular pattern of growth in a malignant/invasive tumor;

b) absence of the conventional nuclear features of papillary carcinoma;

c) presence of at least one of the following features: convoluted nuclei, mitotic activity ≥3 x 10 high power microscopic fields (HPF) and tumor necrosis.

PDTC represents the main cause of morbidity and mortality from non-anaplastic follicular cell-derived thyroid cancer (Ibrahimpasic et al, 2019), and distant disease, most commonly in lung and bone, represent the major cause of death in PDTC, accounting for up to 85% of disease-related deaths (Sanders et al, 2007; Chao et al, 2004; Ibrahimpasic et al, 2014). According to most of the available molecular data, PDTC and DHGTC may arise from differentiated thyroid carcinoma, but they may also originate de novo, in association with iodine deficiency (Baloch et al, 2022).

In terms of treatment, due to their rarity and heterogeneity of inclusion criteria, therapeutic strategies of PDTC have still not been standardized, and surgery is the first treatment of choice for PDTC (Ibrahimpasic et al, 2019). PDTC patients are partially responsive to radioiodine (RAI) therapy, but 10-year survival is below 10% (Dierks et al, 2021). Molecular targeted therapies, as tyrosine kinase inhibitors (TKIs) represent promising therapeutic options for thyroid carcinoma patients (Valerio et al,2017), but only patients with specific genetic mutations can have some benefits from TKIs therapy (Borson-Chazot et al, 2018; Iwasaki et al, 2018).

Therefore, increase in the knowledge of PDTC molecular background is of pathogenetic interest but it also has a prime aim to identify potential therapeutic targets that might offer novel strategies in patients developing radio-iodine refractory disease.

There have been several studies using next generation sequencing (NGS) techniques as a tool to unravel genomic alterations in PDTC (Gerber et al, 2018; Landa et al, 2016; Sykorova et al, 2015; Nikiforova et al, 2013). Genetic alterations include "Early" and "Late" molecular events, where "early changes are found in combination with "Late", in a model of multistep progression from well differentiated to poorly differentiated to anaplastic thyroid carcinoma.

"Early" mutations are mainly in *RAS* and *BRAF* genes, whereas other mutations such as in *EIF1AX*, *ATM* and *ERBB4* are less frequent (Landa et al,2 016; Chen et al, 2018; Gerber et al, 2017). "Late" changes (similarly to anaplastic thyroid carcinoma – ATC) are mainly somatic mutations in *TP53*, and *TERTp*, and dysregulation of the *PIK3/PTEN/AKT*

pathway (Volante et al, 2021). In particular, *TERT* gene plays a dominant role in the activation of telomerase during malignant transformation cells (Liu et al, 2016). There are two *TERTp* mutations that are common in thyroid cancer and are located at two hotspots: chr5:1295228 C>T (C228T) and chr5:1295250 C>T (C250T), corresponding to the positions 124 and 146, respectively (Liu et al,2016).

The C228T mutation is more common than C250T in most cancers; both mutations generate a consensus binding site in the *TERTp* for E-twenty-six (ETS) transcription factors, which has been shown to confer the *TERTp* increased transcriptional activities (Huang et al, 2013; Horn et al, 2013; Na et al, 2022).

In thyroid cancer, *TERTp* mutations increases significantly from well to poorly differentiated and undifferentiated carcinomas, up to 50% of all cases (Gandolfi et al, 2015), and are associated with poor prognosis (Ibrahimpasic et al, 2017).

Gene fusions, such as *RET/PTC*, *ALK*, *NTRK1* and *3* and *PAX8/PPARG*, also occur in thyroid cancer (Gatalica et al, 2019; Panebianco et al, 2019). Although most data are on well-differentiated histotypes, they been found in a significant proportion in PDTC, also but data are still limited to relatively small series.

DNA Mismatch Repair (MMR) proteins are important players in the post-replication repair by correcting base spontaneous mutations that results from replication errors (Hsieh et al, 2008). Mutations in genes coding for MMR proteins, namely *MLH1*, *MSH2*, *MSH6* and *PMS2*, can lead to the development of malignant transformation and tumorigenesis (Luchini et al, 2019; Li, 2008).

Usually, mutations in MMR genes that alter the expression of one or couples of MMR proteins are associated with the onset of microsatellite instability (MSI), since the loss of function of the MMR pathway increases the occurrence of errors in the replication of microsatellite regions of the DNA.

DNA MMR alterations can be identified using immunohistochemistry to detect loss of MMR proteins and/or molecular tests to show microsatellite alterations (Luchini et al, 2019). The occurrence of MMR defects in thyroid cancer (in particular involving MSH2 and MSH6) has been investigated in thyroid cancer, but data in PDTC are few and limited to a small number of cases (Qiao et al, 2022).

References

Asa SL. The Current Histologic Classification of Thyroid Cancer. Endocrinol Metab Clin North Am. 2019 Mar;48(1):1-22.

Asioli S, Erickson LA, Righi A, Jin L, Volante M, Jenkins S, Papotti M, Bussolati G, Lloyd RV. Poorly differentiated carcinoma of the thyroid: validation of the Turin proposal and analysis of IMP3 expression. Mod Pathol. 2010 Sep;23(9):1269-78.

Baloch ZW, Asa SL, Barletta JA, Ghossein RA, Juhlin CC, Jung CK, LiVolsi VA, Papotti MG, Sobrinho-Simões M, Tallini G, Mete O. Overview of the 2022 WHO Classification of Thyroid Neoplasms. Endocr Pathol. 2022 Mar;33(1):27-63.

Borson-Chazot F, Dantony E, Illouz F, Lopez J, Niccoli P, Wassermann J, Do Cao C, Leboulleux S, Klein M, Tabarin A, Eberle MC, Benisvy D, de la Fouchardière C, Bournaud C, Lasolle H, Delahaye A, Rabilloud M, Lapras V, Decaussin-Petrucci M, Schlumberger M. Effect of Buparlisib, a Pan-Class I PI3K Inhibitor, in Refractory Follicular and Poorly Differentiated Thyroid Cancer. Thyroid. 2018 Sep;28(9):1174-1179.

Chao TC, Lin JD, Chen MF. Insular carcinoma: infrequent subtype of thyroid cancer with aggressive clinical course. World J Surg. 2004 Apr;28(4):393-6.

Chen H, Luthra R, Routbort MJ, Patel KP, Cabanillas ME, Broaddus RR, Williams MD. Molecular Profile of Advanced Thyroid Carcinomas by Next-Generation Sequencing: Characterizing Tumors Beyond Diagnosis for Targeted Therapy. Mol Cancer Ther. 2018 Jul;17(7):1575-1584.

Cracolici V. No Longer Well-Differentiated: Diagnostic Criteria and Clinical Importance of Poorly Differentiated/High-Grade Thyroid Carcinoma. Surg Pathol Clin. 2023 Mar;16(1):45-56.

Dettmer MS, Schmitt A, Komminoth P, Perren A. Poorly differentiated thyroid carcinoma: An underdiagnosed entity. Pathologe. 2020 Jun;41(Suppl 1):1-8.

Dierks C, Seufert J, Aumann K, Ruf J, Klein C, Kiefer S, Rassner M, Boerries M, Zielke A, la Rosee P, Meyer PT, Kroiss M, Weißenberger C, Schumacher T, Metzger P, Weiss H, Smaxwil C, Laubner K, Duyster J, von Bubnoff N, Miething C, Thomusch O. Combination of Lenvatinib and Pembrolizumab Is an Effective Treatment Option for Anaplastic and Poorly Differentiated Thyroid Carcinoma. Thyroid. 2021 Jul;31(7):1076-1085.

Duan H, Li Y, Hu P, Gao J, Ying J, Xu W, Zhao D, Wang Z, Ye J, Lizaso A, He Y, Wu H, Liang Z. Mutational profiling of poorly differentiated and anaplastic thyroid carcinoma by the use of targeted next-generation sequencing. Histopathology. 2019 Dec;75(6):890-899.

Gandolfi G, Ragazzi M, Frasoldati A, Piana S, Ciarrocchi A, Sancisi V. TERT promoter mutations are associated with distant metastases in papillary thyroid carcinoma. Eur J Endocrinol. 2015 Apr;172(4):403-13.

Gatalica Z, Xiu J, Swensen J, Vranic S. Molecular characterization of cancers with NTRK gene fusions. Mod Pathol. 2019 Jan;32(1):147-153.

Gerber TS, Schad A, Hartmann N, Springer E, Zechner U, Musholt TJ. Targeted next-generation sequencing of cancer genes in poorly differentiated thyroid cancer. Endocr Connect. 2018 Jan;7(1):47-55.

Hiltzik D, Carlson DL, Tuttle RM, Chuai S, Ishill N, Shaha A, Shah JP, Singh B, Ghossein RA. Poorly differentiated thyroid carcinomas defined on the basis of mitosis and necrosis: a clinicopathologic study of 58 patients. Cancer. 2006 Mar 15;106(6):1286-95.

Horn S, Figl A, Rachakonda PS, Fischer C, Sucker A, Gast A, Kadel S, Moll I, Nagore E, Hemminki K, Schadendorf D, Kumar R. TERT promoter mutations in familial and sporadic melanoma. Science. 2013 Feb 22;339(6122):959-61.

Hsieh P, Yamane K. DNA mismatch repair: molecular mechanism, cancer, and ageing. Mech Ageing Dev. 2008 Jul-Aug;129(7-8):391-407.

Huang FW, Hodis E, Xu MJ, Kryukov GV, Chin L, Garraway LA. Highly recurrent TERT promoter mutations in human melanoma. Science. 2013 Feb 22;339(6122):957-9.

Ibrahimpasic T, Ghossein R, Carlson DL, Nixon I, Palmer FL, Shaha AR, Patel SG, Tuttle RM, Shah JP, Ganly I. Outcomes in patients with poorly differentiated thyroid carcinoma. J Clin Endocrinol Metab. 2014 Apr;99(4):1245-52.

Ibrahimpasic T, Xu B, Landa I, Dogan S, Middha S, Seshan V, Deraje S, Carlson DL, Migliacci J, Knauf JA, Untch B, Berger MF, Morris L, Tuttle RM, Chan T, Fagin JA, Ghossein R, Ganly I. Genomic Alterations in Fatal Forms of Non-Anaplastic Thyroid Cancer: Identification of *MED12* and *RBM10* as Novel Thyroid Cancer Genes Associated with Tumor Virulence. Clin Cancer Res. 2017 Oct 1;23(19):5970-5980.

Ibrahimpasic T, Ghossein R, Shah JP, Ganly I. Poorly Differentiated Carcinoma of the Thyroid Gland: Current Status and Future Prospects. Thyroid. 2019 Mar;29(3):311-321.

Iwasaki H, Yamazaki H, Takasaki H, Suganuma N, Nakayama H, Toda S, Masudo K. Lenvatinib as a novel treatment for anaplastic thyroid cancer: A retrospective study. Oncol Lett. 2018 Dec;16(6):7271-7277.

Landa I, Ibrahimpasic T, Boucai L, Sinha R, Knauf JA, Shah RH, Dogan S, Ricarte-Filho JC, Krishnamoorthy GP, Xu B, Schultz N, Berger MF, Sander C, Taylor BS, Ghossein R, Ganly I, Fagin JA. Genomic and transcriptomic hallmarks of poorly differentiated and anaplastic thyroid cancers. J Clin Invest. 2016 Mar 1;126(3):1052-66.

Li GM. Mechanisms and functions of DNA mismatch repair. Cell Res. 2008 Jan;18(1):85-98.

Liu R, Xing M. TERT promoter mutations in thyroid cancer. Endocr Relat Cancer. 2016 Mar;23(3):R143-55.

Luchini C, Bibeau F, Ligtenberg MJL, Singh N, Nottegar A, Bosse T, Miller R, Riaz N, Douillard JY, Andre F, Scarpa A. ESMO recommendations on microsatellite instability testing for immunotherapy in cancer, and its relationship with PD-1/PD-L1 expression and tumour mutational burden: a systematic review-based approach. Ann Oncol. 2019 Aug 1;30(8):1232-1243.

Na HY, Yu HW, Kim W, Moon JH, Ahn CH, Choi SI, Kim YK, Choi JY, Park SY. Clinicopathological indicators for TERT promoter mutation in papillary thyroid carcinoma. Clin Endocrinol (Oxf). 2022 Jul;97(1):106-115.

Nikiforova MN, Wald AI, Roy S, Durso MB, Nikiforov YE. Targeted next-generation sequencing panel (ThyroSeq) for detection of mutations in thyroid cancer. J Clin Endocrinol Metab. 2013 Nov;98(11):E1852-60.

Panebianco F, Nikitski AV, Nikiforova MN, Kaya C, Yip L, Condello V, Wald AI, Nikiforov YE, Chiosea SI. Characterization of thyroid cancer driven by known and novel ALK fusions. Endocr Relat Cancer. 2019 Nov;26(11):803-814.

Qiao PP, Tian KS, Han LT, Ma B, Shen CK, Zhao RY, Zhang Y, Wei WJ, Chen XP. Correlation of mismatch repair deficiency with clinicopathological features and programmed death-ligand 1 expression in thyroid carcinoma. Endocrine. 2022 Jun;76(3):660-670.

Sanders EM Jr, LiVolsi VA, Brierley J, Shin J, Randolph GW. An evidence-based review of poorly differentiated thyroid cancer. World J Surg. 2007 May;31(5):934-45.

Sykorova V, Dvorakova S, Vcelak J, Vaclavikova E, Halkova T, Kodetova D, Lastuvka P, Betka J, Vlcek P, Reboun M, Katra R, Bendlova B. Search for new genetic biomarkers in poorly differentiated and anaplastic thyroid carcinomas using next generation sequencing. Anticancer Res. 2015 Apr;35(4):2029-36.

Valerio L, Pieruzzi L, Giani C, Agate L, Bottici V, Lorusso L, Cappagli V, Puleo L, Matrone A, Viola D, Romei C, Ciampi R, Molinaro E, Elisei R. Targeted Therapy in Thyroid Cancer: State of the Art. Clin Oncol (R Coll Radiol). 2017 May;29(5):316-324.

Volante M, Landolfi S, Chiusa L, Palestini N, Motta M, Codegone A, Torchio B, Papotti MG. Poorly differentiated carcinomas of the thyroid with trabecular, insular, and solid patterns: a clinicopathologic study of 183 patients. Cancer. 2004 Mar 1;100(5):950-7.

Volante M, Collini P, Nikiforov YE, Sakamoto A, Kakudo K, Katoh R, Lloyd RV, LiVolsi VA, Papotti M, Sobrinho-Simoes M, Bussolati G, Rosai J. Poorly differentiated thyroid carcinoma: the Turin proposal for the use of uniform diagnostic criteria and an algorithmic diagnostic approach. Am J Surg Pathol. 2007 Aug;31(8):1256-64.

Volante M, Lam AK, Papotti M, Tallini G. Molecular Pathology of Poorly Differentiated and Anaplastic Thyroid Cancer: What Do Pathologists Need to Know? Endocr Pathol. 2021 Mar;32(1):63-76.

Volante M, Rapa I, Papotti M. Poorly differentiated thyroid carcinoma: diagnostic features and controversial issues. Endocr Pathol. 2008 Fall;19(3):150-5.

Wong KS, Barletta JA. Thyroid Tumors You Don't Want to Miss. Surg Pathol Clin. 2019 Dec;12(4):901-919.

5.1 Study 3

Molecular heterogeneity of poorly differentiated thyroid carcinomas associated with a well differentiated carcinoma component.

Aim

The aim of the present study was to characterize the molecular landmark of poorly differentiated carcinomas associated with a well-differentiated component, to underpin possible molecular pathways of tumor progression and to verify a possible clonal origin for these tumors.

Methods

DNA and RNA extraction, targeted Next Generation Sequencing, Focus Assay; Sanger sequencing.

Patients and tissue samples

Cases enrolled in the study were selected from the databases of the Department of Oncology, University of Turin, at both San Luigi (Orbassano, Turin) and Città della Salute (Turin) Hospitals, from the Mauriziano Hospital (Turin) and from the Institute of Pathology, University of Bern (Bern). A total of 27 cases were identified meeting the following criteria: i) a diagnosis of poorly differentiated carcinoma confirmed after histological revision (by MV and JM) according to the diagnostic criteria assessed in the Turin Consensus as defined in the most recent WHO classification of thyroid tumors (Baloch et al.,2022); ii) the presence of a clearly recognizable associated well differentiated carcinoma component, and iii) leftover paraffin embedded material adequate for molecular analysis. Match pairs of poorly differentiated and well differentiated components were obtained by means of stereo-microscopically assisted manual microdissection (performed in all cases by the same pathologist, MV) from serial sections.

Results

Clinical and pathological characteristics

Among the 27 selected cases, 23 yielded nucleic acids adequate for further molecular testing. Of these, 13 were associated with a papillary carcinoma component, 8 with a follicular carcinoma component and two with an oncocytic carcinoma component (**Figure 3_1**). In those with an associated papillary carcinoma component, six were of the classical type, five of the follicular type and one of the tall-cell type. The age, sex and pathological stage distribution of the cases is reported in **Table 3_1**, together with the summary of detected molecular alterations. Male to female ratio was 2:1, and the mean age was 65.9 years.

Prevalence of TERT mutations

Two out of 23 cases (cases T2 and T7) gave inadequate results for *TERT* promoter sequencing. Six out of 21 adequate cases (28.5%) harbored a *TERT* promoter mutation (three with associated papillary carcinoma, classic type, and three with associated follicular carcinoma components). All *TERT* promoter mutations detected were C228T (c.-124 C>T). In all but one case, the *TERT* promoter mutation was identified in both the well differentiated and the poorly differentiated components of the tumor. In the last case (case T18), the *TERT* promoter mutation was detected in the poorly differentiated component, only (**Figure 3_2**). In all but one case (T22), the *TERT* promoter mutation was coexistent with other driver mutations.

Next generation sequencing analysis

Seven cases lack any molecular alteration in the genes covered by the NGS panel. DNA analysis in the 16 samples with detectable molecular alterations identified a total of 38 pathogenic variants in one or in both the two tumor component analyzed (**Table 3_1**). *RAS* mutations, exclusive or concurrent with other alterations, were the most prevalent, detectable in 12/23 cases (52.2%), being *NRAS* mutations the most frequent (7 cases). *BRAF* mutations were detected in three cases (13%), being the single pathogenic variant in one of them. Overall, the *RAS/RAF* pathway was altered in 14/23 cases (60.8%). *PIK3CA* mutations occurred in four cases (17.4%), either associated with *RAS* mutations (2 cases) or co-mutated with *BRAF* (1 case) and *EGFR* (1 case). *AKT1* mutations occurred in two cases (8.7%), both co-occurring with *NRAS* mutations. Overall, the *PI3K/AKT*

pathway was altered in 6/23 cases (26.1%); one single case lacked co-mutations with *RAS* genes. *EGFR* mutations were the second most prevalent and were detected in five cases (21.7%) all but one co-occurring with *RAS*, *PIK3CA* and/or *BRAF* mutations. Finally, non-recurrent mutations (one mutation for each gene) were detected in *MED12*, *FGFR1*, *FGFR2*, *RET*, *PDGFRA*, *MET*, *GNA11*, *GNAQ* and *KIT*. Copy number variations (CNV) were not detected.

Concerning RNA analysis, 13 cases failed in sequencing. In the 10 adequate cases, one *PAX8-PPARγ* and one *ETV/NTRK3* fusion were detected.

Comparison of genomic alterations detected in the two separate tumor components (well differentiated and poorly differentiated) of each case are illustrated in **Figures 3_3** and **3_4**, except for *TERTp* mutations and gene fusions whose allelic frequencies cannot be expressed.

Based on the overall agreement of molecular features in the tumor components, 7 cases (T1, T4, T5, T9, T10, T11 and T22) were coded as monoclonal/homogeneous genotype, because of the overlapping molecular alterations in the well differentiated and poorly differentiated carcinoma components. Allelic frequencies of shared mutations, when available, were strongly similar in the two tumor components in all cases.

Six other cases (T3, T8, T12, T15, T16, T17) showed a monoclonal/heterogeneous molecular profile. In these cases, one or two gene mutations were shared by the two tumor components, but additional molecular alterations (from 1 to 3) were detected in the poorly differentiated carcinoma component. Additional co-mutations included the two gene fusions, together with *AKT1* and *EGFR* (2 cases, each), and *KRAS*, *BRAF*, *GNA11*, *GNAQ*, *PIK3CA* and *KIT* (1 case, each). In most cases, allelic frequencies of these genes, when assessable, were lower than those detected for mutations in shared genes. Finally, four cases (T2, T6, T7, T18) were considered polyclonal since no molecular alteration detected in the case was shared by the two tumor components, or – as for case T7 – the shared mutations demonstrated a significantly different allelic frequency together with additional molecular alterations exclusively present in the well differentiated component. Interestingly, all these four cases were enriched in one of the two tumor components for mutations in genes encoding for proteins active as tyrosine kinases.

Discussion

The coexistence of PDTC and WDTC components within an individual lesion is well known (Dettmer et al, 2020), and postulate the hypothesis of the existence of PDTC cases progressing from pre-existing WDTC, in contrast to others arising de novo (Volante et al, 2021).

However, at variance with the model of anaplastic carcinoma where this phenomenon has been also investigated at the molecular level, cases with coexisting WDTC and PDTC have not been investigated, so far, in terms of the definition of possible molecular pathways of progression. The molecular data available on anaplastic carcinoma support the existence of driver early alterations (mainly *RAS* and *BRAF* mutations) common in WDTC and anaplastic components, but also that the WDTC component possess a genomic signature that is different to what expected in WDTC without associated anaplastic components (Mika et al, 2021).

Based on these observations, we designed this study to investigate if PDTC with coexistent WDTC component are distinct from pure PDTC in their genomic background, and if a clonal evolution could be designed based on the observed molecular alterations in the two components.

As a first observation, in our series of cases the WDTC component was made of every type of differentiated thyroid cancer, from papillary to follicular to oncocytic, thus showing that there is not a unique pattern of association, and that PDTC may theoretically arise from every type of WDTC.

In terms of genomic profiling, *RAS* mutations were the most frequently observed, as it has been described in the literature since several years (Nikiforova et al, 2003; Pita et al, 2014), especially when the Turin criteria for PDTC classification are applied (Volante et al, 2009; Landa et al, 2016). Interestingly, the *PI3K*/*AKT* pathway was the second most altered, but in almost all cases by mutations co-occurring with those in *RAS* genes. Mutations in *PIK3CA* and *AKT1* genes were either mutated in both WDTC and PDTC tumor components or were present exclusively in the PDTC component, suggesting that they may represent either mechanisms of tumor progression or characterize WDTC samples with a peculiar genotype favoring dedifferentiation. This second hypothesis is even more evident considering the mutation profile of *TERTp*. In fact, *TERTp* mutations had the expected prevalence (about 30%), but they were early event in our series of tumors since in all but one case they were already detectable in the WDTC component. Therefore, in these cases, the WDTC component harbored already a genetic hallmark of aggressiveness in thyroid carcinogenesis (Liu et al, 2016; Dettmer et al, 2015). Other mutations, such as those in

genes coding for tyrosine kinases (i.e. EGFR), were detected at low prevalence and generally at a low allelic frequency, similarly to previous reports (Gerber et al, 2018; Soares et al, 2011). Mutations in tyrosine kinase genes occurred both in WDTC and PDTC tumor components, but generally in a discordant pattern within individual tumors. Apart from their hypothetical role in the molecular mechanisms of tumor progression in PDTC, it is important to underline that these mutations are potential targets for therapy, as suggested by some preclinical data (Sa et al, 2022).

The two gene fusions identified in our series were both exclusively detected in PDTC tumor samples. The prevalence of fusions in our series of PDTC is similar to what reported in the literature (Yakushina et al, 2018), but our data are limited by the high rate of failure in RNA analysis.

The overall molecular comparison between WDTC and PDTC components of the same case could divide the cases into 4 major groups:

a) not informative, due to the lack of any molecular marker

b) monoclonal/homogeneous, due to a very similar genotype in the two components

c) monoclonal/heterogeneous, due to the coexistence of shared mutations between the two components and additional mutations, more frequently recognized in the PDTC component

d) polyclonal, due to distinct genomic profiles in the two components.

Although patterns b and c were predominant, pattern d was present in four cases, both with a papillary and a follicular WDTC component, and without morphological signs suggestive of a collision phenomenon of two separate tumors. In conclusion, monoclonal homogeneous or heterogeneous samples reinforce the hypothesis that PDTC may arise from progression/dedifferentiation steps from WDTC cases that might already possess a genotype characterized by mutations in genes associated with clinical aggressiveness. However, a few cases showing both WDTC and PDTC components may be clonally unrelated and develop independently as a consequence of a pro-tumorigenic milieu in the thyroid tissue.

Figures and Tables

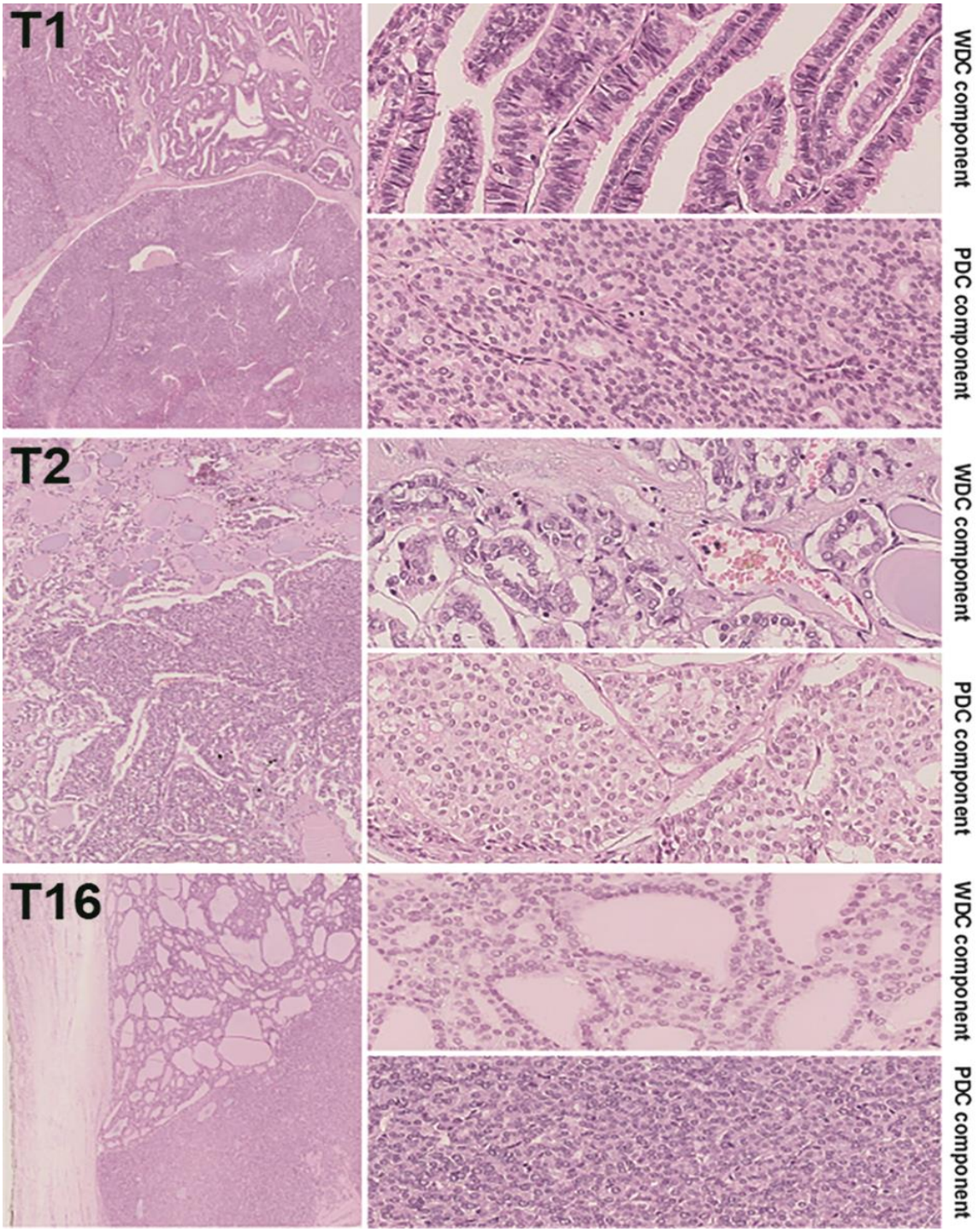

Figure 3_1: Illustrative examples of cases with coexistent well differentiated (WDC) and poorly differentiated (PDC) carcinoma components.

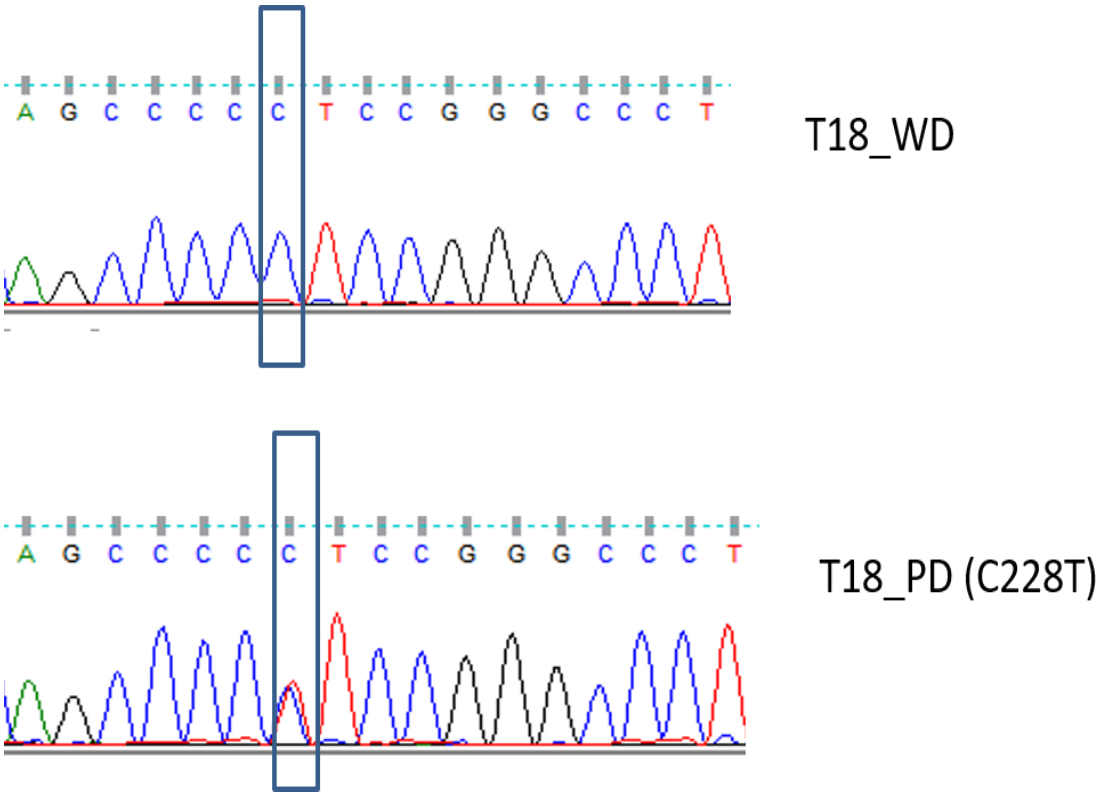

Figure 3_2: Sanger sequencing results of TERT promoter in the two separate components of case T18. (WD: well differentiated; PD: poorly differentiated).

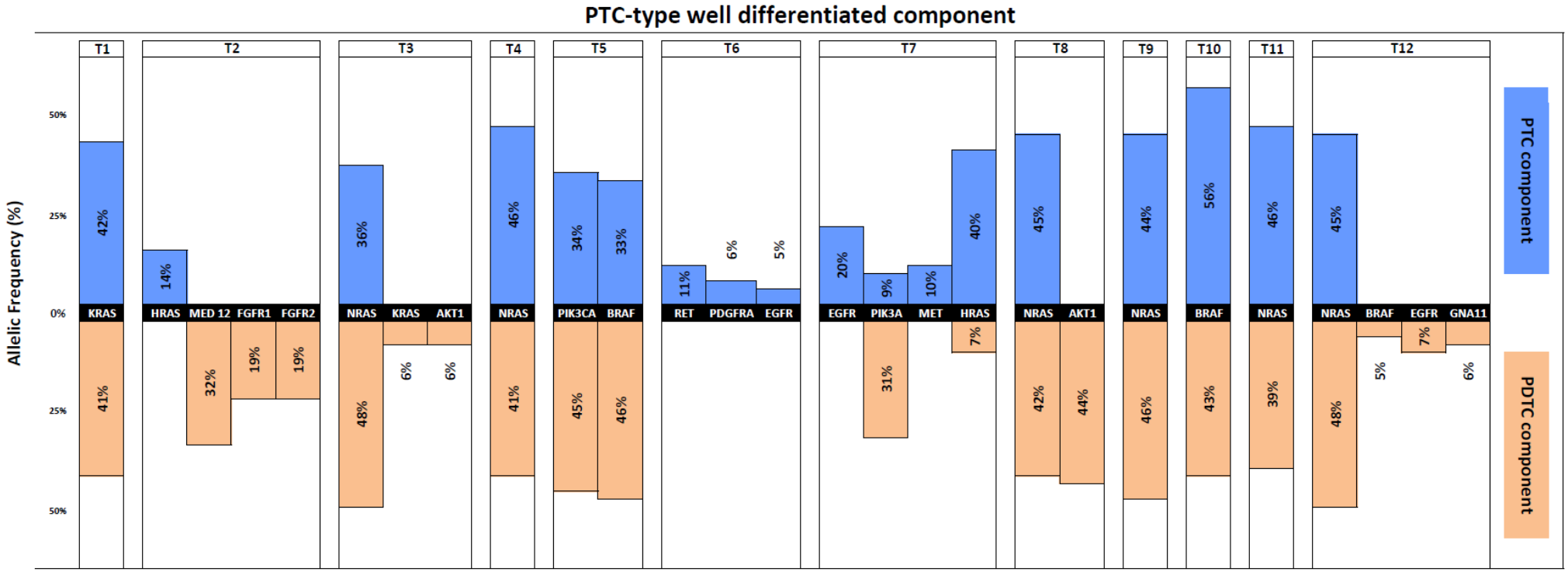

Figure 3_3: Genomic DNA data obtained using NGS in cases of poorly differentiated carcinomas (PDTC) associated with a well differentiated component of the papillary carcinoma-type (PTC).

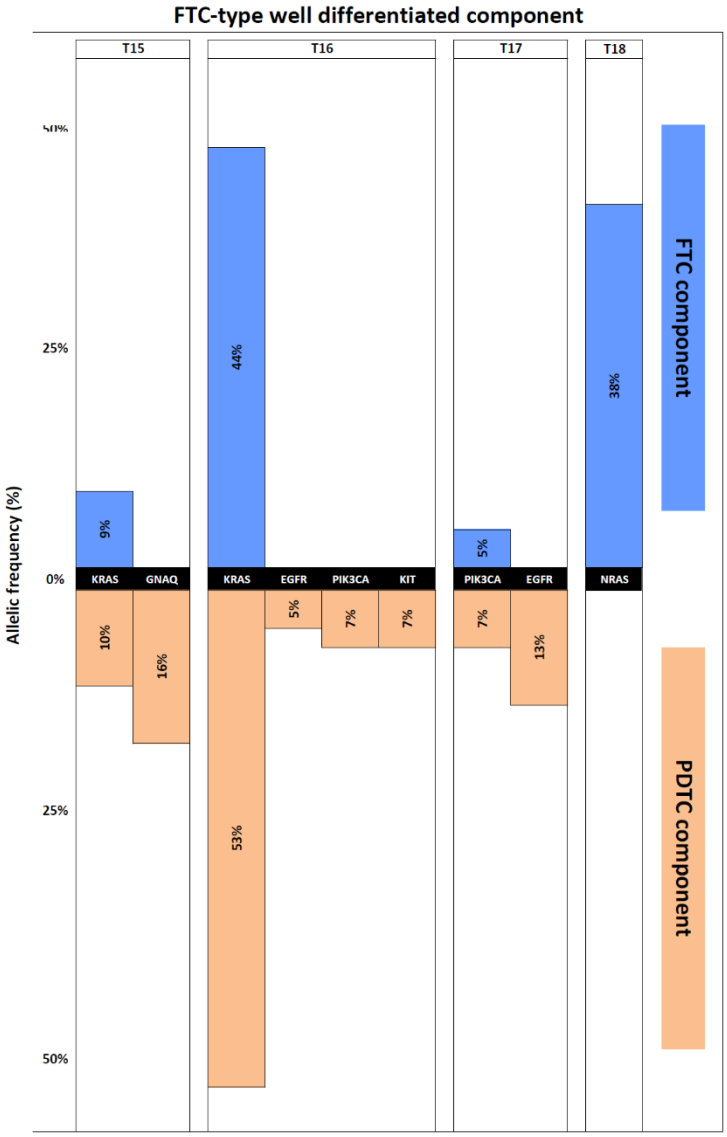

Figure 3_4: Genomic DNA data obtained using NGS in cases of poorly differentiated carcinomas (PDTC) associated with a well differentiated component of the follicular carcinoma-type (FTC). The figure includes case T17 that was associated with an oncocytic carcinoma component.

Sample ID	**Sex**	**Age**	**Histological type of WDC**	**pTN stage**	**Molecular features**		
					Component	***Alteration(s) detected***	***Molecular pattern***
T1	M	74	PTC, tall cell	pT3 pNx	WDC	KRAS (p.Gln61Arg)	Monoclonal, homogeneous
					PDC	KRAS (p.Gln61Arg)	
T2	M	48	PTC, classic	pT3 pN1b	WDC	HRAS (p.Asp57Asn)	Polyclonal
					PDC	MED 12 (p.Gln1212Ter); FGFR1 (p.Gly291Arg); FGFR2 (p.Pro253Ser)	
T3	M	58	PTC, follicular variant	pT3 pNx	WDC	NRAS (p.Gln61Lys)	Monoclonal, heterogeneous
					PDC	NRAS (p.Gln61Lys); KRAS (p.Gly10Glu); AKT1 (p.Arg25His)	
T4	M	73	PTC, classic	pT3b pN0	WDC	NRAS (p.Gln61Arg) TERT (c.-124 C>T)	Monoclonal, homogeneous
					PDC	NRAS (p.Gln61Arg) TERT (c.-124 C>T)	
T5	M	75	PTC, classic	pT4b pN1b	WDC	PIK3CA (p.His1047Arg); BRAF (p.Val600Glu); TERT (c.-124 C>T)	Monoclonal, homogeneous
					PDC	PIK3CA (p.His1047Arg); BRAF (p.Val600Glu); TERT (c.-124 C>T)	
T6	M	79	PTC, follicular variant	pT2 pN1b	WDC	RET (p.Arg912Trp); PDGFRA (p.Asp842Asn); EGFR (p.Pro772Ser)	Polyclonal
					PDC	//	
T7	F	51	PTC, follicular variant	pT3 pN1b	WDC	PIK3CA (p.Glu547Lys); MET (p.Met1268Ile); HRAS (p.Asp57Asn); EGFR (p.Glu746_Ser752delinsVal)	Polyclonal
					PDC	PIK3CA (p.His450Tyr); HRAS (p.Lys16Glu)	
T8	F	89	PTC, follicular variant	pT3a pNx	WDC	NRAS (p.Gln61Arg) TERT (c.-124 C>T)	Monoclonal, heterogeneous
					PDC	NRAS (p.Gln61Arg); AKT1 (p.Glu17Lys); TERT (c.-124 C>T) PPARG-fusion	

T9	M	80	PTC, follicular variant	pT2 pN0	WDC	NRAS (p.Gln61Arg)	Monoclonal, homogeneous
					PDC	NRAS (p.Gln61Arg)	
T10	M	54	PTC, classic	pT3 pN1a	WDC	BRAF (p.Gly469Ala)	Monoclonal, homogeneous
					PDC	BRAF (p.Gly469Ala)	
T11	F	66	PTC, follicular variant	pT3 pN0	WDC	NRAS (p.Gln61Arg)	Monoclonal, homogeneous
					PDC	NRAS (p.Gln61Arg)	
T12	M	76	PTC, columnar	pT3 pN0	WDC	NRAS (p.Gln61Arg)	Monoclonal, heterogeneous
					PDC	NRAS (p.Gln61Arg); BRAF (p.Val600Met); EGFR (p.Pro741Leu);GNA11 (p.Val182Ile)	
T13	M	44	PTC, columnar	pT3b pN1b	WDC	No alterations detected	Not assessable
					PDC	No alterations detected	
T14	M	71	FTC	pT2 pNx	WDC	No alterations detected	Not assessable
					PDC	No alterations detected	
T15	F	64	FTC	pT3 pNx	WDC	KRAS (p.Ala59Val)	Monoclonal, heterogeneous
					PDC	KRAS (p.Ala59Val); GNAQ (p.Gly188Arg)	
T16	M	82	FTC	pT3 pNx	WDC	KRAS (p.Gln61Arg) TERT (c.-124 C>T)	Monoclonal, heterogeneous
					PDC	KRAS (p.Gln61Arg); EGFR (p.Cys797Tyr); PIK3CA (p.Gly29Glu); KIT (p.Val569Ile) TERT (c.-124 C>T)	
T17	F	68	OTC	pT3 pNx	WDC	PIK3CA (p.Arg38Cys)	Monoclonal, heterogeneous
					PDC	PIK3CA (p.Arg38Cys); EGFR (p.Gly283Asp)	
T18	F	34	FTC	pT3a pN0	WDC	NRAS (p.Gln61Arg)	Polyclonal
					PDC	TERT (c.-124 C>T) NTRK3-fusion	
T19	F	73	FTC	pT3 pN0	WDC	No alterations detected	Not assessable
					PDC	No alterations detected	
T20	M	70	OTC	pT3 pN1a	WDC	No alterations detected	Not assessable
					PDC	No alterations detected	
T21	F	82	FTC	pT3b pN1b	WDC	No alterations detected	Not assessable
					PDC	No alterations detected	
T22	M	77	FTC	pT3 pNx	WDC	TERT (c.-124 C>T)	

					PDC	TERT (c.-124 C>T)	Monoclonal, homogeneous
T23	M	27	FTC	pT3 pNx	WDC	No alterations detected	Not assessable
					PDC	No alterations detected	

Legend. M: male; F: female; PTC: papillary thyroid carcinoma; FTC: follicular thyroid carcinoma; OTC: oncocytic thyroid carcinoma; WDC: well differentiated carcinoma; PDC: poorly differentiated carcinoma

Table 3_1: Main clinical, pathological, and molecular features of the series analyzed.

References

Baloch ZW, Asa SL, Barletta JA, Ghossein RA, Juhlin CC, Jung CK, LiVolsi VA, Papotti MG, Sobrinho-Simões M, Tallini G, Mete O. Overview of the 2022 WHO Classification of Thyroid Neoplasms. Endocr Pathol. 2022 Mar;33(1):27-63.

Basolo F, Macerola E, Poma AM, Torregrossa L. The 5th edition of WHO classification of tumors of endocrine organs: changes in the diagnosis of follicular-derived thyroid carcinoma. Endocrine. 2023 Jun;80(3):470-476.

Dettmer MS, Schmitt A, Steinert H, Capper D, Moch H, Komminoth P, Perren A. Tall cell papillary thyroid carcinoma: new diagnostic criteria and mutations in BRAF and TERT. Endocr Relat Cancer. 2015 Jun;22(3):419-29.

Dettmer MS, Schmitt A, Komminoth P, Perren A. Poorly differentiated thyroid carcinoma : An underdiagnosed entity. Pathologe. 2020 Jun;41(Suppl 1):1-8.

Gerber TS, Schad A, Hartmann N, Springer E, Zechner U, Musholt TJ. Targeted next-generation sequencing of cancer genes in poorly differentiated thyroid cancer. Endocr Connect. 2018 Jan;7(1):47-55.

Kopanos C, Tsiolkas V, Kouris A, Chapple CE, Albarca Aguilera M, Meyer R, Massouras A. VarSome: the human genomic variant search engine. Bioinformatics. 2019 Jun 1;35(11):1978-1980.

Landa I, Ibrahimpasic T, Boucai L, Sinha R, Knauf JA, Shah RH, Dogan S, Ricarte-Filho JC, Krishnamoorthy GP, Xu B, Schultz N, Berger MF, Sander C, Taylor BS, Ghossein R, Ganly I, Fagin JA. Genomic and transcriptomic hallmarks of poorly differentiated and anaplastic thyroid cancers. J Clin Invest. 2016 Mar 1;126(3):1052-66.

Liu R, Xing M. TERT promoter mutations in thyroid cancer. Endocr Relat Cancer. 2016 Mar;23(3):R143-55. doi: 10.1530/ERC-15-0533.

Mika J, Łabaj W, Chekan M, Abramowicz A, Pietrowska M, Polański A, Widłak P. The mutation profile of differentiated thyroid cancer coexisting with undifferentiated

anaplastic cancer resembles that of anaplastic thyroid cancer but not that of archetypal differentiated thyroid cancer. J Appl Genet. 2021 Feb;62(1):115-120.

Nikiforova MN, Kimura ET, Gandhi M, Biddinger PW, Knauf JA, Basolo F, Zhu Z, Giannini R, Salvatore G, Fusco A, Santoro M, Fagin JA, Nikiforov YE. BRAF mutations in thyroid tumors are restricted to papillary carcinomas and anaplastic or poorly differentiated carcinomas arising from papillary carcinomas. J Clin Endocrinol Metab. 2003 Nov;88(11):5399-404.

Pita JM, Figueiredo IF, Moura MM, Leite V, Cavaco BM. Cell cycle deregulation and TP53 and RAS mutations are major events in poorly differentiated and undifferentiated thyroid carcinomas. J Clin Endocrinol Metab. 2014 Mar;99(3):E497-507.

Sa R, Liang R, Qiu X, He Z, Liu Z, Chen L. IGF2BP2-dependent activation of ERBB2 signaling contributes to acquired resistance to tyrosine kinase inhibitor in differentiation therapy of radioiodine-refractory papillary thyroid cancer. Cancer Lett. 2022 Feb 28;527:10-23

Soares P, Lima J, Preto A, Castro P, Vinagre J, Celestino R, Couto JP, Prazeres H, Eloy C, Máximo V, Sobrinho-Simões M. Genetic alterations in poorly differentiated and undifferentiated thyroid carcinomas. Curr Genomics. 2011 Dec;12(8):609-17.

Thorvaldsdóttir H, Robinson JT, Mesirov JP. Integrative Genomics Viewer (IGV): high-performance genomics data visualization and exploration. Brief Bioinform. 2013 Mar;14(2):178-92.

Volante M, Collini P, Nikiforov YE, Sakamoto A, Kakudo K, Katoh R, Lloyd RV, LiVolsi VA, Papotti M, Sobrinho-Simoes M, Bussolati G, Rosai J. Poorly differentiated thyroid carcinoma: the Turin proposal for the use of uniform diagnostic criteria and an algorithmic diagnostic approach. Am J Surg Pathol. 2007 Aug;31(8):1256-64.

Volante M, Rapa I, Gandhi M, Bussolati G, Giachino D, Papotti M, Nikiforov YE. RAS mutations are the predominant molecular alteration in poorly differentiated thyroid

carcinomas and bear prognostic impact. J Clin Endocrinol Metab. 2009 Dec;94(12):4735-41.

Volante M, Lam AK, Papotti M, Tallini G. Molecular Pathology of Poorly Differentiated and Anaplastic Thyroid Cancer: What Do Pathologists Need to Know? Endocr Pathol. 2021 Mar;32(1):63-76.

Yakushina VD, Lerner LV, Lavrov AV. Gene Fusions in Thyroid Cancer. Thyroid. 2018 Feb;28(2):158-167.

5.2 Study 4

High prevalence of potential molecular therapeutic targets in poorly differentiated thyroid carcinoma.

Aim

The aim of this study was to characterize a series of PDTC, homogeneously coded according to the most recent WHO classification of thyroid tumors, by means of a multimodal molecular approach with the objective of identifying the prevalence and potential clinical usefulness of molecular targets for therapy.

Methods

DNA and RNA extraction, immunohistochemistry, mismatch repair status, Next Generation Sequencing, OCA v3 assay, Sanger sequencing, fluorescence in situ hybridization.

Patient and tissue samples

Fifty-nine samples of PDTC were selected from the files of the Pathology Units at "San Luigi" and "Città della Salute e della Scienza" Hospitals and tested for the presence of mismatch repair defects and for DNA and RNA alterations through a wide targeted NGS approach. Due to the high number of failures in RNA analysis (see below), 25 additional PDTC samples from Mauriziano (Turin) and Reggio Emilia Hospitals were added to RNA analysis. All samples were represented by formalin fixed and paraffin embedded surgical material, retrieved from years 1993 to 2022. For all enrolled cases, histological slides were re-assessed by a pathologist (MV) to confirm the diagnosis following diagnostic criteria for PDTC proposed in the Turin Consensus (Volante et al, 2007) and embraced by the current WHO classification (Baloch et al, 2022). Major clinical and pathological data were collected and included sex, age, presence of predominant oncocytic features (>75% of the

tumor), pTN stage according to AJCC system 8th edition, presence of recurrences/metastases, site of metastases, and patient status. The study was approved by the local Ethical Committee (#610, date December 20th, 2017), and conducted in accordance with the principles set out in the Declaration of Helsinki. Considering the retrospective nature of this research protocol and that it had no impact on patients' care, no specific written informed consent was required.

Results

Mismatch repair status

All samples were adequate for analysis, with representative positivity for the tested markers in positive control cells within the tissue sections. Seven out of 59 cases (11.9%) resulted with an altered MMR protein pattern (**Figure 4_1**). In particular, four cases have MSH2-MSH6 loss, one sample MLH1-PMS2 loss, one sample MSH6 loss and one sample PMS2 loss. MSI molecular analysis on samples that showed an altered pattern of protein expression resulted with a microsatellite stable result in all cases with the panel of markers employed.

Molecular profiling

Fifty-one over 59 PDTC samples (86%) were suitable for DNA NGS analysis. The eight cases with inadequate DNA for NGS analysis had an age of blocks ranging from 2002 to 2016. Mean age in years of blocks in adequate and inadequate samples was 14 vs 11 (p=0.36).

Genomic alterations found in the series are summarized in **Figure 4_2**.

Three cases were wild type for all genes included in the NGS panel. The number of overall mutations per case ranged from 1 to 25. The most prevalent mutations were in *NRAS* (13/51, 25%) and *TP53* (13/51, 25%), all mutually exclusive each other. *TERTp* mutations were detected in 11/51 of overall cases (21.6%; 10/11 C228T [c.-124 C>T] and 1/11 C250T [c.-146 C>T]). All *TERTp* mutations detected through NGS analysis were confirmed by means of Sanger sequencing. No additional mutations in *TERTp* were detected by Sanger sequencing analysis in NGS negative cases, with an overall concordance between the two methods of 100%.

Mutations in MMR genes were detected in 10 cases (19.6%). Mutational profile in MMR genes was concordant in three samples with protein loss at immunohistochemistry, including two cases with *MSH2* mutation (one with and one without associated *MSH6* mutations) and one case with *MLH1* mutation. One additional case harbored *MLH1* mutation but loss of PMS2 protein, only. In the remaining three cases with altered expression of MMR proteins, no mutations in MMR genes were detected. Six additional cases harbored mutations in MMR genes (two *MLH1*, two *MSH2*, one *MSH6* and one *PMS2*) with no loss of MMR proteins expression.

Other genes with a prevalence of alterations more than 10% were *PTEN* (15.7%), *NF1* (13.7%), *ATM* (13.7%), *NOTCH3* (11.8%) and *BAP1* (11.8%).

NRAS mutated and *TP53* mutated cases showed different molecular characteristics. Mean number of alterations was higher in *TP53*-mutated cases (5.8 mutations/case) than in NRAS-mutated cases (2.8 mutations/case). *PIK3CA* and *TERTp* were the most prevalent co-mutated genes (three cases, each, mutually exclusive) in *NRAS*-mutated cases. *TP53*-mutated samples lacked *TERTp* co-mutations but were associated with mutations in *PTEN* and significantly in genes related to MMR system and/or loss of MMR proteins (up to 53.8% of cases, p=0.005 as compared with the other molecular subgroups). Overall, most co-mutated alterations in TP53 mutated as compared to *NRAS* mutated cases were mutually exclusive (**Figure 4_3**). A third heterogeneous group (25 cases) lacked *NRAS* or *TP53* mutations, had a low mean number of alterations (2.7 mutations/case) but was enriched for *TERTp* mutations (up to 32%). One case with *HRAS* mutation was aggregated within this group because of the co-presence of different other mutations and a low allelic frequency (14%). Copy number variations were not detected.

Twenty-eight out of 59 cases were adequate for RNA NGS analysis (47%). Due to this high rate of failure, additional 25 cases were selected. Overall, 84 samples were tested, with 43 cases passing quality controls for analysis (52%). Mean age of blocks in adequate and inadequate samples was 11 vs 12 (p=0.38).

Chromosomal rearrangements involving genes known to be translocated in thyroid cancer were found in two samples, including one case with *RET* rearrangement involving the common *RET* partner *CCDC6* and one case with the *PAX8-PPARG* fusion. Two other cases harbored a *TBL1XR1-PIK3CA* fusion (**Figure 4_4**). In the remaining 39 samples no gene fusions were detected. The presence of the *TBL1XR1-PIK3CA* fusion was associated with an altered pattern by FISH in both the two positive cases, whereas fusion negative samples showed the expected non-altered pattern (**Figure 4_5**).

Clinical and pathological correlations

The most prevalent molecular findings in our series were compared with major clinical and pathological characteristics available (**Table 4_1**). Cases showing MMR protein loss and *TERTp* mutated cases were not associated with significant clinical or pathological characteristics in our series. The three distinct molecular subgroups did not show any significant association with clinical or pathological parameters, except for a higher prevalence of oncocytic PDTC in the *TP53* mutated group. Moreover, although not reaching statistical significance, *TP53* and *TERTp* mutated cases had a higher prevalence of adverse events as compared with *NRAS* mutated cases. Survival data were available in 47 cases. The two cases with the *TBL1XR1-PIK3CA* fusion showed pathological features consistent with PDTC with no peculiar findings (**Figure 4_6**). Median survival times were calculated in the tree major subgroups. Median disease-free survival was 17, 15 and 64 months in *NRAS*-mutated, *TP53*-mutated and *TERTp*-enriched cases, respectively, with a trend to statistical significance with Log Rank test (p=0.079). Median disease-specific survival was 145, 111 and 274 months in *RAS*-mutated, *TP53*-mutated and *TERTp*-enriched cases, respectively, without a statistically significant difference.

Discussion

In the present study, we aimed at the molecular characterization of a series of PDTC diagnosed using strict classification criteria with a specific focus on the detection of alterations that might represent potential therapeutic targets.

One part of the study was designed to assess the presence and prevalence of alterations in the MMR system. Data on MMR alterations in thyroid carcinomas are relatively scarce. In a recent study on 241 thyroid carcinomas with different histologies, 7.5% of cases showed loss of MMR proteins, including two cases of PDTC (with a prevalence of MMR deficiency in 4.7% of PDTC in the Authors' series) (Qiao et al, 2022). Interestingly, the presence of MMR-deficiency or germline mutations in MMR genes in thyroid cancer have been significantly correlated with the occurrence of double primary cancers (Liu et al, 2021; Fujita et Al, 2021). In our series, nearly 12% of cases presented a MMR-deficient immunophenotype, thus showing a prevalence higher than what expected in the overall thyroid cancer population. Moreover, other six cases have mutations in MMR genes, with

an overall prevalence of 22% of cases with an alteration affecting proteins and/or genes of the pathway. This prevalence supports the hypothesis that defects in the MMR-system are sustaining molecular mechanisms of progression other than representing driver alterations (Juhlin, 2020). In terms of type of protein alterations, loss of MSH6 protein, alone or in combination with loss of MSH2, represented the most prevalent pattern, in line with the recent literature (Qiao et al, 2022). Microsatellite instability analysis using a clinically approved panel for colon and endometrial cancer failed to detect profiles of instability in all protein-altered cases. This result strongly suggest that patterns of microsatellite instability are tumor-type specific and targeted panels based on real time PCR developed for other cancer types may be not efficient to determine MMR defects in thyroid cancer (Long et al, 2020).

As for the gene-to-protein correlation, half of the cases with MMR deficiency at the protein level had mutations in MMR genes. Six other cases with MMR gene mutations had no altered protein profile, supporting that these mutations were in either heterozygosity or impaired protein functionality but not expression. Moreover, three cases with MMR-altered protein expression had no mutations in MMR genes. This observation supports the hypothesis that epigenetic regulation (i.e. promoter methylation) may be an alternative active mechanism of inactivation, as it is described for *MLH1* in colorectal and endometrial cancer. However, this mechanism is not clearly described in the literature for *MSH6*, so far. Cases with MMR defects were not associated with any clinical or pathological feature.

DNA analysis through NGS testing using a wide targeted panel revealed three major molecular types, namely a *NRAS*-mutated, a *TP53*-mutated and a *TERTp*-enriched group. *NRAS* mutations were mutually exclusive with *TP53* mutations. Key molecular features of the three subgroups were:

a) *NRAS*-mutated cancers had a low mean number of mutations and were frequently co-mutated with *PIK3CA*;

b) *TP53*-mutated cancers had the highest mean number of mutations, were frequently co-mutated with *PTEN* but lacked co-mutations in *TERTp*; moreover, all but one MMR-deficient tumor, as defined by immunohistochemistry, belonged to this group;

c) *TERTp*-enriched (double negative *NRAS* & *TP53*) cases had a mean number of mutations comparable with *NRAS*-mutated group and lacked recurrent specific mutations.

This overall scenario is in line with some previous literature data. In particular, our data strongly support that PDTC as defined by Turin consensus criteria are separate even molecularly from high-grade differentiated thyroid cancer, mainly because of the high

prevalence of *NRAS* mutations and the extremely low prevalence of *BRAF* mutations (Landa et al, 2016; Wong et al, 2021). Moreover, the mutually exclusive presence of *NRAS* and *TP53* mutations was already present in the recent study by Xu et al (Xu et al, 2022) although with a different prevalence of mutations. Finally, we observed an overall prevalence of *TERTp* mutations (all validated by Sanger sequencing) lower than in previous studies, and with a lower coincidence with *NRAS* mutations (Xu et al, 2022).

The three molecular subgroups were not associated with peculiar clinical or pathological characteristics except for the presence of predominant oncocytic features that was more prevalent in the *TP53*-mutated group as opposed to *NRAS*-mutated tumors. In terms of outcome and disease-free and disease-specific survivals, the three groups did not differ significantly. *TP53*-mutated and *TERTp*-enriched groups showed a higher proportion of cases with adverse outcome (alive with disease status or death because of cancer) but survival analyses failed to reach statistical significance. We could not confirm the adverse impact on survival of *TP53* and *TERTp* mutations observed by Xu et al (Xu et al, 2022). However, this is most probably related to the fact that PDTC cases only, and not high-grade differentiated carcinomas, were included in our study.

In terms of detection of gene fusions by RNA targeted sequencing, the prevalence of fusions already known to be present in thyroid cancer was low (2 cases, 4.6%) but comparable with previous data. More interestingly, two cases harbored the *TBL1XR1-PIK3CA* fusion, a molecular alteration never described in thyroid cancer, so far. *TBL1XR1* (Transducin beta-like 1X related protein 1, also known as TBLR1) encodes for a protein that acts as an integral subunit of the NCoR (nuclear receptor corepressor) and SMRT (silencing mediator of retinoic acid and thyroid hormone receptors) repressor complexes (Li et al, 2015). *TBL1XR1* mRNA is highly expressed in many human tissues, including thyroid, prostate and breast tissues, and may function as an oncogene by activating many signal transduction pathways, such as Wnt-β-catenin, NF-κB, and Notch (Gu et al, 2020). Rearrangement of *TBL1XR1* (3q26.32) have been identified in various cancers involving different genes, including *RARA* (17q21) (Chen et al, 2014), *HMGA1* (6p21) (Panagopoulos et al, 2016), *TP63* (3q28) (Peterson et al.,2020), *RET* (10q11.2) (Santoro et al,2020) and *PIK3CA* (3q26.32) (Stransky et al, 2014; Taghizadeh et al, 2020). In the case of *TBL1XR1-PIK3CA* fusion, the first exon of *TBL1XR1* is fused with the second exon of *PIK3CA* by inversion and leads to the complete transcription of the wild-type sequence of *PIK3CA* in the fusion transcript. *TBL1XR1* is thought to regulate the expression of nuclear hormone receptor co-repressor (Zhang et al, 2006), and tissue types in which the

TBL1XR1–PIK3CA fusions were found (invasive breast carcinoma and prostate cancer) are hormonally regulated (Stransky et al, 2014, Piscuoglio et al, 2017, Yun et al, 2020). Furthermore, TBL1XR1-PIK3CA fusions were detected in chordoma and pancreatic cancer (Taghizadeh et al, 2020; Kirchner et al, 2019). The recurrence of this alteration in our series supports the potential role of the *TBL1XR1-PIK3CA* fusion as a novel additional driver event in PDTC. The interest for this recurrent molecular event is also associated with the potential role as druggable target for therapy, as suggested in other cancer models (Taghizadeh et al, 2020).

Apart from the impact of our results in the knowledge of the pathogenesis of PDTC, the translational relevance of our data into the clinics is evincible by two main aspects. The first is the high prevalence of MMR defects in PDTC that paves the way for clinical studies testing the potential benefit of immunotherapy specifically in these tumors, as recently suggested for anaplastic thyroid cancer (Rocha et al, 2021). Secondly, a relevant number of cases harbored mutations in potentially druggable genes, mainly coding for tyrosine kinases (i.e. *PDGFRA* and *PDGFRB*, *MET*, *EGFR*, *ERBB3*, *FGFR1* and *FGFR2*). Although such mutations were individually rare (from 2 to 7% of cases), 31% of patients had at least one of such targetable alterations, thus supporting a role of tyrosine kinase inhibitors in the future clinical scenario of PDTC patients, especially when poorly responsive or progressive along radio-iodine treatment. Preclinical data on the effective activation of tyrosine kinase pathways in thyroid cancer cells further support this hypothesis (Liang et al, 2021; Sa et al, 2022).

In conclusion, PDTC in our series were genomically clustered into *NRAS*-mutated tumors (with low mutational burden and co-mutations affecting genes involved in the same pathway), *TP53*-mutated cancers (with high mutational burden, absence of *TERTp* mutations, strong association with MMR defects and predominant oncocytic features) and a third heterogeneous group enriched for *TERTp* mutations. Overall, currently or potentially targetable gene fusions have a prevalence of 9%, including the *TBL1XR1-PIK3CA* fusion that has never been described in the thyroid, so far, thus increasing the number of driver alterations and possible therapeutic targets for this aggressive disease. Finally, 38% of overall cases harbor mutations in genes coding for tyrosine kinases potentially targetable and/or have defects in the MMR that claim a high prevalence of cases candidates for target therapies including immunotherapy.

Figures and Tables

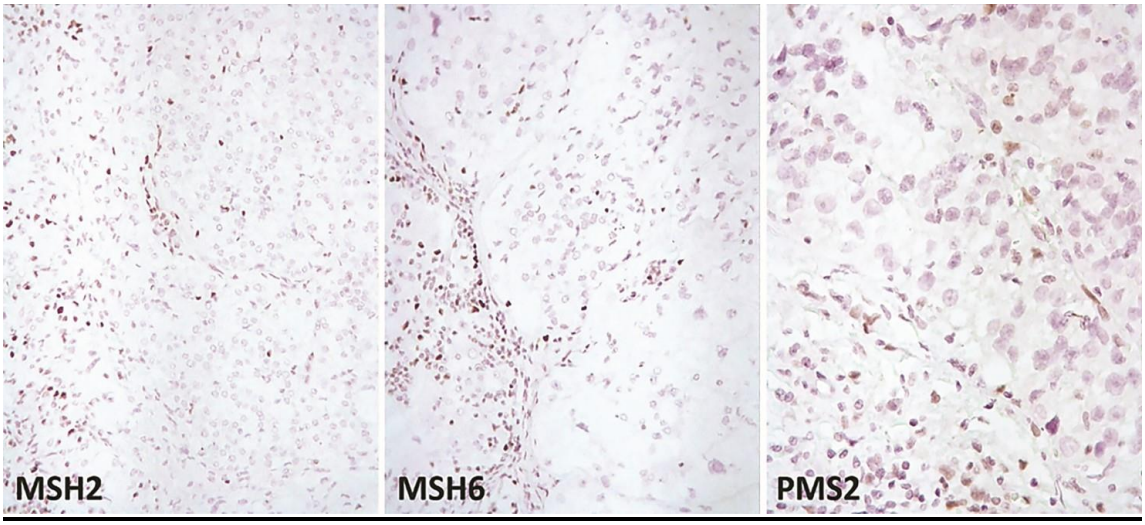

Figure 4_1: Representative images of MSH2, MSH6 and PMS2 altered expression, with negative nuclear staining in tumor cells and positive nuclear staining in non-neoplastic elements (endothelial cells and lymphocytes).

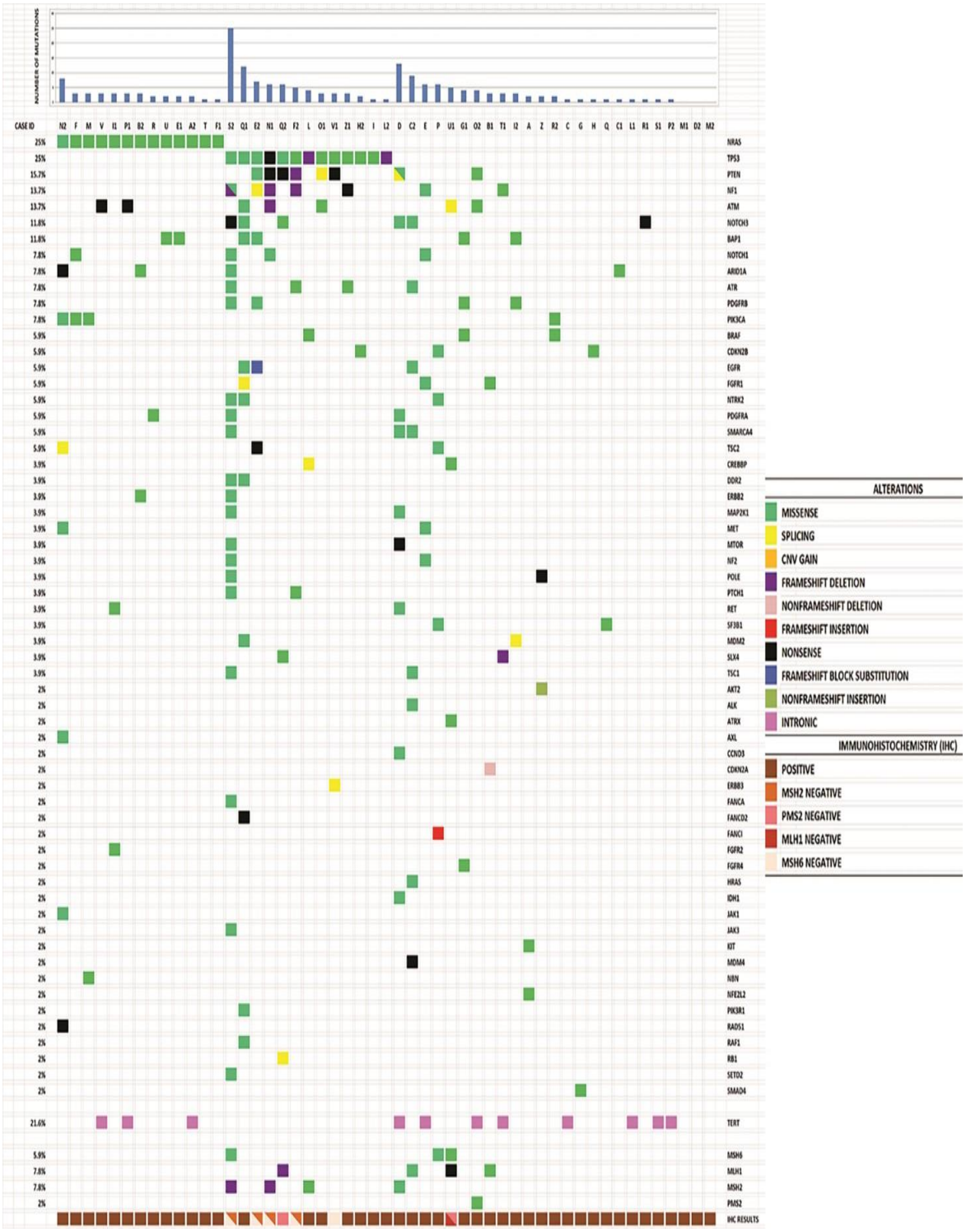

Figure 4_2: Heat map of genomic DNA alterations detected in 51 PDTCs.

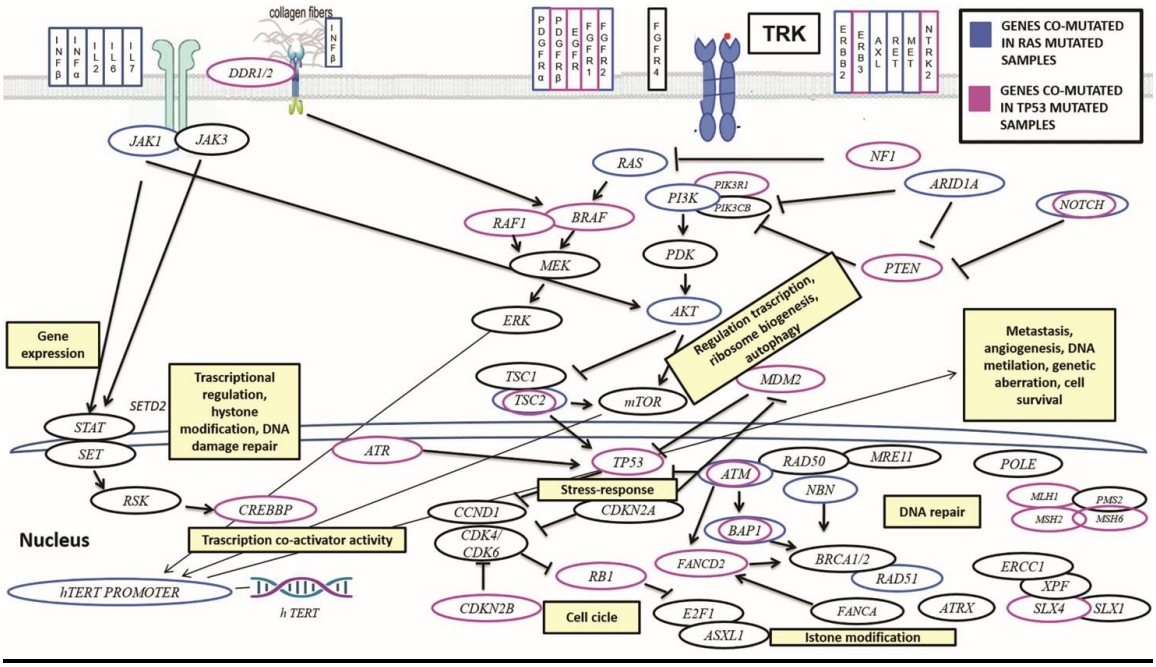

Figure 4_3: Co-mutated genes in RAS-mutated and TP53-mutated cases belong to alternative molecular pathways.

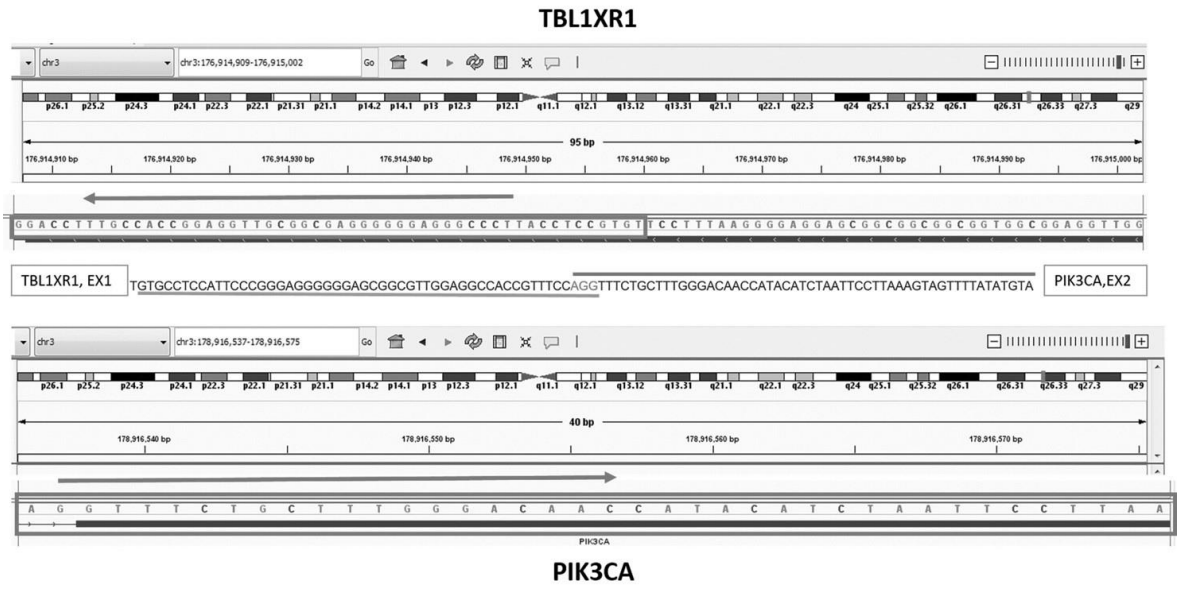

Figure 4_4: IGV image of genes involved in fusion *TBL1XR1-PIK3CA* (the first exon of *TBL1XR1* is fused to the second exon of *PIK3CA* by inversion) and overlap point between *TBL1XR1* and *PIK3CA* sequences (3 grey nucleotides, AGG).

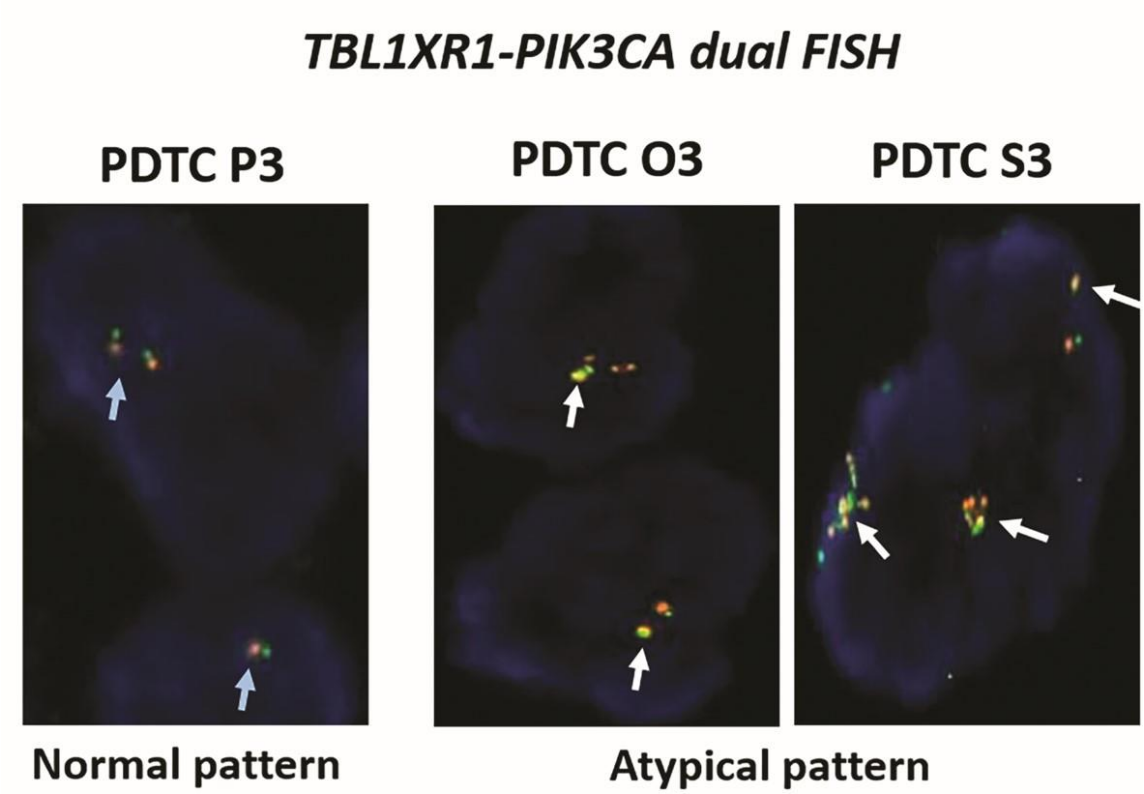

Figure 4_5: Dual FISH analysis showing abnormal pattern in two cases with TBL1XR1-PIK3CA fusion and normal pattern in a wild type case (see General Methods Chapter and corresponding Figure 1 for reference).

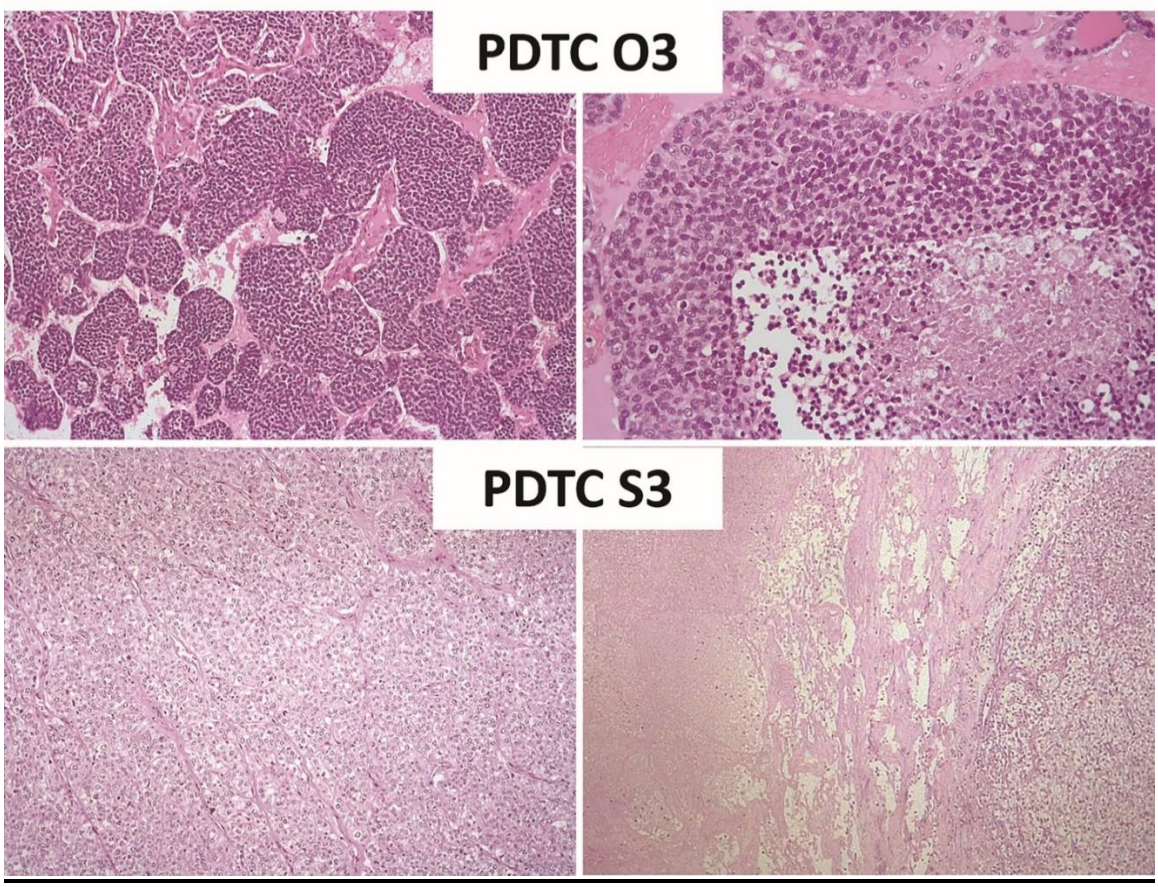

Figure 4_6: Pathological features of the two cases harboring the *TBL1XR1-PIK3CA* fusion (all hematoxylin and eosin stainings). PDTC O3 case displayed an insular growth pattern (left panel) and foci of comedonecrosis (right panel). PDTC S3 case had a solid growth (left panel) and extensive areas of necrosis (right panel).

Parameter	**MMRp**	**MMRd**	***p value***	***NRAS* mutated**	***TP53* mutated**	***TERTp* enriched**	***p value***	***TERTp* wt**	***TERTp* mutated**	***p value***
Sex (M/F)	18/26	4/3	*0.45*	5/8	6/7	11/14	*0.92*	18/22	4/7	*0.61*
Age (median, range)	62	67	*0.56*	68	67	61	*0.33*	65	61	*0.40*
Predominant oncocytic features (yes/no)	21/23	6/1	*0.10*	3/10	11/2	13/12	*0.007*	19/21	8/3	*0.13*
pT stage (pT1-2/pT3-4) (3 cases missing)	8/33	1/6	*0.99*	2/11	2/10	5/18	*0.87*	8/30	1/9	*0.42*
pN stage (pN0-NX/pN+)(3 cases missing)	25/16	3/4	*0.43*	8/5	6/6	14/9	*0.79*	21/17	7/3	*0.40*
Recurrences/metastases (Yes/no) (9 cases missing)	28/8	5/1	*0.12*	9/3	9/2	15/4	*0.92*	25/8	8/1	*0.39*
Site of metastases (lung/bone/others)	18/13/21	3/2/4	*0.97*	3/4/5	6/4/7	12/7/13	*0.92*	18/12/18	3/3/7	*0.52*
Status (NED-DOC/AWD-DOD) (2 cases missing)	14/28	1/6	*0.41*	7/6	2/11	6/17	*0.08*	12/27	2/8	*0.50*

Legend. M: male, F: female; NED: no evidence of disease; DOC: died other causes; AWD: alive with disease; DOD: died other causes; MMRp: mismatch repair proficient; MMR: mismatch repair deficient; wt: wild type

Table 4_1: Clinical pathological correlations according to molecular subgroups

References

Baloch ZW, Asa SL, Barletta JA, Ghossein RA, Juhlin CC, Jung CK, LiVolsi VA, Papotti MG, Sobrinho-Simões M, Tallini G, Mete O. Overview of the 2022 WHO Classification of Thyroid Neoplasms. Endocr Pathol. 2022 Mar;33(1):27-63.

Chen Y, Li S, Zhou C, Li C, Ru K, Rao Q, Xing H, Tian Z, Tang K, Mi Y, Wang B, Wang M, Wang J. TBLR1 fuses to retinoid acid receptor α in a variant t(3;17)(q26;q21) translocation of acute promyelocytic leukemia. Blood. 2014 Aug 7;124(6):936-45.

Fujita S, Masago K. Alteration of DNA mismatch repair capacity underlying the co-occurrence of non-small-cell lung cancer and nonmedullary thyroid cancer. Sci Rep. 2021 Feb 11;11(1):3597.

Gu JF, Fu W, Qian HX, Gu WX, Zong Y, Chen Q, Lu L. TBL1XR1 induces cell proliferation and inhibit cell apoptosis by the PI3K/AKT pathway in pancreatic ductal adenocarcinoma. World J Gastroenterol. 2020 Jul 7;26(25):3586-3602.

Juhlin CC. Aberrant DNA repair as a potential contributor for the clonal evolution in subsets of anaplastic thyroid carcinomas arising through dedifferentiation: implications for future therapeutic algorithms? Cancer Drug Resist. 2020 Nov 3;3(4):992-1000.

Kirchner M, Neumann O, Volckmar AL, Stögbauer F, Allgäuer M, Kazdal D, Budczies J, Rempel E, Brandt R, Talla SB, von Winterfeld M, Leichsenring J, Bochtler T, Krämer A, Springfeld C, Schirmacher P, Penzel R, Endris V, Stenzinger A. RNA-Based Detection of Gene Fusions in Formalin-Fixed and Paraffin-Embedded Solid Cancer Samples. Cancers (Basel). 2019 Sep 5;11(9):1309.

Landa I, Ibrahimpasic T, Boucai L, Sinha R, Knauf JA, Shah RH, Dogan S, Ricarte-Filho JC, Krishnamoorthy GP, Xu B, Schultz N, Berger MF, Sander C, Taylor BS, Ghossein R, Ganly I, Fagin JA. Genomic and transcriptomic hallmarks of poorly differentiated and anaplastic thyroid cancers. J Clin Invest. 2016 Mar 1;126(3):1052-66.

Liang J, Jin Z, Kuang J, Feng H, Zhao Q, Yang Z, Zhan L, Shen B, Yan J, Cai W, Cheng X, Qiu W. The role of anlotinib-mediated EGFR blockade in a positive feedback loop of CXCL11-EGF-EGFR signalling in anaplastic thyroid cancer angiogenesis. Br J Cancer. 2021 Aug;125(3):390-401.

Liang J, Jin Z, Kuang J, Feng H, Zhao Q, Yang Z, Zhan L, Shen B, Yan J, Cai W, Cheng X, Qiu W. The role of anlotinib-mediated EGFR blockade in a positive feedback loop of CXCL11-EGF-EGFR signalling in anaplastic thyroid cancer angiogenesis. Br J Cancer. 2021 Aug;125(3):390-401.

Long DR, Waalkes A, Panicker VP, Hause RJ, Salipante SJ. Identifying Optimal Loci for the Molecular Diagnosis of Microsatellite Instability. Clin Chem. 2020 Oct 1;66(10):1310-1318.

Xu B, David J, Dogan S, Landa I, Katabi N, Saliba M, Khimraj A, Sherman EJ, Tuttle RM, Tallini G, Ganly I, Fagin JA, Ghossein RA. Primary high-grade non-anaplastic thyroid carcinoma: a retrospective study of 364 cases. Histopathology. 2022 Jan;80(2):322-337.

Panagopoulos I, Gorunova L, Bjerkehagen B, Lobmaier I, Heim S. Fusion of the TBL1XR1 and HMGA1 genes in splenic hemangioma with t(3;6)(q26;p21). Int J Oncol. 2016 Mar;48(3):1242-50.

Peterson JF, Pearce KE, Meyer RG, Greipp PT, Knudson RA, Baughn LB, Ketterling RP, Feldman AL. Fluorescence in-situ hybridisation for TP63 rearrangements in T cell lymphomas: single-site experience of 470 patients and implications for clinical testing. Histopathology. 2020 Feb;76(3):481-485.

Piscuoglio S, Ng CKY, Geyer FC, Burke KA, Cowell CF, Martelotto LG, Natrajan R, Popova T, Maher CA, Lim RS, Bruijn I, Mariani O, Norton L, Vincent-Salomon A, Weigelt B, Reis-Filho JS. Genomic and transcriptomic heterogeneity in metaplastic carcinomas of the breast. NPJ Breast Cancer. 2017 Dec 1;3:48.

Qiao PP, Tian KS, Han LT, Ma B, Shen CK, Zhao RY, Zhang Y, Wei WJ, Chen XP. Correlation of mismatch repair deficiency with clinicopathological features and programmed death-ligand 1 expression in thyroid carcinoma. Endocrine. 2022 Jun;76(3):660-670.

Rocha ML, Schmid KW, Czapiewski P. The prevalence of DNA microsatellite instability in anaplastic thyroid carcinoma - systematic review and discussion of current therapeutic options. Contemp Oncol (Pozn). 2021;25(3):213-223.

Sa R, Liang R, Qiu X, He Z, Liu Z, Chen L. IGF2BP2-dependent activation of ERBB2 signaling contributes to acquired resistance to tyrosine kinase inhibitor in differentiation therapy of radioiodine-refractory papillary thyroid cancer. Cancer Lett. 2022 Feb 28;527:10-23.

Santoro M, Moccia M, Federico G, Carlomagno F. RET Gene Fusions in Malignancies of the Thyroid and Other Tissues. Genes (Basel). 2020 Apr 15;11(4):424.

Stransky N, Cerami E, Schalm S, Kim JL, Lengauer C. The landscape of kinase fusions in cancer. Nat Commun. 2014 Sep 10;5:4846.

Taghizadeh H, Müllauer L, Mader RM, Schindl M, Prager GW. Applied precision medicine in metastatic pancreatic ductal adenocarcinoma. Ther Adv Med Oncol. 2020 Jul 10;12:1758835920938611.

Ticha I, Hojny J, Michalkova R, Kodet O, Krkavcova E, Hajkova N, Nemejcova K, Bartu M, Jaksa R, Dura M, Kanwal M, Martinikova AS, Macurek L, Zemankova P, Kleibl Z, Dundr P. A comprehensive evaluation of pathogenic mutations in primary cutaneous melanomas, including the identification of novel loss-of-function variants. Sci Rep. 2019 Nov 19;9(1):17050.

Volante M, Collini P, Nikiforov YE, Sakamoto A, Kakudo K, Katoh R, Lloyd RV, LiVolsi VA, Papotti M, Sobrinho-Simoes M, Bussolati G, Rosai J. Poorly differentiated thyroid carcinoma: the Turin proposal for the use of uniform diagnostic criteria and an algorithmic diagnostic approach. Am J Surg Pathol. 2007 Aug;31(8):1256-64.

Wong KS, Dong F, Telatar M, Lorch JH, Alexander EK, Marqusee E, Cho NL, Nehs MA, Doherty GM, Afkhami M, Barletta JA. Papillary Thyroid Carcinoma with High-Grade Features Versus Poorly Differentiated Thyroid Carcinoma: An Analysis of Clinicopathologic and Molecular Features and Outcome. Thyroid. 2021 Jun;31(6):933-940.

Xu B, David J, Dogan S, Landa I, Katabi N, Saliba M, Khimraj A, Sherman EJ, Tuttle RM, Tallini G, Ganly I, Fagin JA, Ghossein RA. Primary high-grade non-anaplastic thyroid carcinoma: a retrospective study of 364 cases. Histopathology. 2022 Jan;80(2):322-337.

Yun JW, Yang L, Park HY, Lee CW, Cha H, Shin HT, Noh KW, Choi YL, Park WY, Park PJ. Dysregulation of cancer genes by recurrent intergenic fusions. Genome Biol. 2020 Jul 6;21(1):166.

Zhang XM, Chang Q, Zeng L, Gu J, Brown S, Basch RS. TBLR1 regulates the expression of nuclear hormone receptor co-repressors. BMC Cell Biol. 2006 Aug 7;7:31.

6.0 LUNG CARCINOIDS WITH HIGH PROLIFERATION INDEX

<u>Study 5</u>: High prevalence of potentially druggable molecular alterations in high-grade lung neuroendocrine tumors with carcinoid morphology.

Vanessa Zambelli[1], Francesca Napoli[1], Susanna Cappia[1], Angela Listì[1], Ida Rapa[2], Luisella Righi[1], Fabrizio Tabbò[1], Jasna Metovic[3], Mauro Papotti[3], Giorgio Scagliotti[1], Silvia Novello[1], Marco Volante[1]

[1]Department of Oncology, University of Turin, San Luigi Hospital, Orbassano, Turin, Italy
[2]Pathology Unit, San Luigi Hospital, Orbassano, Turin, Italy
[3]Department of Oncology, University of Turin, Città della Salute e della Scienza Hospital, Turin, Italy

(paper status: manuscript in preparation)

Neuroendocrine neoplasms (NENs) represent a rare group of tumors that are characterized by a neuroendocrine morphology and expression of neuroendocrine markers (Rindi et al, 2018; Rindi et al, 2022).

NEN may arise in different organs, including the lungs (Rindi et al, 2018). In particular, pulmonary NENs have an incidence of approximately 15% to 20% of all lung cancers (Derks et al, 2021), and can be subdivided, following the current WHO 2021 classification, into four main categories: typical carcinoids (TC) and atypical carcinoids (AC) are considered well differentiated neuroendocrine tumors (WD-NET), whereas large cell neuroendocrine carcinoma (LCNEC) and small cell neuroendocrine carcinoma (SCLC) are considered poorly differentiated neuroendocrine carcinomas (PD-NECs) (Hermans et al, 2020).

This classification is based on three histological criteria, which are:

1. the morphological differentiation status, based on architectural and cytological features;
2. the mitotic count, by counting the number of mitoses over a 2 mm^2 surface;
3. the presence or absence of tumor necrosis

AC and TC together constitutes 20-25% of all neuroendocrine tumors, and 1-2% of lung tumors (Prinzi et al, 2021; Baudin et al, 2021; Chiappetta et al, 2020) and occur in younger patients than high-grade neuroendocrine carcinomas (Hermans et al, 2020).

Lung NENs prognosis depends on histological subtypes of the tumor: TC have the best prognosis, with 10-year survival over 85% (Terzi et al, 2004); LCNEC have a median survival between 28% and 62% in 5 years; SCLC have the worst survival time around 7-11 months (Cattoni et al, 2018; Lee et al, 2015; Filosso et al, 2015); AC have a 5-year overall survival between 55% and 77% which is in between the good prognosis of TC and the poor prognosis of LCNEC and SCLC (Filosso et al, 2015; Cattoni et al, 2018).

Ki-67 index is a known prognostic parameter in lung NENs but cannot be used to separate NET from NEC (Vyas et al, 2021) despite it may be used to distingue lung carcinoids from high-grade neuroendocrine carcinomas in small biopsies (Ramirez et al, 2017; Rekhtman et al, 2022). However, TC and AC in the vast majority of cases have Ki-67 values not overcoming 10%.

Currently, gastro-entero-pancreatic (GEP) WD-NET are graded as G1, G2 or G3 depending on the mitotic rate and Ki-67 labeling index (Rindi et al, 2018). G1 and G2 are considered well differentiated, while G3 is a new category, characterized by high proliferative capacities despite well differentiated morphology of tumor cells (Rindi et

al, 2022). This category has been termed as “NET G3” and has been included, first in 2017 WHO classification of pancreatic neuroendocrine neoplasms (NENs) (Guilmette et al, 2019).

Indeed, there are recent studies that suggest the existence of well-differentiated NENs with carcinoid morphology and high proliferative index also in the lung that are characterized by a more aggressive clinical behavior as compared to TC and AC (Rubino et al, 2020; Quinn et al, 2017; Kasajima et al, 2019; Oka et al, 2020; Marchiò et al, 2017; Cros et al, 2021; Kasajima et al, 2020). These recent data claim the introduction in the lung also of a “NET G3” tumor entity (Vyas et al, 2021).

At the molecular level, the most frequently mutated gene in lung carcinoids is *MEN1* (10% of cases) (Simbolo et al, 2017; Fernandez-Cuesta et al, 2014; Derks et al, 2018), together with *ARID1A* and *EIFAX* genes (Alcala et al, 2019). On the other hand, mutations in *TP53* and *RB1* are frequently found in SCLC and in LCNEC and are rare in carcinoids (Simbolo et al, 2017). By contrast molecular alterations in genes that are treatable with a targeted inhibitor (i.e. *EGFR*, *ALK*, *ROS1*, and *BRAF*) are rare in neuroendocrine tumors, except for case reports (Grosse et al, 2019; Capodanno et al, 2012; Armengon et al, 2015). However, data on the genomic profile of lung carcinoids with high proliferation index are scarce.

References

Alcala N, Leblay N, Gabriel AAG, Mangiante L, Hervas D, Giffon T, Sertier AS, Ferrari A, Derks J, Ghantous A, Delhomme TM, Chabrier A, Cuenin C, Abedi-Ardekani B, Boland A, Olaso R, Meyer V, Altmuller J, Le Calvez-Kelm F, Durand G, Voegele C, Boyault S, Moonen L, Lemaitre N, Lorimier P, Toffart AC, Soltermann A, Clement JH, Saenger J, Field JK, Brevet M, Blanc-Fournier C, Galateau-Salle F, Le Stang N, Russell PA, Wright G, Sozzi G, Pastorino U, Lacomme S, Vignaud JM, Hofman V, Hofman P, Brustugun OT, Lund-Iversen M, Thomas de Montpreville V, Muscarella LA, Graziano P, Popper H, Stojsic J, Deleuze JF, Herceg Z, Viari A, Nuernberg P, Pelosi G, Dingemans AMC, Milione M, Roz L, Brcic L, Volante M, Papotti MG, Caux C, Sandoval J, Hernandez-Vargas H, Brambilla E, Speel EJM, Girard N, Lantuejoul S, McKay JD, Foll M, Fernandez-Cuesta L. Integrative and comparative genomic analyses identify clinically relevant pulmonary carcinoid groups and unveil the supra-carcinoids. Nat Commun. 2019 Aug 20;10(1):3407.

Armengol G, Sarhadi VK, Rönty M, Tikkanen M, Knuuttila A, Knuutila S. Driver gene mutations of non-small-cell lung cancer are rare in primary carcinoids of the lung: NGS study by ion Torrent. Lung. 2015 Apr;193(2):303-8.

Baudin E, Caplin M, Garcia-Carbonero R, Fazio N, Ferolla P, Filosso PL, Frilling A, de Herder WW, Hörsch D, Knigge U, Korse CM, Lim E, Lombard-Bohas C, Pavel M, Scoazec JY, Sundin A, Berruti A; ESMO Guidelines Committee. Electronic address: clinicalguidelines@esmo.org. Lung and thymic carcinoids: ESMO Clinical Practice Guidelines for diagnosis, treatment and follow-up☆. Ann Oncol. 2021 Apr;32(4):439-451.

Capodanno A, Boldrini L, Alì G, Pelliccioni S, Mussi A, Fontanini G. Phosphatidylinositol-3-kinase α catalytic subunit gene somatic mutations in bronchopulmonary neuroendocrine tumours. Oncol Rep. 2012 Nov;28(5):1559-66.

Cattoni M, Vallières E, Brown LM, Sarkeshik AA, Margaritora S, Siciliani A, Filosso PL, Guerrera F, Imperatori A, Rotolo N, Farjah F, Wandell G, Costas K, Mann C, Hubka M, Kaplan S, Farivar AS, Aye RW, Louie BE. Improvement in TNM staging of pulmonary

neuroendocrine tumors requires histology and regrouping of tumor size. J Thorac Cardiovasc Surg. 2018 Jan;155(1):405-413.

Chiappetta M, Sperduti I, Ciavarella LP, Leuzzi G, Bria E, Mucilli F, Lococo F, Filosso P, Ratto G, Spaggiari L, Facciolo F, Margaritora S. Prognostic score for survival with pulmonary carcinoids: the importance of associating clinical with pathological characteristics. Interact Cardiovasc Thorac Surg. 2020 Sep 1;31(3):315-323.

Cros J, Théou-Anton N, Gounant V, Nicolle R, Reyes C, Humez S, Hescot S, Thomas de Montpréville V, Guyétant S, Scoazec JY, Guyard A, de Mestier L, Brosseau S, Mordant P, Castier Y, Gentien D, Ruszniewski P, Zalcman G, Couvelard A, Cazes A. Specific Genomic Alterations in High-Grade Pulmonary Neuroendocrine Tumours with Carcinoid Morphology. Neuroendocrinology. 2021;111(1-2):158-169.

Derks JL, Leblay N, Lantuejoul S, Dingemans AC, Speel EM, Fernandez-Cuesta L. New Insights into the Molecular Characteristics of Pulmonary Carcinoids and Large Cell Neuroendocrine Carcinomas, and the Impact on Their Clinical Management. J Thorac Oncol. 2018 Jun;13(6):752-766.

Derks JL, Rijnsburger N, Hermans BCM, Moonen L, Hillen LM, von der Thüsen JH, den Bakker MA, van Suylen RJ, Speel EM, Dingemans AC. Clinical-Pathologic Challenges in the Classification of Pulmonary Neuroendocrine Neoplasms and Targets on the Horizon for Future Clinical Practice. J Thorac Oncol. 2021 Oct;16(10):1632-1646.

Fernandez-Cuesta L, Peifer M, Lu X, Sun R, Ozretić L, Seidal D, Zander T, Leenders F, George J, Müller C, Dahmen I, Pinther B, Bosco G, Konrad K, Altmüller J, Nürnberg P, Achter V, Lang U, Schneider PM, Bogus M, Soltermann A, Brustugun OT, Helland Å, Solberg S, Lund-Iversen M, Ansén S, Stoelben E, Wright GM, Russell P, Wainer Z, Solomon B, Field JK, Hyde R, Davies MP, Heukamp LC, Petersen I, Perner S, Lovly C, Cappuzzo F, Travis WD, Wolf J, Vingron M, Brambilla E, Haas SA, Buettner R, Thomas RK. Frequent mutations in chromatin-remodelling genes in pulmonary carcinoids. Nat Commun. 2014 Mar 27;5:3518.

Filosso PL, Rena O, Guerrera F, Moreno Casado P, Sagan D, Raveglia F, Brunelli A, Welter S, Gust L, Pompili C, Casadio C, Bora G, Alvarez A, Zaluska W, Baisi A, Roesel C, Thomas PA; ESTS NETs-WG Steering Committee. Clinical management of atypical carcinoid and large-cell neuroendocrine carcinoma: a multicentre study on behalf of the European Association of Thoracic Surgeons (ESTS) Neuroendocrine Tumours of the Lung Working Group†. Eur J Cardiothorac Surg. 2015 Jul;48(1):55-64.

Grosse A, Grosse C, Rechsteiner M, Soltermann A. Analysis of the frequency of oncogenic driver mutations and correlation with clinicopathological characteristics in patients with lung adenocarcinoma from Northeastern Switzerland. Diagn Pathol. 2019 Feb 11;14(1):18.

Guilmette JM, Nosé V. Neoplasms of the Neuroendocrine Pancreas: An Update in the Classification, Definition, and Molecular Genetic Advances. Adv Anat Pathol. 2019 Jan;26(1):13-30.

Hermans BCM, Derks JL, Moonen L, Habraken CHJ, der Thüsen JV, Hillen LM, Speel EJM, Dingemans AC. Pulmonary neuroendocrine neoplasms with well differentiated morphology and high proliferative activity: illustrated by a case series and review of the literature. Lung Cancer. 2020 Dec;150:152-158.

Kasajima A, Konukiewitz B, Oka N, Suzuki H, Sakurada A, Okada Y, Kameya T, Ishikawa Y, Sasano H, Weichert W, Klöppel G. Clinicopathological Profiling of Lung Carcinoids with a Ki67 Index > 20. Neuroendocrinology. 2019;108(2):109-120.

Kasajima A, Klöppel G. Neuroendocrine neoplasms of lung, pancreas and gut: a morphology-based comparison. Endocr Relat Cancer. 2020 Nov;27(11):R417-R432.

Lee KW, Lee Y, Oh SW, Jin KN, Goo JM. Large cell neuroendocrine carcinoma of the lung: CT and FDG PET findings. Eur J Radiol. 2015 Nov;84(11):2332-8.

Marchiò C, Gatti G, Massa F, Bertero L, Filosso P, Pelosi G, Cassoni P, Volante M, Papotti M. Distinctive pathological and clinical features of lung carcinoids with high proliferation index. Virchows Arch. 2017 Dec;471(6):713-720.

Oka N, Kasajima A, Konukiewitz B, Sakurada A, Okada Y, Kameya T, Weichert W, Ishikawa Y, Suzuki H, Sasano H, Klöppel G. Classification and Prognostic Stratification of Bronchopulmonary Neuroendocrine Neoplasms. Neuroendocrinology. 2020;110(5):393-403.

Prinzi N, Rossi RE, Proto C, Leuzzi G, Raimondi A, Torchio M, Milione M, Corti F, Colombo E, Prisciandaro M, Cascella T, Spreafico C, Beninato T, Coppa J, Lo Russo G, Di Bartolomeo M, de Braud F, Pusceddu S. Recent Advances in the Management of Typical and Atypical Lung Carcinoids. Clin Lung Cancer. 2021 May;22(3):161-169.

Quinn AM, Chaturvedi A, Nonaka D. High-grade Neuroendocrine Carcinoma of the Lung With Carcinoid Morphology: A Study of 12 Cases. Am J Surg Pathol. 2017 Feb;41(2):263-270.

Ramirez RA, Beyer DT, Diebold AE, Voros BA, Chester MM, Wang YZ, Boudreaux JP, Woltering EA, Uhlhorn AP, Ryan P, Campeau RJ, Anthony LB. Prognostic Factors in Typical and Atypical Pulmonary Carcinoids. Ochsner J. 2017 Winter;17(4):335-340.

Rekhtman N. Lung neuroendocrine neoplasms: recent progress and persistent challenges. Mod Pathol. 2022 Jan;35(Suppl 1):36-50.

Rindi G, Klimstra DS, Abedi-Ardekani B, Asa SL, Bosman FT, Brambilla E, Busam KJ, de Krijger RR, Dietel M, El-Naggar AK, Fernandez-Cuesta L, Klöppel G, McCluggage WG, Moch H, Ohgaki H, Rakha EA, Reed NS, Rous BA, Sasano H, Scarpa A, Scoazec JY, Travis WD, Tallini G, Trouillas J, van Krieken JH, Cree IA. A common classification framework for neuroendocrine neoplasms: an International Agency for Research on Cancer (IARC) and World Health Organization (WHO) expert consensus proposal. Mod Pathol. 2018 Dec;31(12):1770-1786.

Rindi G, Mete O, Uccella S, Basturk O, La Rosa S, Brosens LAA, Ezzat S, de Herder WW, Klimstra DS, Papotti M, Asa SL. Overview of the 2022 WHO Classification of Neuroendocrine Neoplasms. Endocr Pathol. 2022 Mar;33(1):115-154.

Rubino M, Scoazec JY, Pisa E, Faron M, Spaggiari L, Hadoux J, Spada F, Planchard D, Cella CA, Leboulleux S, De Marinis F, Ducreux M, Lamartina L, Baudin E, Fazio N. Lung carcinoids with high proliferative activity: Further support for the identification of a new tumor category in the classification of lung neuroendocrine neoplasms. Lung Cancer. 2020 Oct;148:149-158.

Simbolo M, Mafficini A, Sikora KO, Fassan M, Barbi S, Corbo V, Mastracci L, Rusev B, Grillo F, Vicentini C, Ferrara R, Pilotto S, Davini F, Pelosi G, Lawlor RT, Chilosi M, Tortora G, Bria E, Fontanini G, Volante M, Scarpa A. Lung neuroendocrine tumours: deep sequencing of the four World Health Organization histotypes reveals chromatin-remodelling genes as major players and a prognostic role for TERT, RB1, MEN1 and KMT2D. J Pathol. 2017 Mar;241(4):488-500.

Terzi A, Lonardoni A, Feil B, Spilimbergo I, Falezza G, Calabrò F. Bronchoplastic procedures for central carcinoid tumors: clinical experience. Eur J Cardiothorac Surg. 2004 Dec;26(6):1196-9.

Vyas M, Tang LH, Rekhtman N, Klimstra DS. Alterations in Ki67 Labeling Following Treatment of Poorly Differentiated Neuroendocrine Carcinomas: A Potential Diagnostic Pitfall. Am J Surg Pathol. 2021 Jan;45(1):25-34.

6.1 Study 5:

High prevalence of potentially druggable molecular alterations in high-grade lung neuroendocrine tumors with carcinoid morphology

Aim

The aim of this work was to investigate the genomic background of lung carcinoid with high proliferation index, with special reference to alterations in genes of potential therapeutic relevance.

Methods

DNA and RNA extraction; next generation sequencing (OCAv3); immunohistochemistry; fluorescence in situ hybridization; quantitative Real Time PCR; MiRNome profiling.

Patients and tissue samples

A cohort of twenty-eight lung carcinoids with high proliferation index (LC-HP) defined by the presence of a carcinoid/well differentiated neuroendocrine tumor morphology and Ki-67 index >20% were selected from the pathology files of the San Luigi and Città della Salute e della Scienza Hospitals of Turin. The series included twenty surgical and eight biopsy samples.
For gene expression analysis, an additional cohort of 20 LCNEC and 23 TC was added to build control groups. For Global miRNome profiling analysis six samples each of LC-HP, TC and LCNEC were selected, based on the quality and quantity of RNA extracts.

Results

Patients and sample characteristics

Mean age of patients was 67 years, with a range from 23 to 80 years, and most of the cases were male. Original diagnoses were AC in 16, TC in two and LCNEC in one. Nine cases diagnosed on biopsy material had a diagnosis of carcinoid, not otherwise specified. Most cases were surgical samples, whereas 11 were bronchial biopsies, transbronchial fine needle aspiration biopsies or liver biopsies.
A summary of the case series is represented in **Table 5_1**.

Gene expression patterns

By means of unsupervised cluster analysis, patterns of gene expression were able to stratify the cases into 3 major group (**Figure 5_1**), being one outlier case excluded.
The first small cluster was composed of 3 LCNEC and one LC-HP. The other two groups had a similar number of cases, with two separate patterns of distribution. One cluster, enriched for *ASCL1* and *DLL3* overexpressing cases, had four TC, 14 LCNEC and 14 LC-HP. Moreover, LC-HP cases in this cluster were mostly segregated into a sub-cluster enriched for cases with NEUROD1 overexpression. The other cluster was composed of 19 TC, two LCNEC and 5 LC-HP, and was characterized by low *ASCL1*, *DLL3* and *NEUROD1* expression. The distribution of LC-HP cases among clusters was statistically significant (Chi square test $p<0.0001$).

Global miRNome profiling

A total number of six surgical sample per group was selected to perform miRNome profiling. Unsupervised cluster analysis of surgical samples clearly segregated samples int three major groups: one group composed of six TC and one LC-HP, one group composed of one TC and 5 LCNEC and a third group composed of 2 LCNEC and 5 LC-HP (**Figure 5_2**). The distribution of LC-HP cases among clusters was statistically significant (Chi square test $p=0.0006$).
We then analyzed the expression of individual miRNAs differentially expressed among groups. MiRNAS with a p value <0.005 and a fold regulation > +/-2 were considered. LC_HP had 54 up and 20 down regulated miRNA as compared to TC, whereas LC-HP had 19 up and 11 down regulated miRNA as compared to LCNEC (**Figure 5_3**). Three miRNAs were in common between the two groups of comparison and were excluded. The list of differentially expressed miRNAs is represented in **Table 5_2**.

Identification of pathways regulated by miRNAs differentially expressed

In silico analysis of target genes of miRNAs differentially expressed between LC-HP and TC or between LC-HP and LCNEC identified a bunch of genes that act in several cellular processes, thus showing a wide complexity of pathway interactions that were different comparing TC vs LC-HP or LCNEC vs LC-HP. In the first comparison, regulation of metabolic processes (GO:0019222) was mostly represented. By contrast in LCNEC vs LC-HP comparison the differential miRNA profile mostly impacted in multicellular organismal process (GO:0032501) and developmental process (GO:0032502).

The corresponding protein interaction network of main pathways impaired by miRNA deregulation among groups obtained by STRING is showed in **Figure 5_4**.

Next generation sequencing analysis

Twenty-seven cases were suitable for NGS analysis, whereas 1 case was excluded after nucleic acid extraction due to low quality control. A total of 25 cases (92.5%) showed molecular alteration, whereas two cases lacked any molecular alteration in the genes covered by the NGS panel.

Genomic alterations found in the series are illustrated in **Figure 5_5** and listed in **Table 5_3**.

The number of overall mutations per case ranged from 1 to 18.

The most prevalent mutations were in *ATM*, *MSH2*, and *PIK3CA* (5/25, 18.5%). Mutations in *ATR*, *ERBB2*, *KRAS*, *MLH1*, *FGFR1*, *NF1*, *NOTCH3*, *POLE*, *STK11* and *TP53* were found in a high number of cases (4/27, 14.8%).

Other genes with a prevalence of alterations more than 10% were: *MSH6*, *MYCL*, *SMARCA4*, *TERT* all 11.1%.

Eleven out of 27 cases (40%) harbored mutations (single or co-occurrent) in genes that are potential therapeutic targets. Mutation in genes involved in DNA repair mechanism were found in 8 cases (29.6%), including 5 (18.5%) affecting the mismatch repair. Among tyrosine-kinases, *ERBB2/HER2*

showed the highest mutation rate, being found in two cases.

Three gene fusion were detected in three samples (11%): *ETV6/NTRK2*, *KIF5B/RET* and *EML4/ALK*.

The presence of these gene fusions was confirmed by ALK immunohistochemistry and *RET* and *NTRK* FISH (**Figure 5_6**).

Moreover, additional potential druggable molecular alterations, all not exclusive, were found in *RET*, *FGFR1*, *NTRK1* (in one sample, each) and *KRAS* G12C (in two samples).

Discussion

The existence of LC-HP is supported by both morphological and clinical data. In fact, morphology recognizes cases with a discordant pattern in terms of well differentiated morphology but high proliferation index (Hermans et al, 2020) that behave intermediate between carcinoids (TC and AC) and high grade neuroendocrine carcinomas (Rubino et al, 2020). The discrepancy between morphology and proliferation/mitotic index is responsible for a possible dishomogeneity of classification in these tumors. In fact, in our series one sample was originally diagnosed as LCNEC despite a well differentiated tumor morphology.

The few molecular data available on LC-HP, so far, reinforce the concept that these tumors occupy an intermediate position between carcinoids and neuroendocrine carcinomas. Gene expression profiling studies support the existence of a grey zone between atypical carcinoids and large cell neuroendocrine carcinomas. In one study, atypical carcinoids and large cell neuroendocrine carcinomas have been clustered into three groups. Two groups were enriched for atypical carcinoids or large cell neuroendocrine carcinomas, respectively, and the genomic findings and outcome of the patients were as would be expected for the respective histotype. A third group was composed of mixed histologies, intermediate molecular features and a survival similar to atypical carcinoid-type cluster (Simbolo et al, 2019). In another study, four samples classified as borderline neuroendocrine tumor because of the presence of well differentiated neuroendocrine morphology and increased Ki-67 or mitotic rates were clustered mostly with carcinoids but one case with LCNEC (Sazonova et al, 2020). Our data focusing on gene expression patterns of transcriptional regulators of neuroendocrine differentiation showed an overall picture that supports the concept that LC-HP are more similar to LCNEC but falling into a separate category. In particular, LC-HP were characterized by high levels of expression of *ASCL1* and *DLL3*, that are described to be highly expressed in LCNEC (Yoshimura et al, 2022; Hermans et al, 2019).

As to concern miRNA profiling data, LC-HP were segregated more closely to LCNEC but - as for gene expression data - most cases fell in a separate cluster. Although our data cannot be compared with the literature, this observation reinforce the same hypothesis generated by gene expression profiling. The predicted consequence of miRNA

deregulation in the two groups of comparison (TC vs LC-HP and LCNEC vs LC-HP) identified different pathways specifically impaired. Although pathway classification is generalistic and descriptive in purpose, since the predicted pathways are not shared in the two groups of comparison, we can conclude that LC-HP have a distinct position between TC and LCNEC.

A few small studies in the literature were specifically aimed at the molecular characterization of LC-HP. In a series of cases at advanced stage of disease, no alterations in *RB1* or *TP53* were detected, whereas mutations on chromatin-modifier genes (*MEN1*, *ARID1A*, *ARID1B*, and *KDM5C*) were present in more than 50% of cases (Rekhtman et al, 2019). In another study (Cros et al, 2021) LC-HP displayed molecular alterations in tumor suppressor genes belonging to pathways commonly altered in both carcinoids and neuroendocrine carcinomas of the lung, including chromatin remodeling, DNA repair and cell cycle. Moreover, based on data in cases with spatial and/or temporal heterogeneity, this study proposes an evolutionary model from clones of lower aggressivity through the accumulation of "neuroendocrine carcinoma-like" genetic alterations, such as *TP53*/*RB1* alterations. Our data are slightly in contrast with what above. In fact, although mutations affecting both chromatin remodeling genes and *TP53*/*RB1* were detected, a significant proportion of cases harbored mutations in genes characterizing non-small cell lung carcinoma, such as those in *PIK3CA*, *ERBB2*, *KRAS* or *STK11*. In particular, we detected *PIK3CA* and *KRAS* mutations in about 18 and 15% of cases, respectively, percentages that are pretty much higher than what described in lung carcinoids (Volante et al, 2021; Armengol et al, 2015; Simbolo et al, 2017). We also found four cases with *ERBB2* mutation, a gene that is usually altered in LCNEC (Baine et al, 2020) but not in carcinoids. Finally, gene fusions were detected in more than 10% of cases. Although described in lung carcinoids as cases reports, *ALK* and *RET* fusions are of particular interest since they are potential clinically relevant targets for therapy in these tumors (Gococo-Benore et al, 2022; Kander et al, 2021; Lei et al, 2022)

In conclusion, despite these tumors needs to be investigated more deeply, we have found a high prevalence of potential druggable molecular alterations, most of them not included in the classical molecular genotype of carcinoids, supporting the need to identify these tumors as a separate group among lung neuroendocrine neoplasms and opening the way to novel potential therapies.

Figures and Tables

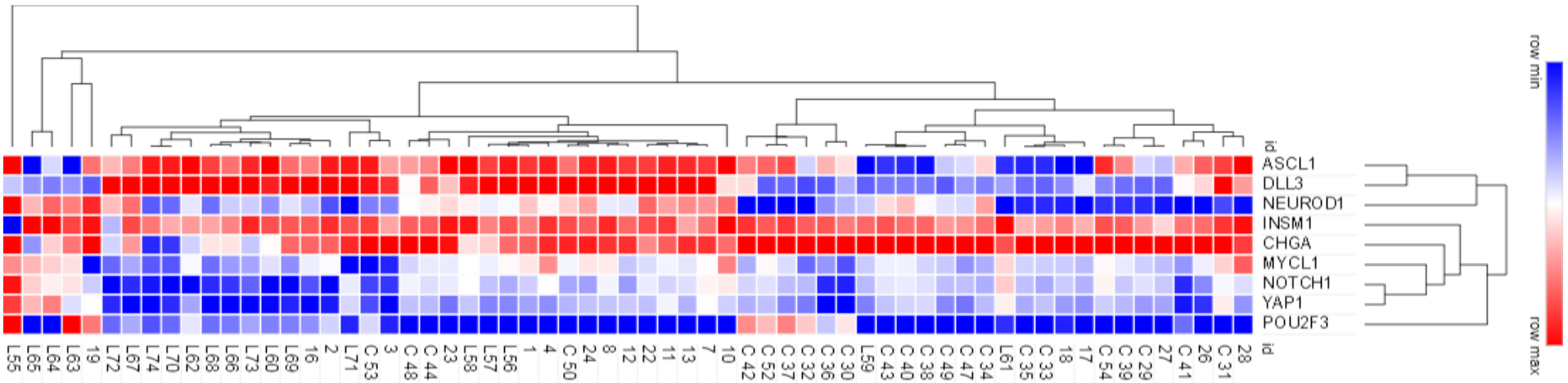

Figure 5_1: Unsupervised cluster analysis of the entire cohort, with subgroup division indicated. LC-HP are listed as numbers; LCNEC are indicated as “L” and carcinoids are indicated with “C”, these last two are listed as the representative letter followed by a number.

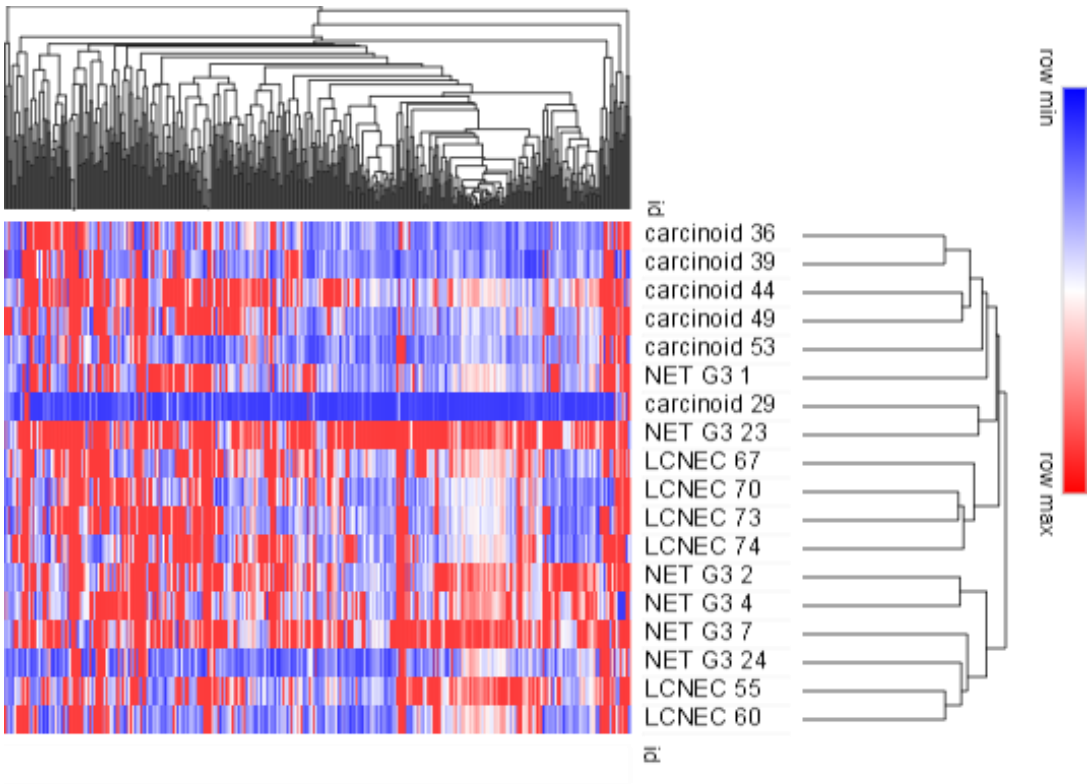

Figure 5_2: Unsupervised cluster analysis based on global microRNA profiling of LCNEC, TC (carcinoids) and LC-HP (indicated as NET G3 in the figure).

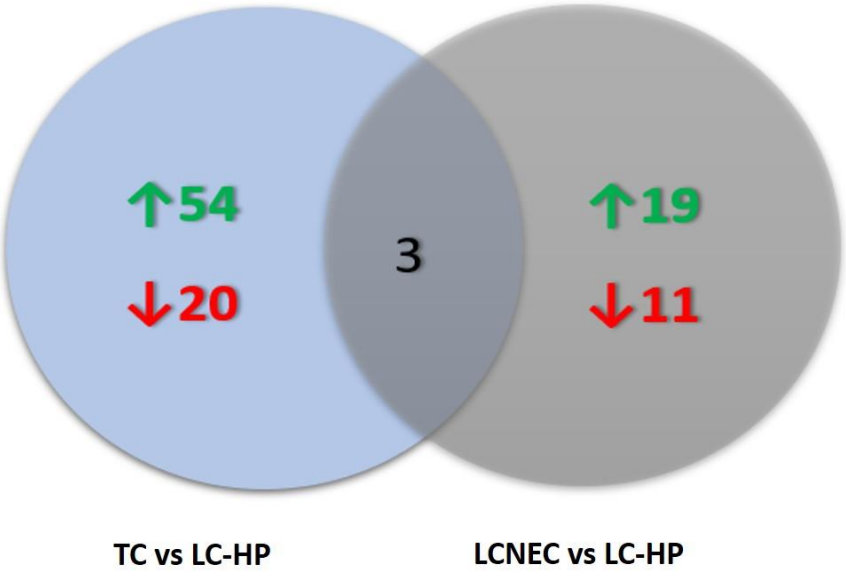

Figure 5_3: miRNAs differentially expressed between: carcinoid/LC-HP and LCNEC/LC-HP

up

hsa-miR-659-3p
hsa-miR-520d-3p
hsa-miR-646
hsa-miR-155-5p
hsa-miR-650
hsa-miR-619-3p
hsa-miR-766-3p
hsa-miR-202-3p
hsa-miR-623
hsa-miR-629-5p
hsa-miR-632
hsa-miR-216a-5p
hsa-miR-216b-5p
hsa-miR-302d-5p
hsa-miR-33b-5p
hsa-miR-146b-3p
hsa-miR-1299
hsa-miR-1207-3p
hsa-miR-1291
hsa-miR-920
hsa-miR-943
hsa-miR-18b-3p
hsa-miR-218-2-3phsa-miR-1257
hsa-miR-1276
hsa-miR-323b-5p
hsa-miR-19b-1-5p
hsa-miR-10a-3p
hsa-miR-4316
hsa-miR-2278
hsa-miR-4315
hsa-miR-642b-3p
hsa-miR-3666
hsa-miR-3667-3p
hsa-miR-593-5p
hsa-miR-3186-3p
hsa-miR-2276-3p
hsa-miR-3654
hsa-miR-3147
hsa-miR-16-1-3p
hsa-miR-3132
hsa-miR-3688-3p
hsa-miR-3127-5p
hsa-miR-214-5p
hsa-miR-4257
hsa-miR-2116-3p
hsa-miR-4303
hsa-miR-3617-5p
hsa-miR-4290
hsa-miR-4299
hsa-miR-101-5p
hsa-miR-3121-3p
hsa-miR-1914-3p
hsa-miR-3134

down

hsa-miR-375
hsa-miR-130a-3p
hsa-miR-183-5p
hsa-miR-324-5p
hsa-miR-24-3p
hsa-miR-185-5p
hsa-miR-125a-5p
hsa-miR-23b-3p
hsa-miR-361-5p
hsa-miR-23a-3p
hsa-miR-103a-3p
hsa-miR-182-5p
hsa-miR-129-5p
hsa-miR-140-3p
hsa-miR-7-5p
hsa-miR-151a-3p
hsa-miR-99b-5p
hsa-miR-1301-3p
hsa-miR-1180-3p
hsa-miR-374c-5p

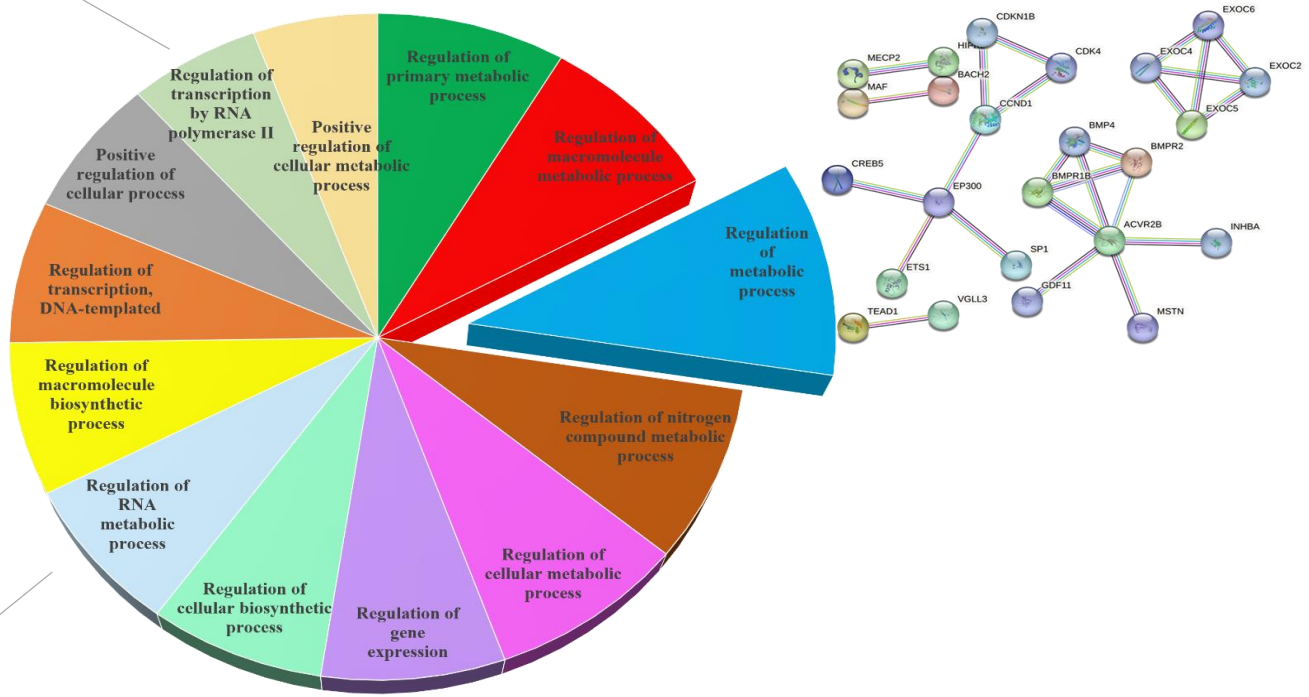

A

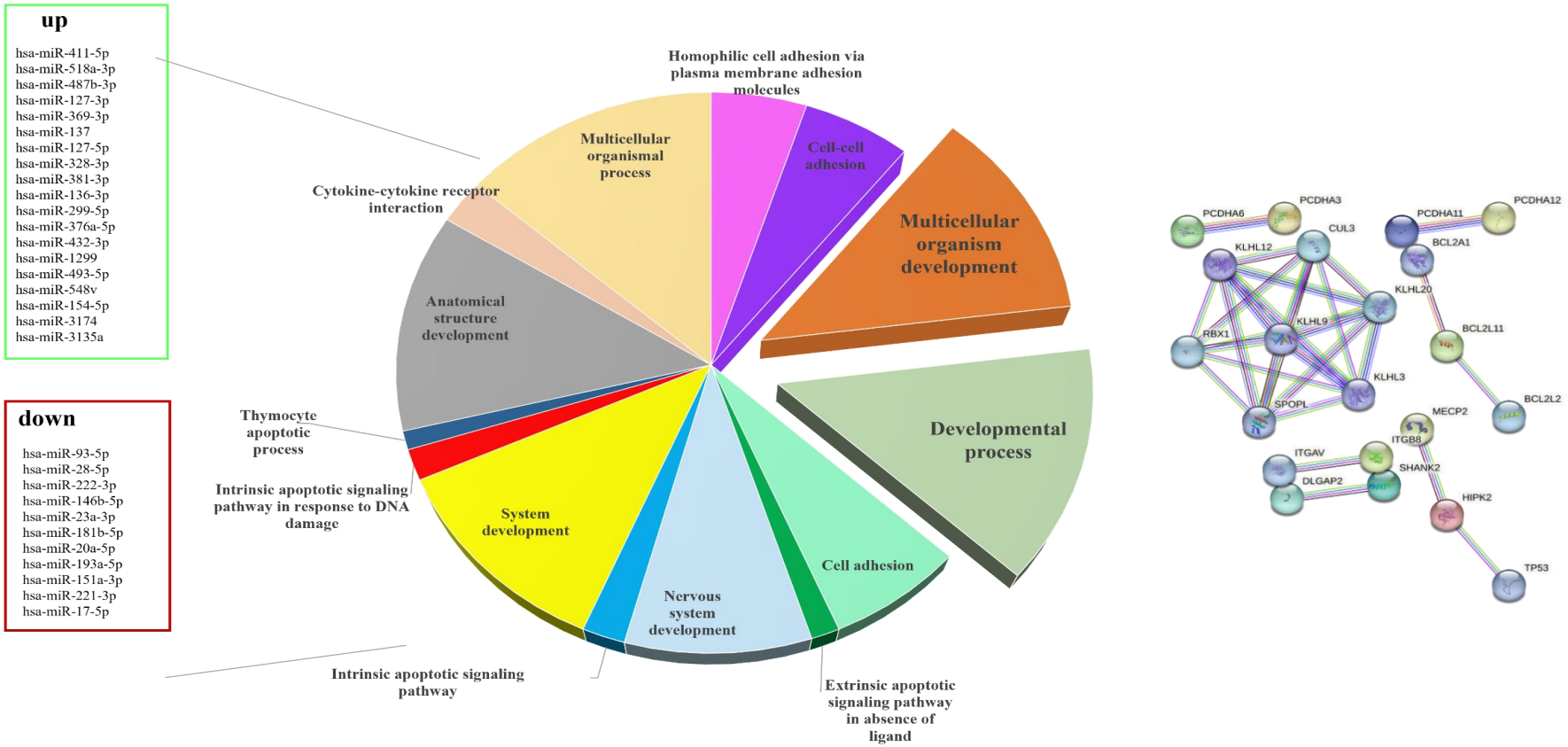

B

Figure 5_4: A) List of miRNAs up and down regulated between TC and LC-HP. B) List of miRNAs up and down regulated between LCNEC and LC-HP. The cake graphics represent pathways that are regulated by those miRNAs. Protein interactions that are related to these pathways are shown on the left.

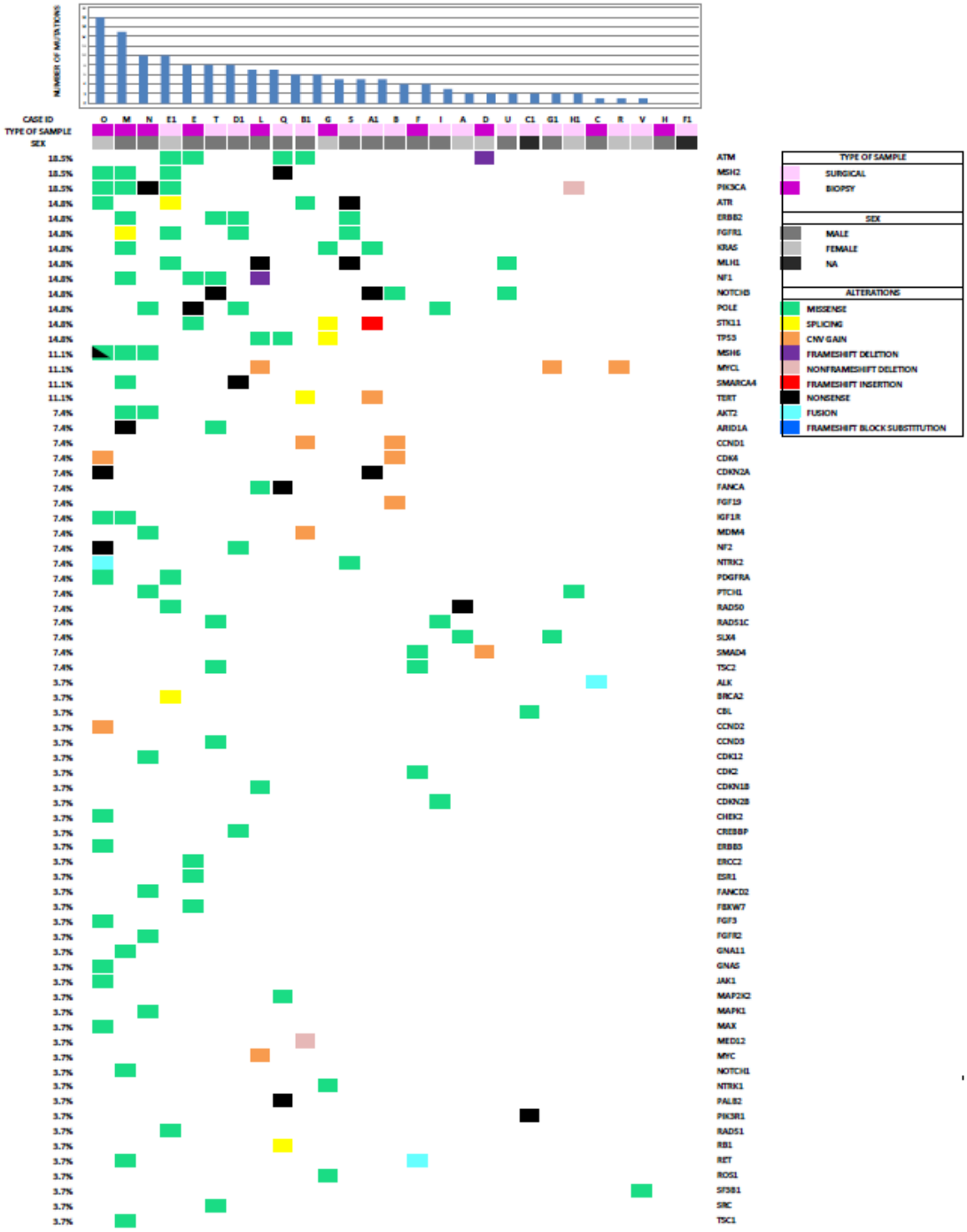

Figure 5_5: Gene mutation representative heatmap.

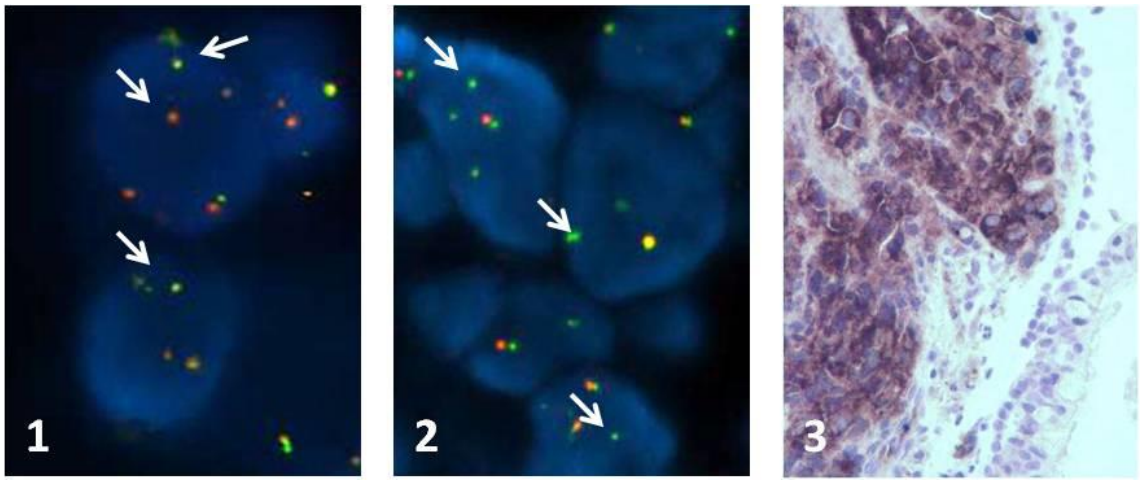

Figure 5_6: 1) and 2) dual FISH analysis showing abnormal pattern in cases with fusions: *ETV6/NTRK2* and *KIF5B/RET* respectively (see General methods for reference); and 3) immunohistochemistry showing ALK overexpression in the case harboring the *EML4/ALK* fusion.

ID SAMPLE	SEX	AGE	ORIGINAL DIAGNOSIS	KI67 (%)	MITOTIC INDEX (in $2mm^2$)	TYPE OF SAMPLE
A	F	78	TYPICAL CARCINOID	30	1	SURGICAL, LUNG
B	M	79	ATYPICAL CARCINOID	40	5	SURGICAL, LUNG
C	M	79	CARCINOID NAS	22	//	BRONCHIAL BIOPSY
D	F	60	CARCINOID NAS	30	//	TBNA
E	M	80	ATYPICAL CARCINOID	50	//	BRONCHIAL BIOPSY
F	M	75	CARCINOID NAS	20	//	BRONCHIAL BIOPSY
G	F	53	CARCINOID NAS	20	//	BRONCHIAL BIOPSY
H	M	75	CARCINOID NAS	22	//	BRONCHIAL BIOPSY
I	M	60	ATYPICAL CARINOID	28	5	SURGICAL, LUNG
L	M	75	CARCINOID NAS	30	//	TBNA
M	M	76	CARCINOID NAS	20	//	LIVER BIOPSY
N	M	53	CARCINOID NAS	35	//	LIVER BIOPSY
O	F	53	CARCINOID NAS	50	//	BRONCHIAL BIOPSY
P	M	74	ATYPICAL CARCINOID	20	//	TBNA
Q	M	45	ATYPICAL CARCINOID	43	5	SURGICAL, LYMPHNODE
R	F	75	ATYPICAL CARCINOID	27	3	SURGICAL, LUNG
S	M	72	ATYPICAL CARCINOID	40	5	SURGICAL, LUNG
T	M	69	ATYPICAL CARCINOID	20	3	SURGICAL, LUNG
U	M	23	LCNEC	35	12	SURGICAL, LUNG
V	F	65	ATYPICAL CARCINOID	30	4	SURGICAL, LUNG
A1	M	77	ATYPICAL CARCINOID	36	10	SURGICAL, LUNG
B1	M	79	ATYPICAL CARCINOID	20	8	SURGICAL, LUNG
C1	NA	NA	ATYPICAL CARCINOID	25	9	SURGICAL, LUNG
D1	M	44	ATYPICAL CARCINOID	20	3	SURGICAL, LUNG
E1	F	72	TYPICAL CARCINOID	20	1	SURGICAL, LUNG
F1	NA	NA	ATYPICAL CARCINOID	20	2	SURGICAL, LUNG
G1	M	71	ATYPICAL CARCINOID	35	10	SURGICAL, LUNG
H1	F	78	ATYPICAL CARCINOID	45	6	SURGICAL, LUNG

Table 5_1: Main data of cases of LC-HP collected for the study. TBNA: transbronchial needle aspiration.

TC *vs* LC-HP				**LCNEC *vs* LC-HP**			
Up-regulated miRNA	**Fold regulation**	***p value***	**Target genes**	**Up-regulated miRNA**	**Fold regulation**	***p value***	**Target genes**
hsa-miR-659-3p	3.7	0.000112	ONECUT2	**hsa-miR-411-5p**	3.67	0.000729	MECP2
hsa-miR-520d-3p	5.79	0.004818	CPEB2	**hsa-miR-518a-3p**	2.84	0.002877	CUGBP2
hsa-miR-646	2.8	0.012586	MECP2	**hsa-miR-487b-3p**	6.06	0.004128	HIPK2
hsa-miR-155-5p	4.16	0.013657	PURB	**hsa-miR-127-3p**	4.32	0.003752	
hsa-miR-650	4.76	0.058153	TNRC6B	**hsa-miR-369-3p**	3.66	0.000892	
hsa-miR-619-3p	4.56	0.003696	SH3PXD2A	**hsa-miR-137**	3.27	0.00344	
hsa-miR-766-3p	2.45	0.016212	NUFIP2	**hsa-miR-127-5p**	4.1	0.000231	
hsa-miR-202-3p	4.35	0.035013	KCNA1	**hsa-miR-328-3p**	3.74	0.000939	
hsa-miR-623	3.16	0.059954	AAK1	**hsa-miR-381-3p**	3.5	0.001874	
hsa-miR-629-5p	4.8	0.003036	JHDM1D	**hsa-miR-136-3p**	5.54	0.000017	
hsa-miR-632	4.23	0.037849	BNC2	**hsa-miR-299-5p**	6.96	0.003494	
hsa-miR-216a-5p	5.83	0.035984	ZNF618	**hsa-miR-376a-5p**	2.99	0.000914	
hsa-miR-216b-5p	6.17	0.041165	CREB5	**hsa-miR-432-3p**	2.9	0.00187	
hsa-miR-302d-5p	2.69	0.013668	POU2F2	**hsa-miR-1299**	3.76	0.002387	
hsa-miR-33b-5p	3.78	0.014792	NFAT5	**hsa-miR-493-5p**	3.86	0.000952	
hsa-miR-146b-3p	4.66	0.04246	CBL	**hsa-miR-548v**	3.46	0.001178	
hsa-miR-1299	3.78	0.032199	DCX	**hsa-miR-154-5p**	4.41	0.001854	
hsa-miR-1207-3p	5.49	0.00256	BAHD1	**hsa-miR-3174**	3.48	0.001467	
hsa-miR-1291	3.73	0.031526	BCAT1	**hsa-miR-3135a**	2.53	0.002251	
hsa-miR-920	5.65	0.034263	KPNA6				
hsa-miR-943	2.38	0.06878	ETS1				
hsa-miR-18b-3p	4.2	0.000936	DLGAP2				
hsa-miR-218-2-3p	3.3	0.046368	GATAD2B				
hsa-miR-1257	3.36	0.006189	HIPK2				
hsa-miR-1276	4.63	0.044866	CCND1				

hsa-miR-323b-5p	3.61	0.020791	CREBZF				
hsa-miR-19b-1-5p	4.73	0.020122	TEAD1				
hsa-miR-10a-3p	6.22	0.00053	ARL4C				
hsa-miR-4316	4.34	0.032911	CPEB4				
hsa-miR-2278	4.98	0.000406	RPS6KA3				
hsa-miR-4315	4.56	0.051813	SERBP1				
hsa-miR-642b-3p	4.05	0.044861	ACVR2B				
hsa-miR-3666	5.17	0.03514	RNF165				
hsa-miR-3667-3p	5.82	0.011775					
hsa-miR-593-5p	2.22	0.144825					
hsa-miR-3186-3p	2.88	0.012551					
hsa-miR-2276-3p	4.37	0.017139					
hsa-miR-3654	4.06	0.060378					
hsa-miR-3147	4.09	0.001615					
hsa-miR-16-1-3p	3.26	0.032506					
hsa-miR-3132	4.74	0.023913					
hsa-miR-3688-3p	6.05	0.013536					
hsa-miR-3127-5p	4.23	0.042221					
hsa-miR-214-5p	4.28	0.04101					
hsa-miR-4257	4.72	0.035693					
hsa-miR-2116-3p	4.01	0.032798					
hsa-miR-4303	3.29	0.057111					
hsa-miR-3617-5p	6.33	0.034053					
hsa-miR-4290	3.83	0.00127					
hsa-miR-4299	2.34	0.078983					
hsa-miR-101-5p	4.47	0.039095					
hsa-miR-3121-3p	4.37	0.023918					
hsa-miR-1914-3p	3.74	0.043431					
hsa-miR-3134	6.05	0.03422					

Down-regulated miRNA	Fold regulation	*p value*	Target genes	Down-regulated miRNA	Fold regulation	*p value*	Target genes
hsa-miR-375	-8.04	0.003785	TNRC6B	**hsa-miR-93-5p**	-5.13	0.042819	NUFIP2
hsa-miR-130a-3p	-2.15	0.002091	CUGBP2	**hsa-miR-28-5p**	-4.12	0.023429	ANKRD52
hsa-miR-183-5p	-4.67	0.002168	BACH2	**hsa-miR-222-3p**	-6.3	0.046045	PCDHA6
hsa-miR-324-5p	-4.15	0.003083	TET3	**hsa-miR-146b-5p**	-10.83	0.064327	PCDHA11
hsa-miR-24-3p	-6.2	0.003218	NFIB	**hsa-miR-23a-3p**	-4.02	0.019324	PCDHA1
hsa-miR-185-5p	-4.78	0.003645	TRPS1	**hsa-miR-181b-5p**	-5.93	0.050025	PCDHA7
hsa-miR-125a-5p	-4.03	0.000149	SP1	**hsa-miR-20a-5p**	-12.4	0.052374	PCDHA5
hsa-miR-23b-3p	-7.21	0.001819	BMPR1B	**hsa-miR-193a-5p**	-2.86	0.001298	PCDHA4
hsa-miR-361-5p	-4.65	0.173135	ESRRG	**hsa-miR-151a-3p**	-2.57	0.059039	PCDHA2
hsa-miR-23a-3p	-3.99	0.001819	FLJ20309	**hsa-miR-221-3p**	-7.34	0.017586	DNAL1
hsa-miR-103a-3p	-4.19	0.001975	PURB	**hsa-miR-17-5p**	-8.65	0.018193	PCDHA12
hsa-miR-182-5p	-3.65	0.001256	MECP2				THRB
hsa-miR-129-5p	-14.54	0.003074	ATXN1				PCDHA3
hsa-miR-140-3p	-2.8	0.000288	BMPR2				PCDHA8
hsa-miR-7-5p	-10.61	0.000537	SNX27				PCDHAC1
hsa-miR-151a-3p	-2.37	0.004077	BRWD1				TANC2
hsa-miR-99b-5p	-4.96	0.000445	NUFIP2				ATXN1
hsa-miR-1301-3p	-2.66	0.003948	SOX11				TNRC6B
hsa-miR-1180-3p	-4.54	0.001712	BNC2				PCDHA10
hsa-miR-374c-5p	-4.02	0.000548	EXOC5				AAK1
			TEAD1				PCDHA13
			ATRN				TRPS1
			EBF3				WDR37
			ZNF395				CUL3
			SPOPL				PCDHAC2
			ANKRD52				PLCXD3
			YWHAG				NFAT5
			CPEB2				ABL2
			PTAR1				ZNF618
			SIRPA				BCL2L11

			MTF1 NFIX VGLL3 KLHL28 SSH2 ACVR2B PITPNA MAF				BCL11B UBE2J1 TMCC1 PPP3R1 CAPRIN2 JAZF1 ITGB8 SLC4A4 DLGAP2 DYRK1A SLAIN2 PURB SHANK2 FRS2 MIDN ZFPM2 ZADH2 EIF5A2 CSNK1G1 FNDC3A

Table 5_2: List of all miRNAs up and down regulated and targeted genes between TC and LC-HP and between LCNEC and LC-HP.

CASE ID	DNA ALTERATIONS			RNA FUSIONS	CNV
	GENE	AMINO ACID CHANGE	ALLELIC FREQUENCY (%)		
O	ERBB3	p.His292Tyr	14.17	ETV6(5)-NTRK2(16)	CDK4 12q14.1(58142245-58145450)
	FGF3	p.Ser108Leu	13.75		CCND2 12p13.32(4383096-4409149)
	GNAS	p.Arg201Cys	9.46		
	MAX	p.Arg35Cys	16.19		
	PIK3CA	p.Arg349Gln	5.69		
	CDKN2A	p.Arg80Ter	53.40		
	CHEK2	p.Gly403Arg	34.76		
	JAK1	p.Arg681Gln	18.06		
	MSH6	p.Arg911Ter	18.18		
	MSH6	p.Gly1002Asp	11.56		
	NF2	p.Arg262Ter	17.66		
	MSH2	p.Ser699Leu	10.03		
	ATR	p.Gly1181Asp	15.40		
	IGF1R	p.Cys455Tyr	17.17		
	PDGFRA	p.Pro553Leu	21.45		
M	AKT2	p.Thr148Ile	12.00	WT	WT
	ERBB2	p.Leu800Pro	12.24		
	IGF1R	p.Val1200Ile	14.12		
	GNA11	p.Arg181Gln	19.14		
	NOTCH1	p.Arg1824Trp	9.87		
	PIK3CA	p.Pro539His	12.97		
	ARID1A	p.Arg1722Ter	21.00		
	KRAS	p.Gly12Cys	9.34		
	TSC1	p.Pro169Ser	11.89		
	MSH2	p.Pro591Ser	23.16		
	SMARCA4	p.Gly775Ser	14.20		
	NOTCH1	p.Asp2108Asn	12.43		
	NF1	p.Ser2064Phe	12.69		
	MSH6	p.Ala481Gly	9.92		
	FGFR1	p.?	6.35		
N	PIK3CA	p.Trp328Ter	15.99	WT	WT
	MAPK1	p.Glu322Lys	12.60		
	FANCD2	p.Arg1321Gln	20.1		
	FGFR2	p.Gly305Arg	17.92		
	AKT2	p.Glu85Lys	14.41		
	CDK12	p.Arg779His	13.54		

	MSH6	p.Ala794Asp	8.63		
	PTCH1	p.Gly1054Arg	10.02		
	POLE	p.Asp1123Tyr	11.91		
	MDM4	p.Ala40Gly	14.07		
E1	PIK3CA	p.Arg108His	7.62	WT	WT
	MLH1	p.Gly67Arg	7.25		
	MSH2	p.Gly587Ser	7.33		
	ATM	p.Ser974Phe	15.74		
	RAD51	p.Ala176Val	7.35		
	PDGFRA	p.Ser851Leu	12.82		
	FGFR1	p.Val279Met	14.01		
	RAD50	p.Arg224His	42.66		
	ATR	p.?	10.36		
	BRCA2	p.?	9.40		
E	ATM	p.Gly2536Glu	8.16	WT	WT
	ATM	p.Leu752Pro	60.45		
	NF1	p.Lys1457Arg	9.52		
	ESR1	p.Gly276Cys	10.93		
	ERCC2	p.Arg112Cys	14.95		
	STK11	p.Pro275Thr	19.92		
	POLE	p.Tyr2269Ter	10.43		
	FBXW7	p.Arg309His	30.46		
T	ERBB2	p.Val773Met	5.00	WT	WT
	NOTCH3	p.Arg1036Ter	6.21		
	NF1	p.Arg720Trp	18.60		
	SRC	p.Arg391His	5.44		
	TSC2	p.Ser174Leu	5.74		
	CCND3	p.Arg114Cys	6.15		
	ARID1A	p.Arg1980His	7.92		
	RAD51C	p.Arg366Gln	5.00		
D1	FGFR1	p.Asp351Asn	5.98	WT	WT
	ERBB2	p.Arg940Gln	6.31		
	CREBBP	p.Arg1664Cys	7.07		
	SMARCA4	p.Arg1653Ter	7.66		
	NF2	p.Arg376Trp	6.48		
	POLE	p.Gly1501Arg	7.24		
	POLE	p.Asp1783Asn	9.17		
	POLE	p.Thr528Met	13.11		

L	TP53	p.Arg158Pro	61.98	WT	MYC 8q24.21(128748724-128753198)
	MLH1	p.Arg659Ter	6.01		MYCL 1p34.2(40362966-40367017)
	NF1	p.Glu1928LysfsTer14	42.58		
	FANCA	p.Thr561Met	5.83		
	CDKN1B	p.Asp17Tyr	55.66		
Q	PALB2	p.Gln759Ter	5.00	FAIL	WT
	MSH2	p.Arg383Ter	5		
	FANCA	p.Arg591Ter	6.12		
	TP53	p.Ser367Asn	8.11		
	MAP2K2	p.Leu105Phe	10.38		
	ATM	p.Glu1978Lys	10.94		
	RB1	p.?	77.22		
B1	MED12	p.Asp34_Leu36delinsVal	93.28	WT	MDM4 1q32.1(204494576-204518712)
	ATR	p.Gly874Arg	7.3		CCND1 11q13.3(69455972-69466035)
	ATM	p.Asp2448His	87.46		
	TERT	p.?	11.54		
G	KRAS	p.Gly12Cys	53.24	WT	WT
	NTRK1	p.Gly595Trp	23.37		
	ROS1	p.Pro2021Ser	25.63		
	STK11	p?	59		
	TP53	p?	36		
S	MLH1	p.Gln409Ter	5.95	WT	WT
	ERBB2	p.Gly909Asp	7.5		
	ATR	p.Gln1638Ter	6.27		
	FGFR1	p.Asn577Lys	46.59		
	NTRK2	p.Ala677Thr	8.33		
A1	CDKN2A	p.Arg80Ter	28.61	WT	TERT 5p15.33(1253820-1295326)x8.15385
	KRAS	p.Gly12Val	33.43		
	STK11	p.Lys124GlufsTer39	67.22		
	NOTCH3	p.Arg244Ter	5.85		
B	NOTCH3	p.Val644Asp	50.61	WT	CCND1 11q13.3(69455972-69466035)x32.1053
					FGF19 11q13.3(69513954-69518740)x35.3263
					CDK4 12q14.1(58142245-58145450)x6.08421
F	SMAD4	p.Arg531Leu	16.75	KIF5B(15)-RET(12)	WT

	TSC2	p.Pro632Leu	16.18		
	CDK2	p.Arg199Cys	15.25		
I	CDKN2B	p.Thr95Met	8.49	WT	WT
	RAD51C	p.Ala175Thr	50.1		
	POLE	p.Arg976His	47.92		
A	RAD50	p.Tyr625Ter	49.62	WT	WT
	SLX4	p.Ala952Met	48.95		
D	ATM	p.Val2288AlafsTer22	81.61	WT	SMAD4 18q21.2(48591842-48604861)x5.24444
U	MLH1	p.Leu622Phe	52.81	WT	WT
	NOTCH3	p.Cys891Trp	45.16		
C1	CBL	p.Tyr368Cys	41.52	WT	WT
	PIK3R1	p.Leu638Ter	11.93		
G1	SLX4	p.Lys68Thr	35.92	FAIL	MYCL 1p34.2(40362966-40367017)
H1	PIK3CA	p.Glu110del	39.74	WT	WT
	PTCH1	p.Phe434Ile	44.57		
C	NOT			EML4(6)-ALK(20)	WT
R	NOT			WT	MYCL 1p34.2(40362966-40367017)
V	SF3B1	p.Arg625Cys	27.68	FAIL	WT
H	NOT			WT	WT
F1	NOT			WT	WT

Table 5_3: List of all molecular alterations identified in 27 samples of LC-HP.

References

Armengol G, Sarhadi VK, Rönty M, Tikkanen M, Knuuttila A, Knuutila S. Driver gene mutations of non-small-cell lung cancer are rare in primary carcinoids of the lung: NGS study by ion Torrent. Lung. 2015 Apr;193(2):303-8.

Baine MK, Rekhtman N. Multiple faces of pulmonary large cell neuroendocrine carcinoma: update with a focus on practical approach to diagnosis. Transl Lung Cancer Res. 2020 Jun;9(3):860-878.

Cros J, Théou-Anton N, Gounant V, Nicolle R, Reyes C, Humez S, Hescot S, Thomas de Montpréville V, Guyétant S, Scoazec JY, Guyard A, de Mestier L, Brosseau S, Mordant P, Castier Y, Gentien D, Ruszniewski P, Zalcman G, Couvelard A, Cazes A. Specific Genomic Alterations in High-Grade Pulmonary Neuroendocrine Tumours with Carcinoid Morphology. Neuroendocrinology. 2021;111(1-2):158-169.

Gococo-Benore DA, Boyle A, Wylie N, Drusbosky L, Khoor A, Starr JS. Atypical Lung Carcinoid With EML4/ALK Fusion Detected With Circulating Tumor DNA. Cureus. 2022 Feb 16;14(2):e22276.

Hermans BCM, Derks JL, Thunnissen E, van Suylen RJ, den Bakker MA, Groen HJM, Smit EF, Damhuis RA, van den Broek EC; PALGA-group; Ruland A, Speel EJM, Dingemans AMC. DLL3 expression in large cell neuroendocrine carcinoma (LCNEC) and association with molecular subtypes and neuroendocrine profile. Lung Cancer. 2019 Dec; 138:102-108.

Hermans BCM, Derks JL, Moonen L, Habraken CHJ, der Thüsen JV, Hillen LM, Speel EJM, Dingemans AC. Pulmonary neuroendocrine neoplasms with well differentiated morphology and high proliferative activity: illustrated by a case series and review of the literature. Lung Cancer. 2020 Dec;150:152-158.

Kander EM, Shah MH, Zhou Y, Goyal A, Palmer JD, Owen DH, Shilo K, Patel G, Raval RR, Gonzalez J, Nguyen M, Olek E, Kherani J, Rothenberg SM, Konda B. Response to

the Selective RET Inhibitor Selpercatinib (LOXO-292) in a Patient With RET Fusion-positive Atypical Lung Carcinoid. Clin Lung Cancer. 2021 May;22(3):e442-e445.

Lei X, Zhu S, Ren D, Ren F, Li T, Zhou N, Li S, Shi T, Zu L, Song Z, Chalubinska-Fendler J, Denis MG, Bernicker EH, Thomas de Montpréville V, Jiang R, Xu S. Metastatic pulmonary carcinoids with *EML4-ALK* fusion response to ALK inhibitors: two case reports and review of literature. Transl Lung Cancer Res. 2022 Jun;11(6):1176-1184.

Rekhtman N, Desmeules P, Litvak AM, Pietanza MC, Santos-Zabala ML, Ni A, Montecalvo J, Chang JC, Beras A, Preeshagul IR, Sabari JK, Rudin CM, Ladanyi M, Klimstra DS, Travis WD, Lai WC. Stage IV lung carcinoids: spectrum and evolution of proliferation rate, focusing on variants with elevated proliferation indices. Mod Pathol. 2019 Jul;32(8):1106-1122.

Rubino M, Scoazec JY, Pisa E, Faron M, Spaggiari L, Hadoux J, Spada F, Planchard D, Cella CA, Leboulleux S, De Marinis F, Ducreux M, Lamartina L, Baudin E, Fazio N. Lung carcinoids with high proliferative activity: Further support for the identification of a new tumor category in the classification of lung neuroendocrine neoplasms. Lung Cancer. 2020 Oct;148:149-158.

Sazonova O, Manem V, Orain M, Khoshkrood-Mansoori B, Gaudreault N, Desmeules P, Bossé Y, Joubert P. Transcriptomic data helps refining classification of pulmonary carcinoid tumors with increased mitotic counts. Mod Pathol. 2020 Sep;33(9):1712-1721.

Simbolo M, Mafficini A, Sikora KO, Fassan M, Barbi S, Corbo V, Mastracci L, Rusev B, Grillo F, Vicentini C, Ferrara R, Pilotto S, Davini F, Pelosi G, Lawlor RT, Chilosi M, Tortora G, Bria E, Fontanini G, Volante M, Scarpa A. Lung neuroendocrine tumours: deep sequencing of the four World Health Organization histotypes reveals chromatin-remodelling genes as major players and a prognostic role for TERT, RB1, MEN1 and KMT2D. J Pathol. 2017 Mar;241(4):488-500.

Simbolo M, Barbi S, Fassan M, Mafficini A, Ali G, Vicentini C, Sperandio N, Corbo V, Rusev B, Mastracci L, Grillo F, Pilotto S, Pelosi G, Pelliccioni S, Lawlor RT, Tortora G, Fontanini G, Volante M, Scarpa A, Bria E. Gene Expression Profiling of Lung Atypical

Carcinoids and Large Cell Neuroendocrine Carcinomas Identifies Three Transcriptomic Subtypes with Specific Genomic Alterations. J Thorac Oncol. 2019 Sep;14(9):1651-1661.

Volante M, Mete O, Pelosi G, Roden AC, Speel EJM, Uccella S. Molecular Pathology of Well-Differentiated Pulmonary and Thymic Neuroendocrine Tumors: What Do Pathologists Need to Know? Endocr Pathol. 2021 Mar;32(1):154-168.

Yoshimura M, Seki K, Bychkov A, Fukuoka J. Molecular Pathology of Pulmonary Large Cell Neuroendocrine Carcinoma: Novel Concepts and Treatments. Front Oncol. 2021 Apr 22; 11:671799.

7.0 CONCLUSIONS

This work presents five selected research projects followed by the Candidate during her 4-years PhD program as the Principal Investigator. As already stated in the overview, and discussed in the specific chapters that are the main core of this Thesis, three different models of rare endocrine tumors were studied, all faced with the similar intent of investigating mechanism of progression and of identifying novel targets for therapy.

Papers described in this Thesis can be separated in three main subgroups:

a) the study of molecular mechanism of tumor progression, analyzing cases showing tumor components of benign morphology or less aggressive malignancy;

b) the identification of novel molecular therapeutic targets in tumors that are orphan of an individualized therapeutic approach;

c) the study of specific tumor subgroups, as for the study on the characterization of ACC with MMR-deficiency.

In the first setting, we analyzed two different tumor models. On the one side we studied PDTC cases that were morphologically related with a coexistent well differentiated – biologically less aggressive – carcinoma component, whereas the second model consisted of ACC cases with a benign component concurrent within the same lesion. Although different in biological terms, both tumor types represent models of tumor progression that are feasible to analyze comparatively at the molecular level possible steps of tumor development. Both studies gave comparable results. In fact, in both models, a predominant monoclonal origin was suggested, since the majority of cases was characterized by coexistence of molecular alteration in benign/well differentiated and more aggressive tumor populations, these latter in some cases acquiring additional molecular alterations driving tumor progression (i.e. *TERTp* mutations). However, a significant number of cases in both studies unexpectedly presented completely distinct genotypes, even in the presence of a morphological pattern strongly suggestive for a unique tumor. Therefore, it should be assumed that, at least in part, heterogeneous tumors that display in the same lesion tumor components with different aggressiveness may be unrelated and may stem from separate clonal evolutionary pathways.

Concerning the identification of novel therapeutic targets, we focused on a large series of PDTCs and on lung carcinoids with high proliferative index. Both these tumors are rare, poorly characterized and are lacking therapeutic strategies preventing a patient's specific approach in the clinical management. Both studies, among other findings, claimed one main point: that druggable alterations are less rare than expected, irrespective of their type (gene fusions, mutations in TKI genes or MMR-deficiency) and that screening for

targetable alterations should be considered widely also in these rare tumors to raise new data with a strong potential clinical relevance. Moreover, novel drivers were identified in both tumor models, such as *ETV6/NTRK2* in lung carcinoids and *TBL1RX1-PIK3CA* fusion in PDTC.

Finally, we aimed at characterizing one specific subtype of ACC that presents MMR deficiency, as determined by loss of protein expression of MMR proteins. These MMR-deficient ACC cases were associated with peculiar pathological features of aggressiveness and with a distinct genotype, dominated by a relatively high burden of mutations, and a particular enrichment for mutations in *TP53* and in genes belonging to the chromatin remodeling pathway. Apart from a pathogenetic interest, these data claim that molecular characterization should integrate pathological classification in ACC to define specific subgroups with a "blind" morphology but with a distinct biological and possibly clinical behavior. These data again support the need of an individualized approach in rare cancer characterization, to achieve optimal clinical management and the definition of the best therapeutic strategies.

8.0 AKNOWLEDGMENTS

Sinceri ringraziamenti al Professor Marco Volante, per avermi consentito di effettuare questo percorso nel suo gruppo di ricerca e per i preziosi insegnamenti elargiti negli anni.
Grazie alla Professoressa Luisella Righi, per il costante supporto e il ruolo che ha avuto nella mia crescita lavorativa.
Grazie a tutto il gruppo dell'Anatomia Patologica dell'ospedale San Luigi, in particolare grazie a: Francesca N., Susanna, Angela e Ida per avermi trasmesso le loro conoscenze nel campo e per avermi insegnato a non mollare mai; grazie anche a Federica (o Federca come più le piace) e Francesca B., per avermi aiutata e supportata in questo percorso anche quando a volte non era facile e per il bel rapporto di amicizia che si è instaurato.
Grazie ai miei amici che ci sono sempre stati sin dal liceo: ad Allan per le serate giochi, le lunghe chiacchierate e il continuo sostegno; e ad Anna per gli aperitivi, i pomeriggi a chiacchierare e il supporto non indifferente.
Grazie al mio amico Edoardo, per le risate, il sushi ma soprattutto per il sostegno anche da lontano.
Grazie alla Biotech Company (Franci, Fè, Lalla, Rao, Ale, Flavio, Mauro e Rox) per essere diventati negli anni una seconda famiglia ed essermi stati sempre vicini anche se fisicamente lontani.
Infine, grazie alla mia famiglia, ai miei genitori che sono stati un costante supporto in tutti questi anni, fin dall'inizio della mia carriera scolastica; ai miei nonni, Elsa ed Enrico, per avermi sempre sostenuta e a mio nonno Antonio, che sono sicura sarebbe contento del percorso fatto; grazie a mio zio Guido e a Emma, per avermi sempre fatta ridere anche nei momenti bui; e infine, ma non meno importante, grazie a Stefano, che è ormai parte della mia famiglia, per il costante supporto, amore e incondizionata fiducia nelle mie capacità, anche quando io non ci credevo, perciò grazie di cuore.